
POLITECNICO DI TORINO

MASTER OF SCIENCE PROGRAM IN CIVIL ENGINEERING

# Reusing damaged tennis strings in asphalt pavements: experimental investigation on the anti-rutting potential

**Supervisors:**
Prof. Pier Paolo Riviera
Prof. Ezio Santagata
Eng. Hajiali Mozhgan

**Candidate:**
Ochilov Shokhrukh

Academic year 23/24

# Acknowledgment

I would like to express my deepest gratitude to all those who have supported me throughout the development of this thesis.

First and foremost, I am sincerely grateful to my supervisor, Professor Pier Paolo Riviera, for his invaluable guidance, insightful feedback, and constant encouragement throughout this research process. His expertise and patience have greatly shaped the outcome of this work.

Above all, I owe my deepest gratitude to my family, whose unwavering love and support have been the cornerstone of all my achievements. To my parents, who have been my greatest inspiration and my enduring source of strength, I am forever grateful for your sacrifices, guidance, and belief in my dreams. Your constant support has empowered me to confront challenges with confidence and inspired me to strive for greater achievements.

My special thanks to co-tutor Hajiali Mozhgan, I express my sincere gratitude for her precious guidance and support in this research. Her input and thoughtful advice have significantly contributed to the depth and quality of the research. I am deeply thankful for her patience, expertise, and unwavering commitment to helping me succeed.

I would also like to extend my heartfelt thanks to my colleague and friend Enrico Miceli, whose support and companionship have been invaluable during this journey. His assistance, intuitive discussions, and cooperation to share ideas have greatly enriched my experience and contributed to the successful completion of this thesis.

I would like to extend my heartfelt gratitude to Alessandro and Sadegh for their help during the research. Their collaborative spirit, valuable suggestions, and shared perspectives have been instrumental in enriching my experience and advancing this work. I deeply appreciate their generosity, friendship, and readiness to assist whenever I needed help

# Abstract

In today's highly industrialized world, the production of various plastic materials has reached its peak, leading to the widespread issue known as plastic pollution. It is a long-lasting, large-scale concern, with plastic debris and particles found in numerous ecosystems. This pollution disrupts habitats and natural processes, decreasing ecosystems' ability to handle with climate change, and negatively impacts the food security and production, and well-being of millions of people. Additionally, the production, use, and disposal of plastics contribute to about 4% of global greenhouse gas emissions. Plastic waste contaminates food, water, and oceans, with 85% of marine debris being plastic. Since plastic does not biodegrade, 46% of it ends up in landfills, while 22% is improperly managed and becomes litter.

Thanks to modern technology, waste plastic can be utilized in various engineering applications, especially in the civil construction fields. In particular, plastic waste can be incorporated into road construction. One of the typical plastic wastes derived from the sport industry is discarded tennis strings, which constitutes a significant portion of plastic waste. With around 87 million players worldwide, the frequent replacement of strings due to their loss of tension and flexibility over time contributes to this accumulation.

As mentioned before these wasted tennis strings in road pavements can contribute for reducing plastic waste globally. Additionally, it may help to improve pavement performance. Tennis strings are typically made from materials such as nylon, polyester, natural gut, Kevlar, or combination of these. Tennis strings are added to asphalt mixture as fibers and the dry method is used, as their melting point exceeds the binder's mixing temperature. Based on data from the literature, fibers around 5 mm in length are recommended.

The experimental study begins with the initial phase of mix design, aimed at determining the optimal dosage of fibers derived from discarded tennis strings and bitumen content. Three fiber quantities were evaluated: 1.0%, 0.5%, and 0.3% by the weight of the aggregate. Due to volumetric results with 1% fiber is unable to attain the required binder content, while the other evaluated dosages demonstrated appropriate binder content during the mix design. Based on the mix design results and the related studies, 0.3% is selected for the mechanical tests as it provided the most suitable performance.

The specimens of two different type of reference mixture and mixture with fiber are subjected to experimental tests to determine the material's relaxation characteristics and overall dynamic properties using master curve and permanent deformation behaviour of asphalt mixes under repeated loading through the flow number test, above tests are conducted according to AASHTO R 84 (Master Curve by AMPT) and AASHTO T378 (E and Flow Number by AMPT) consequently. The master curve tests are conducted at 4°C, 20°C, and 40°C. While flow number test is done at 58°C. The results, along with the comparison of the two mixtures, indicate that incorporating tennis strings as fibers can enhance the rutting resistance and viscoelastic properties of asphalt mixtures.

Keywords: Plastic waste, recycled tennis strings, road pavements, bituminous mixtures, binder layer, dry method, ITS, stiffness, flow number, rutting behaviour, permanent deformation.

# Contents

# List of figures

# List of tables

# 1. Introduction

Nowadays, our planet is facing severe ecological harm due to millions of tons of plastic waste being generated each year and consequently littering the environment, causing massive amounts of industrial and household leftover in surroundings. Plastic pollution has become one of the most pressing environmental issues, as rapidly increasing production of disposable plastic products overwhelms the world's ability to deal with them. Plastic contamination is most visible issue in the world, where garbage collection systems are often inefficient or non-existent. But the developed world, especially in countries with low recycling rates, also has trouble properly collecting discarded plastics.

The world is producing twice as much plastic waste as two decades ago, with the bulk of it ending up in landfill, incinerated or leaking into the environment, according to a new report of OECD (the Organisation for Economic Co-operation and Development). Ahead of UN talks on international action to reduce plastic debris, the OECD's first Global Plastics Outlook shows that as rising populations and incomes drive a relentless increase in the amount of plastic being used and thrown away, policies to curb its leakage into the environment are falling short. Almost half of all plastic litter is generated in OECD countries, according to the Outlook. Discarded plastics generated annually per person varies from 221 kg in the United States and 114 kg in European OECD countries to 69 kg, on average, for Japan and Korea. Approximately 36% of all plastic produced is used to create packaging, 85% of which ends up in landfills. According to a report by the United Nations Environment Programme, around 400 million tonnes of plastic waste is generated every year globally, whereas recycled amount merely counts to 9%.

A tremendous 91% of plastic isn't recycled. If that amount feels beyond belief, it is. Even the scientists who undertook the world's first comprehensive count of plastic production, discarded, burned or put in landfills, were stunned by the sheer size of the numbers. Plastic is one of the most long-lasting materials that human has produced. Today, it's widely known that it can take hundreds of years for plastic to degrade, and research indicates that plastic might never fully decompose. Plastic poses a significant threat to the world due to its environmental persistence, and harmful effects on ecosystems and human health. From this perspective, the scale of this disaster becomes evident. Immediate action must be taken to focus on these issues effectively in order to mitigate the damage and prevent further harm to the environment. Reducing pollution from plastics will require international co-operation, to decrease plastic production, including through innovation, better product design and developing environmentally friendly alternatives, as well as efforts to improve waste management and increase recycling. These are ongoing challenges that modern industries are addressing with limited efforts, but a fundamental shift is needed in our consumption-driven society.

Till this day over 9200 million metric tonnes (Mt) of plastic have been produced worldwide, among them with approximately 6900 Mt left unrecycled, resulting instead as accumulation in landfills or dispersal within the environment. This situation presents a lost economic opportunity and a substantial detriment to the environmental health. To sustain the long-term value of this multi-billion-dollar material, it is fundamental to address the complexity of plastic waste and take transformative steps to reform plastic products focusing on sustainability and end-of-life.

A key solution to decrease plastic waste is recycling. Plastic recycling incorporates both positive and negative aspects, warranting a comprehensive evaluation to balance environmental benefits and burdens. Recycling plastic waste can significantly reduce fossil fuel utilization, power consumption, and landfilling.

Mechanical recycling is considered as main method for recycling. This involves reprocessing these waste plastics into reusable material without changing its basic chemical structure. In mechanical recycling usually plastics are undergone through shredding process. The process for this recycling includes several steps, such as collecting, sorting, washing, shredding, and melting the plastics before reshaping them into pellets or new products. The recycled plastics can then be utilized to produce new items, reducing the demand for virgin plastic and conserving natural resources. On the other hand, turning plastic into usable heat, or fuel through incineration is another alternative way to deal with plastic waste, it is known as energy recovery process.

Conversely, this plastic contamination can be repurposed across various construction sectors. The suitability of recycled plastic waste for various applications depends on its type and properties. High-density polyethylene (HDPE), being a relatively hard and rigid material, it can be used in the manufacture of plastic lumber, tables, chairs, and other furniture. The light-density polyethylene (LDPE), due to its flexibility, it is suitable for the production of bricks and blocks. Polypropylene (PP) is hard and elastic, and due to these properties, its potential applications are as aggregates in asphalt mixtures. Polystyrene (PS), with its hard and brittle nature, is mainly used for parts that are not highly stressed mechanically, like insulation materials. Polyvinyl chloride (PVC) is hard and rigid, which indicates its potential use as an aggregate in cement-based materials. Finally, polyethylene terephthalate (PET), is both hard and flexible, commonly used as fibers in cementitious composites.

Typically, the attention has been given to household and industrial sources of plastic pollution, however, sports industry contributes enough waste to plastic pollution due to events, venues, and products related to sports, creating what can be termed “sportive plastic waste” - a subset of plastic waste generated through sports-related activities and consumables. This plastic waste can accumulate from individual training sessions or major tournaments. Furthermore, effective and innovative solutions are still needed to cover reprocessing of these plastic contamination.

Due to fact that current level of application and research on waste plastic widely enhanced, including improved recycling practices, experience, utilization of recycled materials in civil engineering provides the waste management. Particularly, one innovative approach involves incorporating plastic waste into bituminous mixtures for pavements. Plastic has proven to be one of the most effectively unite bitumen mixes used in the pavements. The main objective to use of waste plastic is to reduce plastic pollution, while enhancing the durability and sustainability of road infrastructure.

Plastic roads, which first emerged in India two decades ago, these roads are being tested and constructed in more and more countries as globally plastic pollution problem becomes an increasingly pressing issue. India has already laid over 60,000 miles of these roads. The technology is also gaining traction in Britain, Europe, and Asia. Recently, several countries including South Africa, Vietnam, Mexico, the Philippines, and the United States, have built their first plastic roads.

In this contents, various laboratory tests were conducted on different materials used in road superstructures containing recycled plastics. Extensive research has explored the use of different types of fibres depending on the type of polymer used, such as HDPE, LDPE, polyester, PET, PE, PP and others. These studies have demonstrated improvements in the mechanical performance of the bituminous mixtures, for example, from the literature, 0.25% polyester fibres, compared to the mixture and 8 mm in length, gave positive results on the breaking energy of the mixture, compared to the control mixture. On the other hand, different fibre contents, 0.3%, 0.5%, and 1%, were used, which improved the stability, durability, crack resistance, and rutting behaviour of the bituminous mixtures. The available literature shows that mixtures containing a certain amount of plastic will increase properties such as strength, water resistance, binding of the mix, and service life. In this thesis, the use of discarded plastics from sports industry is examined.

In conclusion, a brief summary of this review study is provided. The main purpose of this research is to verify the effect of waste tennis strings, which is made by PET material, on rutting behaviour and materials' relaxation characteristics of the bituminous mixtures. Through an experimental procedure in the laboratory, tests were carried out to evaluate the mechanical properties of the bituminous mixtures containing fibres obtained from discarded tennis strings through cutting. These tests are performed in accordance with AASHTO T378 (E and Flow Number by AMPT) to analyse rutting performance and AASHTO R 84 (Master Curve by AMPT) to assess viscoelastic behaviour of bituminous mixtures. Lastly, the mechanical properties of these plastic-enhanced asphalt mixtures were compared to those of a reference mixture without plastic. This experimental research has conducted in the laboratory of DIATI door 2 (Department of Environment, Land and Infrastructure Engineering, Politecnico di Torino).

# 2. Waste plastic

Plastic pollution is a serious environmental challenge due to its non-biodegradable nature, creating problems for wildlife and their habitats as well as human populations. Mostly plastic products such as single-use items like bags, bottles, and packaging end up in landfill, where they can take centuries to decompose. This buildup of plastic waste is harmful to wildlife, causing to pollution in oceans and soil, impacting food chains and human health which may ingest or become entangled in plastic debris. Addressing this issue requires improving recycling processes, as well as the development of biodegradable alternatives, are essential steps in solving the plastic waste crisis, alongside efforts to reduce plastic production and consumption are crucial for creating a more sustainable future.

Today, the average consumer comes into daily contact with all kinds of plastic materials. These plastic materials are derived from petroleum and non-biodegradable, they tend to persist in natural environments. Additionally, many lightweight single-use plastic products and packaging materials, accounting nearly 50 percent of all plastics produced, are frequently not discarded properly in designated containers for transport to landfills, recycling facilities, or incineration sites. Instead, they are improperly thrown away at or near the location where they end their usefulness to the consumer.

Plastic consumption has thus increased about 180 times from 1950 to 2018. Global plastic production reached an estimated 400.3 million tons in 2022, with expectations for continued exponential growth in the years ahead. Plastics are created from organic compounds, including synthetic and semi-synthetic materials derived from petrochemicals and partially natural sources, which make them soft and flexible. Typically, plastics can be classified as bio-based (organic polymers) or engineered. Engineered plastics are developed using unrefined petroleum, flammable gas, and coal. Approximately about 4 % of fossil fuel is used to produce plastics. Furthermore, sustainable resources such as carbohydrates, vegetable oils, microorganisms, and various natural materials are also used to manufacture bio-based plastics.

Plastics are made from fossil fuels and the plastics industry has become one of the fastest-growing sources of industrial greenhouse gases. In 2019, emissions from plastic production and incineration were equivalent to the those generated by 189 coal power plants. Without proper regulation, plastic pollution can obstruct efforts to keep global temperature increases below 1.5°C. Recent data indicates that this threshold has been temporarily exceeded over the past year. For instance, from June 2023 to May 2024, global temperatures averaged 1.63°C above pre-industrial levels, showing the hottest year on record.

Polymer materials, particularly plastics and rubbers, are notably sensitive to temperature and moisture fluctuations. As temperatures rise, polymers expand, leading to inferior properties. Widely used plastics, such as polyethylene, polypropylene, and polyvinyl chloride can experience over 20% decrease in stiffness when a service temperature rises from 23-24 °C to 40 °C. Beyond these immediate impacts, a warming climate also speeds up the degradation of properties over time by accelerating the ageing process.

Recent studies proves that between 15 and 51 trillion pieces of plastic pollute the world's oceans with over 1.3 million tonnes floating on the ocean surface - covering roughly 40% of it. This means that plastic pollution impacts every square mile of the ocean's surface. It is found in offshore environments that macroplastics from several decades ago, even as far back as

the 1950s and 1960s still remains. Some estimation even approves that some plastic takes a breakdown period of approximately four centuries.

In 2019, a turtle hatchling, small enough to fitting a hand, was discovered dead with more than 100 pieces of plastic in its stomach. Marine animals mistake floating plastic debris for food and end up consuming it. Unfortunately, plastic particles smaller than 5 mm are widespread in the oceans, allowing them to pass through the digestive systems of these creatures. This causes severe health issues and, ultimately, can lead to their death. Alarmingly, they found that 1,557 species worldwide, including many endangered ones, have been documented to have ingested plastic.

*Figure 1. Marine animals entangled with waste plastic*

The solution is to prevent plastic waste from entering rivers and seas in the first place, many scientists and conservationists say. This could be accomplished with improved waste management systems and recycling, better product design that takes into account the short life of disposable packaging, and a reduction in manufacturing of unnecessary single-use plastics.

Recycling is a waste management method which collects waste materials and converts them into raw materials that can be reused to create other valuable products. It is often referred to as "renewing or reusing" to prevent the harmful effect on society and protect the environment. The plastics are non-biodegradable as carbon-based products and other polymers. Plastic contains bottles and other materials that can be melted and transformed into other products like plastic tables and chairs. This recycling process is performed in the following six steps: collecting waste plastics, sorting, or arranging plastics into categories, washing to remove impurities, shredding and resizing, identifying and separating different types of plastics, and compounding them for reuse.

The first steps in plastics waste management include storage, collection, and primary recyclables processing. These are followed by secondary recycling (where material is reused in some other way without reprocessing), tertiary recycling (chemically altering material to reuse it), incineration, or landfilling (sanitary and dumpsites).

Primary recycling, also called mechanical recycling or closed-loop recycling, refers to the process of reusing waste materials by transforming them back into their original form or similar products without altering significantly their chemical composition. In primary recycling, the

items are reused in their original form, keeping products out of recycling plants and landfills. This approach is important as products that are recycled in one town may not be accepted in another. Instead of ending up in landfills, they are repurposed for their original intended use.

Secondary recycling is a process where waste plastics become new products, but unlike primary recycling, they don't preserve their original form. Instead, secondary recycling converts plastics into things of lower quality or value, often with altered properties. This type of recycling is commonly used for materials that are too degraded for primary recycling. For example, waste plastics can be turned into materials like plastic lumber, insulation materials, or textiles. While secondary recycling helps reduce plastic waste but often results in products with limited recyclability.

Tertiary recycling is the process of repurposing items that could otherwise be discarded in a landfill or incineration and turning them into something new and useful. It involves the chemical altering of the products in order to make it reusable. Specifically, this recycling method converts plastics into raw materials, such as monomers, oils, or gases, which can then be used to create new plastic products or other chemicals. Tertiary recycling can handle a wider variety of plastic types, including those that are too degraded or contaminated for mechanical recycling, making it a valuable method for reducing plastic waste on a molecular level.

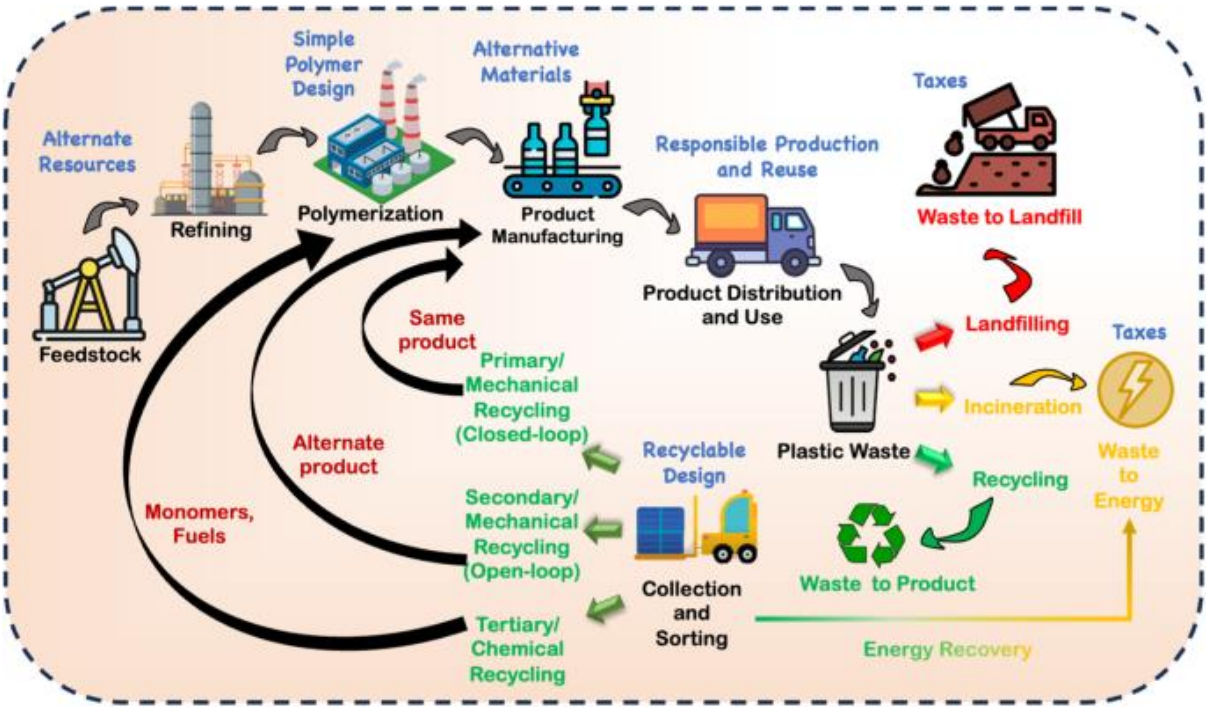


*Figure 2. Recycling process of waste plastic.*

For plastics waste to be diverted for reuse in infrastructure it must have the potential to be sourced and processed in sufficient volume and quality to be useful. Thermoplastics used for durable applications, such as polyvinyl chloride (PVC) sewer pipe and electric wire insulation, and high-density polyethylene (HDPE) storm drainage pipe, rarely become municipal solid

waste. In contrast, nondurable plastics, with service lives lasting less than 3 years, are often recyclable, particularly polyethylene terephthalate (PET) and HDPE items, with the exception of multilayered plastic composite products, biomedical devices, and hard-to-recycle materials such as PVC and polystyrene (PS).

Accordingly, there is a growing global interest in improving the performance of asphalt layers by modifying bitumen or the asphalt mix to extend their lifespan. Fibers have been the most utilized materials in asphalt layers for many decades due to their capability in boosting the mechanical performance of asphalt layers. Adding plastic to bitumen improves the durability of the road, making it more resistant to wear, cracking, and water damage. Roads made with plastic-modified bitumen generally have a longer lifespan and require less maintenance.

Each kilometre of road constructed using recycled plastic can consume 684,000 plastic bottles or 1.8 million plastic bags, effectively diverting substantial amounts of plastic waste from landfills and incineration. Waste plastics, such as low-density polyethylene (LDPE) and polyethylene terephthalate (PET) can enhance the stability and strength of asphalt. Modified mixtures often exhibit higher Marshall stability values, indicating greater resistance to deformation under heavy loads. Studies have shown that roads incorporating waste plastics exhibit improved stability and strength. For example, according to Jalal J. Jafar et al. (2015), the use of waste plastic as a partial aggregate replacement in bituminous increased stiffness by 10%. Previous study (Marco Pasetto, et al. 2022**)** has shown that a proportional increase in the strength and fracture resistance with the corresponding addition of plastic waste was also observed in indirect tensile tests, suggesting the strengthening of the asphalt mastic due to the chemo-physical interaction between the asphalt binder and the plastic particles.

A substantial amount of plastic waste arises annually from construction and demolition activities, as well as municipal solid waste. In Europe, for instance, 27.1 million tonnes of plastic waste is generated each year; of this, 8.4 million tonnes are recycled, while the remaining 18.7 million tonnes are either landfilled, incinerated, stored, or exported. This trend reflects the typical global handling of plastic waste.

Worldwide, managing plastic waste generated by the sports industry receives limited attention, however, the amount of plastic waste generated by the sports industry is substantial. Specifically, in sports sector, the string waste discarded from tennis racket isn't used well for recycling purposes. There are around 87 million tennis players worldwide. If we assume players change strings once per month. From our calculations we assumed standard lengths of string for each racket 12 metres, where it weighs 17 grams. By doing math, 12,528,000 km string waste is obtained and approximately 18000 tons of waste string per year. Burning this amount of plastic waste produces around 50000 tons of carbon-dioxide into atmosphere. Recycling this plastic litter can play a substantial role in lessening its environmental impact.

Discarded strings typically contribute to waste accumulation, posing an environmental alarm. Specifically, polyester string, commonly used, is a non-biodegradable string. Similar to nylon, polyester is a synthetic material that is made from petroleum. Once discarded, it can take up to 200 years to decompose. During this time, it may release harmful chemicals into the environment, which can have a negative impact on both wildlife and human health.

String is a common household item that is used in diverse applications, from tying up packages to hanging decorations, and widely used in sport industry, string is a versatile tool that many

people rely on. In particular in this research, the effect of the tennis strings on bituminous mixtures is examined. An overview of the tennis string information is presented below.

String is made of materials such as nylon, polyester, or natural gut, each offering different characteristics in terms of durability, power, control, and spin potential. Players can also customize their string tension to tailor their racket to their needs further. Overall, tennis string plays a significant role in the overall feel and playability of a tennis racket. There are more than 60 producers of tennis strings throughout the world. Each of them produces different type of string with different pattern and material.

## Material of tennis strings

Modern tennis strings fall under 5 main categories:

- **Synthetic gut**: it is the cheapest type of string. It is typically made of nylon and offers good playability for the price. It is suitable for beginners.
- **Multifilament**: this material offers playability most familiar to natural gut strings. They are made of 1000+ nylon microfibers.
- **Natural gut**: made from animal intestine, mostly cow's intestine. Natural gut strings are the most resilient material. It has better tension retention and is softer. It is the most comfortable string for arm. But it is very expensive material.
- **Polyester (monofilament)**: it is made of polyethylene terephthalate (PET). It is very popular among pro players.
- **Hybrid stringing**: A hybrid string means that there are two different string materials used in the mains and the cross strings of the racket. The most popular hybrid set up is polyester with natural gut.
- **Kevlar**. Longer durable, very rigid material with considerable tension and less comfortable [1]

*Figure 3. Synthetic gut string*

*Figure 4. Multifilament string.*

*Figure 5. Natural gut string*

*Figure 6. Polyester string*

## The reason to change the tennis strings

There are several reasons to change the tennis strings. Each string starts to lose tension after use. Specifically, tennis strings of professional players are more subjected to tension as they play hard during big tournaments. Changing the string helps players to avoid arm and shoulder injuries, because it is difficult to play with distorted strings. Here are a few of the top reasons players should restring their tennis racquet periodically.

**Tension Loss:** The first and most apparent reason to replace the tennis string. Over time, the tennis strings lose their tension, which effects control and power. Tension drops even without single stroke.

**Notching:** As you start playing, your strings will rub together and produce friction, causing the strings to notch. If you look closely, you will notice that notches form at the intersection of strings toward the middle of your racquet.

**Fraying:** Usually, fraying occurs with natural gut, multifilament, and Kevlar strings are composed of tiny fibres that will fray over time. It's a natural part of the wear for these strings, but it can be a great indicator of when you need to make restringing as it intensifies.

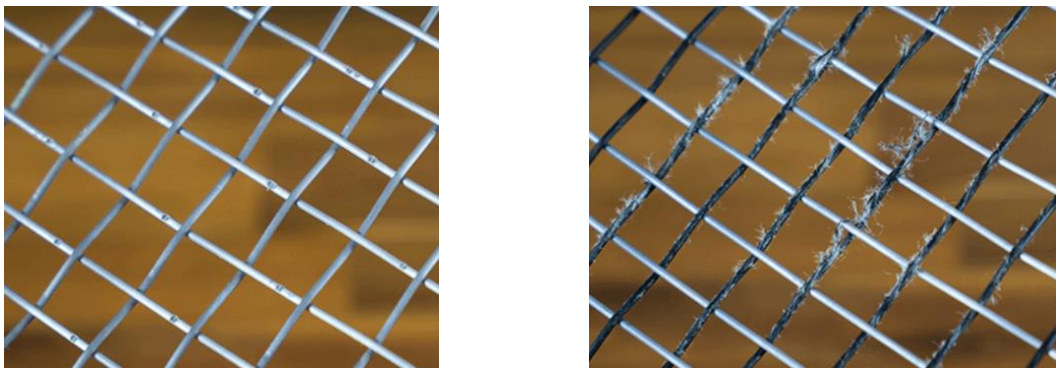

*Figure 7. Notching and fraying of the string*

# 3. Bituminous mixtures

Road pavements, also known as superstructures, upper part of the roadway that is exposed to vehicle traffic. They must fulfil both structural demands, such as minimizing the stresses transferred to the underlying layers and withstanding deterioration, as well as functional demands, including maintaining smoothness and grip for comfort and safety. Typically, these pavements are constructed in multiple layers and can be classified as either flexible or rigid.

Focusing on the flexible ones, they are made up of layers that form the bituminous package where the percentage of bitumen grows upwards, and each layer has different characteristics. Starting from the bottom, there is the base layer that contributes significantly to the structural response, with coarse grain size, high porosity and low percentage of bitumen.

The binder or connecting layer serves to link the base and wear layers, possessing properties that fall between the two. The wear layer, characterized by a fine grain size and high bitumen content, is the most exposed to traffic loads and environmental factors, leading to ongoing deterioration and requiring more frequent maintenance.

Layers of bituminous mixtures experience structural weakening, which can manifest as fatigue failure, the buildup of permanent deformation or distortion, and thermal cracking.

Principally, permanent deformation characteristics of asphalt mixture is studied with the help of a flow number test. Additionally, the dynamic modulus master curve test is carried out. The dynamic modulus master curve describes the temperature dependency of the material.

## 3.1 Bituminous mixtures

Bituminous mixtures, sometimes called asphalt mixtures (AC), are made up of different materials and produced at high temperatures in special plants to create asphalt layers. The composition of these mixtures differs according to the layers, with variation in gradation, binder content, varying volumetric, and mechanical properties. Bituminous mixtures can be categorized into various types based on their composition and characteristics.

As shown in Figure 8, the stone aggregate, characterized by its own internal and surface porosity, is covered by bitumen: in surface porosity the innermost part is permeable to water but not to the binder, while the outermost part to bitumen (called absorbed). A key feature of bituminous mixtures is the presence of voids between the bitumen-covered particles and in the porosity of the water-permeable asphalt mixtures. Voids affect the volume and mechanical properties of asphalt mixtures.

The materials that make up the mixture are:

- Stone aggregates that form the load bearing lithic skeleton of the AC.
- Bituminous binder that provides cohesion to the mixture of particles
- Filler, the finest fraction of grain size to improve workability
- Any additives, such as polymers to improve the performance of AC
- Possible recovered or milled AC also known as RAP (Reclaimed Asphalt Pavement)

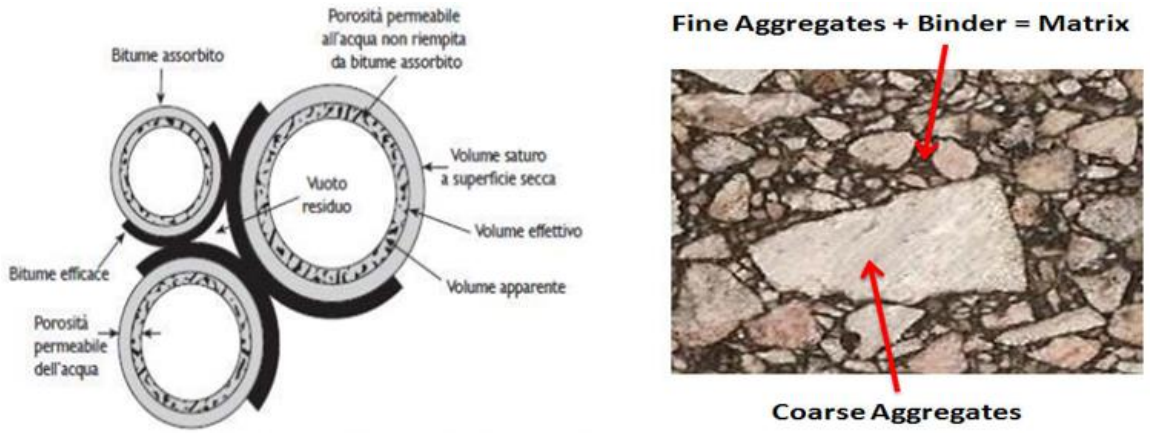


*Figure 8. Bituminous - aggregate cohesion formation*

## 3.2 Materials

A diverse range of materials is employed in road construction, containing soils, aggregates (both fine and coarse, sourced from rocks), binders such as lime, bituminous materials, different type of fillers, it can be mineral filler, cement, or other fine materials, reclaimed asphalt pavement (RAP). The essential component of asphalt mixtures is coarse aggregates, as it plays a vital role in the construction of roads. It consists of granular materials, such as crushed stone, gravel, or recycled concrete.

### 3.2.1 Aggregates

**Coarse Aggregates**

Coarse aggregates provide strengths, stability, and durability to pavement layers. Coarse aggregate refers to the larger particles that constitute most of AC, usually size is over 4.75 mm in diameter. These aggregates can be obtained from natural deposits like quarries or produced by crushing rocks or recycling concrete debris.

**Sand Aggregates**

Sand aggregates are classified into fine, medium, and coarse sands based on particle size. Coarse sand has larger particle size, typically between 2 and 4,75 mm. Sourced from natural deposits such as riverbeds or quarries. Coarse sand enhances the overall stability and strength of concrete mixtures, its coarser texture helps prevent segregation in the concrete and boosts structural integrity. Additionally, it is compactable material.

**Filler**

In pavement mix design, filler is a fine powder used to fill the spaces between larger aggregates in asphalt mixtures. This material is necessary for enhancing the mix by increasing stability, workability, and durability. It aids in compaction and cohesion, which leads to better mechanical interlocking and improved structural integrity.

**Reclaimed asphalt pavement (RAP)**

Reclaimed asphalt pavement is the most commonly used material to substitute virgin raw materials in asphalt mixtures. it is generated during maintenance activities. RAP is a high-

quality material that is rich in valuable constituents. It supplies top-grade aggregates and binder and can be recycled up to 100% in the construction of new roads.

### 3.2.2 Asphalt binder (bitumen)

Bitumen is a sticky, black substance, and highly viscous liquid or semi-solid form of petroleum. It serves as the main binding agent used in of asphalt pavement, binding together aggregates like sand, gravel, and crushed stone. The binder is obtained from crude oil through a refining process.

## 3.3 Type of failures in pavements

Pavement failure occurs due to various factors such as traffic loads, weather conditions, and material deficiencies. The main type of failure is due to fatigue cracking, rutting (permanent deformation), and thermal cracking.

### 3.3.1 Permanent deformation (Rutting)

Permanent deformation, often referred to as rutting, is a common issue in asphalt pavements. Rutting caused by permanent deformation in asphalt pavement layers is a longitudinal depression in wheel paths, caused by the accumulation of the non-recoverable component of responses to load repetitions at high service temperatures.

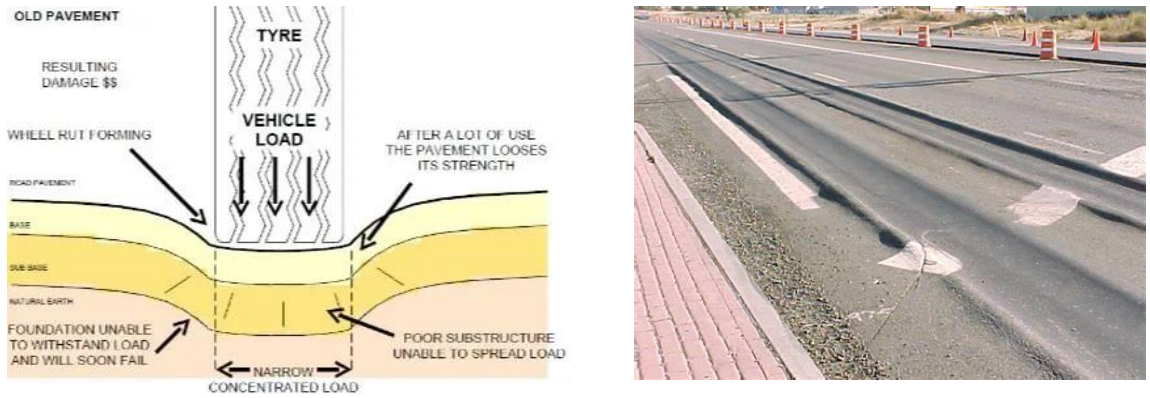


*Figure 9. Accumulation of permanent deformation scheme*

Rutting is an undesired stress in a pavement for several reasons. For the road users, it gives an increase of fuel consumption due to increased friction, and an increased risk of hydroplaning under wet weather conditions. Rutting is caused by several factors such as a low density of the layer, stress conditions, and number of load applications, among others, and occurs in a different layer of the asphalt pavement. In fact, the wider the ruts are, the deeper in the pavement the permanent deformation has occurred.

The accumulation of permanent deformation can be evaluated by means of several tests through which inducing the formation and accumulation of deformations on specimen by making use of:

- Constant load tests
- Repeated loading tests

- Simulative tests

Flow number is the repeated loading test. The test is conducted by applying repeated haversine axial compressive loads to a cylinder specimen at a specific test temperature. The test may be conducted with or without confining pressure. For each load cycle, the recoverable strain and permanent strain are recorded. The flow number is determined as the number of load cycles corresponding to the minimum rate of change of permanent strain (tertiary flow).

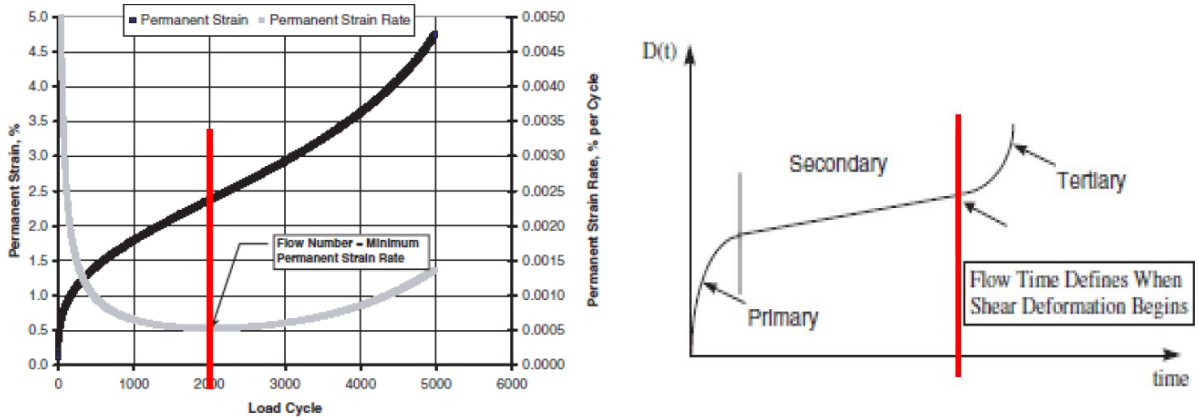


*Figure 10. Flow number and flow time (NCHRP Project 9-33)*

In Figure 10, flow number on the left is a repeated haversine axial compressive load pulse of 0.1 s every 1.0 s. Constant static stress applied up to the onset of tertiary flow.

The flow number is a property related to the resistance of asphalt mixtures to permanent deformation. It can be used to evaluate and design asphalt mixtures with specific resistance to permanent deformation.

### 3.3.2 Fatigue cracking failure

Fatigue failure in pavement is characterized by a series of interconnected cracks resulting from repeated traffic loading. In thinner pavements, these cracks start at the bottom of the asphalt layer where tensile stress is highest, and then propagates to the surface as longitudinal cracks. One criterion for failure is when fatigue cracking covers over 10 percent of the wheel path area.

Cracks usually initiate at the bottom of the asphalt layer and move upward to the surface. Figure 9 highlights the critical points within the asphalt layer that are subjected to wheel path. Generally, the lower section of the asphalt layer experiences bottom tensile strain ($\varepsilon_t$) while the upper part is under compression due to the wheel load. Furthermore, the natural flexibility of asphalt pavements induces surface tensile stresses at the top, particularly in the front, back, and sides.

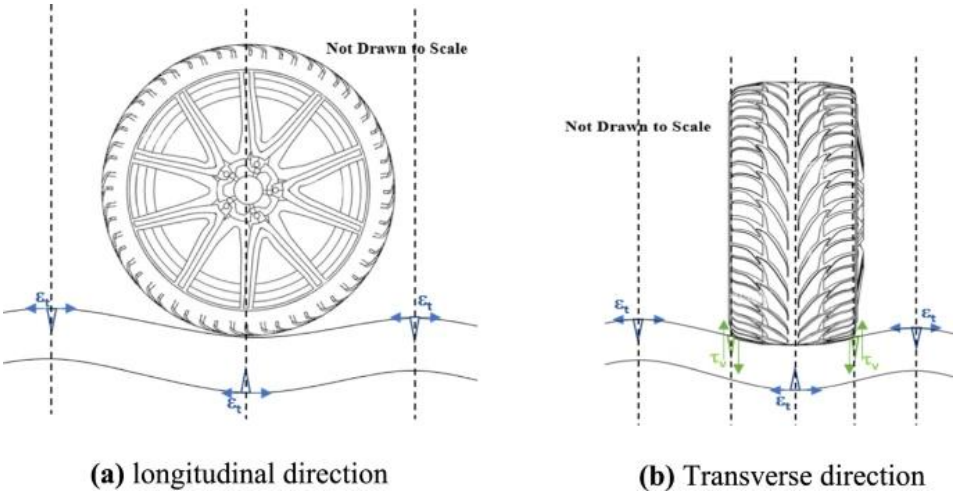


*Figure 11. Tensile stresses in asphalt pavement*

Fatigue cracking in asphalt pavements is generally attributed to two initial factors: bottom-up cracking and top-down cracking. The fatigue cracking initiated by either bottom-up or top-down cracking can be challenging to distinguish, and most of the time it can mix both mechanisms, therefore, coring techniques can be established to accurately determine the real underlying cause of the cracking.

Numerous loading modes is used to evaluate the fatigue responses of asphalt mixture. Including the uniaxial compression/tension (UC/UT), beam bending (BB), semi-circular bending (SCB), indirect tensile (IDT), and dynamic shearing (DS).

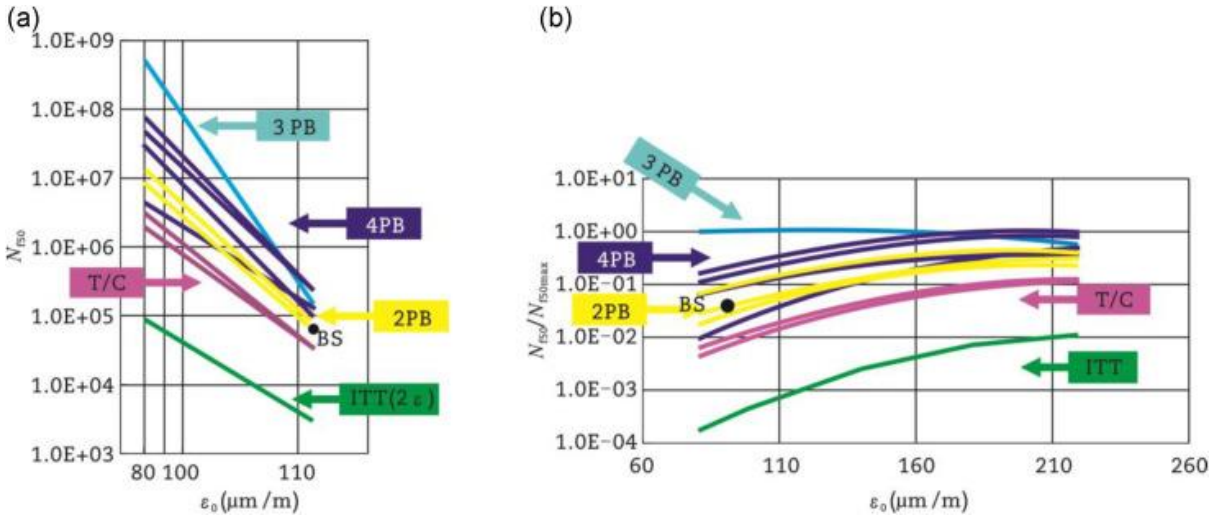


*Figure 12. (a) Obtained classical fatigue lives for strain fatigue tests. (b) Ratio of the fatigue life by the maximum fatigue life*

As shown in Figure 12, different loading models commonly generate dissimilar fatigue test results.

### 3.3.3 Thermal cracking failure

Due to the thermal sensitivity of asphalt mixtures, the thermal cracking is one of the most frequent distresses in asphalt pavements. Asphalt mixtures undergoes thermal stress when the temperature drops suddenly or the temperature gradient along the depth of pavement is significant due to their thermal-dependence and viscoelasticity.

Thermal stress arises due to the constraints of the pavement structure, and damage occurs when this the thermal stress surpasses the tensile strength of the material. Thermal fatigue cracking, on the other hand appears in the regions with relatively moderate climates. After repeated cycles of temperature fluctuations lead to the accumulation of fatigue damage in the material, in the end resulting in thermal fatigue cracking.

To study thermal effect on pavement performance two temperature variation range is applied for cyclic thermal stress simulation, as indicated in Figure 13. 15 typical cycles were chosen for the damage analysis, as indicated in Figure 13. Thermal stress increased progressively as the temperature decreased with a certain delay. Because of the viscoelastic properties of asphalt mixtures, the magnitude of thermal stress within each cycle gradually reduced, demonstrating visible stress relaxation phenomena under cyclic temperature variations. This behaviour associates with the characteristics of asphalt mixtures when exposed to cyclic stress at very low frequencies.

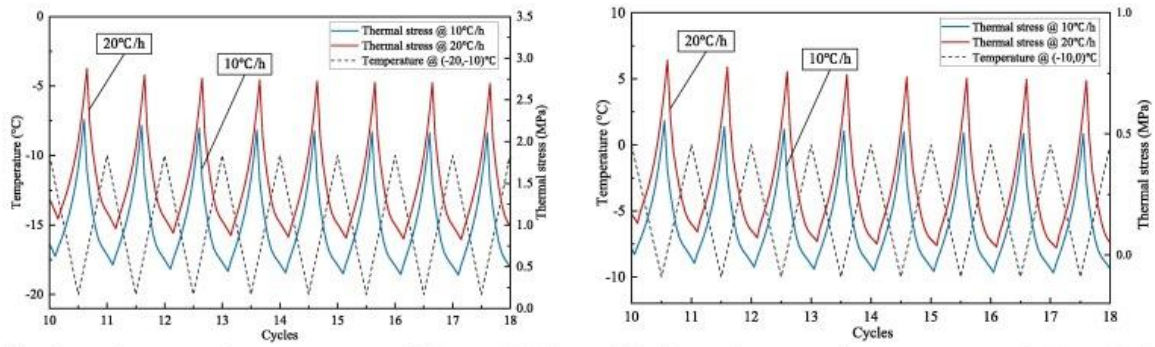


(a) Thermal stress under temperature of -20 to -10 °C (b) Thermal stress under temperature of -10 to 0 °C

*Figure 13. Thermal stress of asphalt mixtures at different temperature ranges and cooling rates*

A faster cooling rate generated larger thermal stress, as it led to a higher accumulation of internal thermal stress. Comparing the thermal stress magnitude within different temperature ranges and cooling rates, it can be obtained that the temperature range had a more noticeable impact on thermal stress than the cooling rate.

# 4. Experimental investigation

The goal of this thesis is to evaluate the mechanical characteristics, particularly the permanent deformation and master curve analysis to determine viscoelastic behaviour of materials, of the bituminous mixture containing the fibres from discarded tennis strings, comparing it with a reference mixture without containing fibres.

The two different mixtures under our interest were created with the help of so-called mix design of bituminous mixtures in which the materials used in mixtures are analysed, including mineral aggregates, bitumen and any additional materials (additives). Based on the characteristics of the materials, design parameters are selected, such as the grain size distribution of the aggregates, and different mixtures with different bitumen contents were studied to identify the optimal bitumen content.

These two different mixtures in specimen form were tested using mechanical tests for master curve and flow number. In addition, specimens were tested in indirect tensile strength test to evaluate their resistance behaviour to cracking.

## 4.1 Experimental program

The preparation of the mixture until the testing is prescribed in the following flow chart:

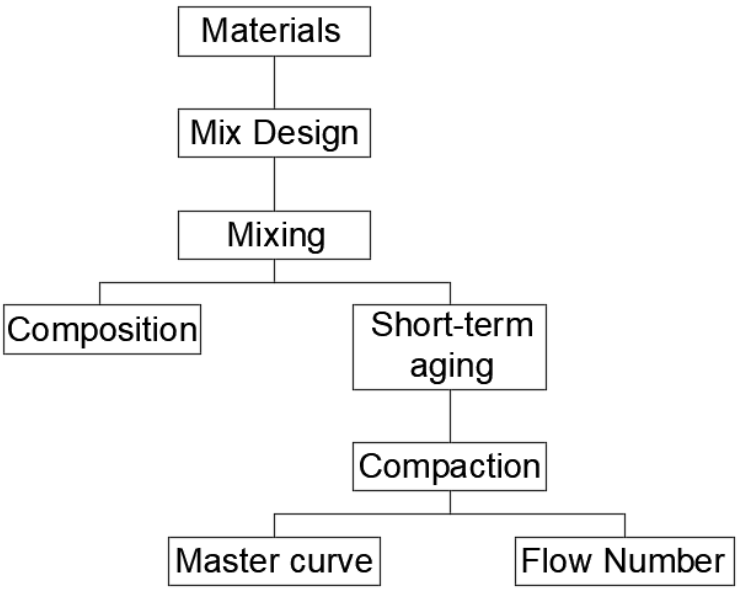


*Figure 14. Experimental method flow chart*

## 4.2 Materials

In this section the materials are described which are used in the laboratory investigation, their properties, and their usage in asphalt mixture. The initial phase of laboratory activity is selection, classification, preparation, measurement and transportation of materials for creation of asphalt mixture.

### 4.2.1 Fiber

The fibers under our studying is discarded tennis string. They are obtained by cutting in lengths less than or at 20 mm, based on the literature data.

*Figure 15. Wasted fibers with 20 mm in length*

These polymeric materials, originating from monofilament ropes, they were analysed by observing both their visual characteristics and their response to high melting temperatures conditions.

These polymeric fibers were taken and placed in a small aluminium container and put at initial temperature which is 170 °C and every one hour this temperature is increased by 15 °C. It was noticed that this polymer began to change its colour at 260°C and then melt at 275°C, with a complete melting at 280°C, afterwards it was deduced that the temperature at 275°C falls within the range of that characteristic of melting of polyester materials, with a density of 1.38 $g/c\ m3$.

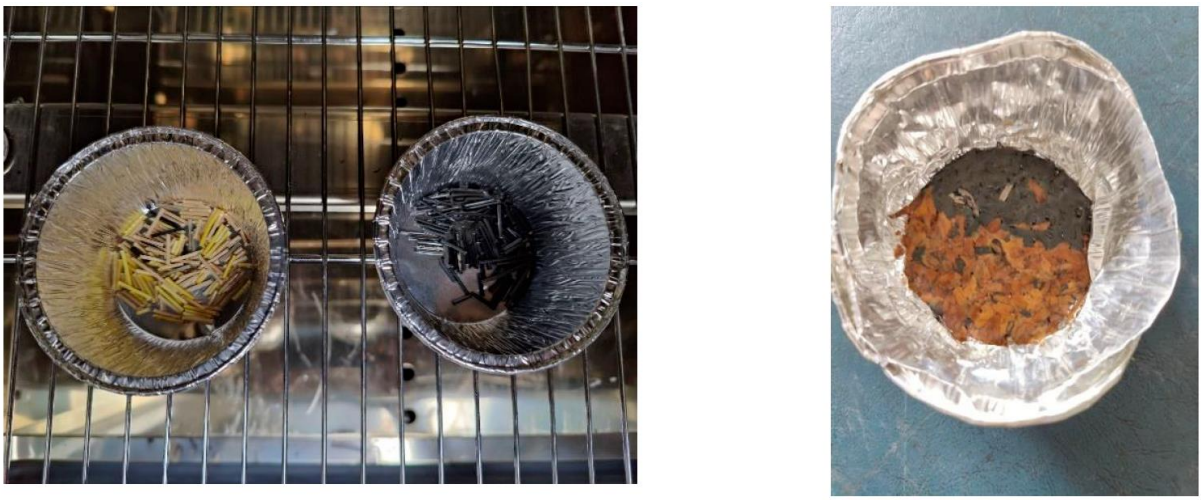

*Figure 16. Fibres in the oven before melting with colour change (left) and melted fiber (right)*

To obtain the melting point of these fibers, geometrically, the fiber lengths are variable, measuring up to 20 mm, with an average value of 10 mm, and their thickness is fixed, equal to 1.2 mm. The fibers with different colour are all discarded tennis strings, probably with similar

characteristics, as flexibility, but for considering the same behaviour of the discarded string, the black fiber was chosen to obtain mixtures.

According to the literature, recycled plastics can be integrated into asphalt mixtures using two methods: the dry process and the wet process. The key difference between these two methods lies in how the plastics are introduced into the mixture.

- **In the dry process**, the plastics are initially mixed with hot aggregates, then hot bitumen is poured. This process is considered more suitable for rigid plastics with a high melting point, such as PET.
- **In the wet process**, first fibers are added as a modifier to the hot liquid bitumen and the modified bitumen is mixed with the hot aggregates to obtain asphalt mixture. This process is more used for plastics with a low melting point, such as LDPE and HDPE.

Therefore, for this experimental observation, the fibers will be introduced into the mixture with dry process, as these fibers do not soften at the mixing temperature.

For this thesis work, at the end the length of the fibers is 5 mm is based on another research. The mechanical testing is performed using these fibers with 5mm in lengths as shown in figure below:

*Figure 17. Fibers with 5 mm in lengths*

### 4.2.2 Aggregates

Based on numerous research laboratories, a maximum aggregate size of 16 mm was chosen for the AC16 layer in the case study. Several classes of aggregates are sourced from the Brillada asphalt plant located in Borgaro Torinese (TO), Piedmont Region, Italy. These aggregates were transported to the Road Materials Laboratory at the Department of Evvironmetal, Land, and Infrastructure Engineering (DIATI) laboratory at the Politecnico di Torino.


*Figure 18. Location of Brillada asphalt plant, Borgaro Torinese (TO)*

*Figure 19. Milling process into fine aggregates*

*Figure 20. Powder*

*Figure 21. Aggregates: 5-15, 0-5, Powder.*

The selected material classes chosen and analysed are 5-15, 3-8, 0-5, “powder” and Reclaimed Asphalt Pavement (RAP), each with distinct dimensions as shown in Figure 22**.** Each of the classes has been subjected to two separate procedures for the calculation of the volumetric properties, specifically the density and the grain size distribution to identify aggregate framework, which are described in the next sections.


*Figure 22. Different aggregates.*

### 4.2.3 Preparation of the aggregates

The initial step with aggregates from the field was spreading the material for air drying for one day. Then, to obtain a representative sample of the material was followed the standard BS EN 932-2:1999 applying method B referred to quartering process, to reduce the large soil sample to an adequate size for sampling as follows:

1. Mix the material by turning over it and leaving it in a conical shape.
2. Flat the surface of the cone until it reaches a uniform thickness and diameter.
3. Divide the material into four equal parts.
4. Discard the opposite quarters and mix the other material.
5. Quarter again until the sample is reduced to the desired size.

*Figure 23. Quartering process*

### 4.2.4 Particle density

Particle density is an important characteristic used for calculating the volume occupied by aggregates in mixtures proportioned by absolute volume. It is determined as a ratio of mass to

volume where the volume is measured by water mass after a certain period of immersion, the process adheres to the guidelines specified in European standard EN 1097-6 Annex H.

To calculate the volumetric properties of the particles, the so-called pycnometer method is used which consists of the following steps:

1. **Calibration of the pycnometer**. To evaluate the density, mass and volume of the empty pycnometers must be measured. These are glass instruments consisting of a conical container and a cap with a capillary tube. First, each pycnometer is weighed empty, obtaining the empty mass of the pycnometer and then weighed after being filled with distilled, deaerated water. The water is added until a convex meniscus is created at the end of the spout of the cap (with a concavity towards the bottom). After recording the masses, the volume of the pycnometer is determined based on the volume of the it contains.

*Figure 24. Convex meniscus at the end of the tube*

2. **Preparation of the test samples.** This test is completed on two samples of the same material to obtain a representative average value. Prior to testing, the aggregates collected from the plant were dried for 12 hours in an oven at 105°C. Once dry, two samples of a defined quantity were taken depending on the maximum size of the aggregates, in accordance with the standard.
3. **Weighing of pycnometer in air.** The pycnometers are filled with test particles and weighed to obtain the total mass of the pycnometer along with the aggregates.
4. **Filling the pycnometers with distilled water and subsequent deaeration.** Distilled water is poured into the pycnometers, leaving a free surface level with 2-3 cm above the material (roughly the width of three fingers). However, due to presence of very fine particles in each aggregate class, it was waited for about 4 hours to allow the water to fully fill voids between the particles. Next, the two pycnometers containing the aggregate samples were connected to an air suction system (or deaerator), to eliminate the trapped air between the particles. This process takes at least 20 minutes, during which the pycnometers were shaken manually and gently.

*Figure 25. Vacuum system and pycnometers with distilled de-aired water.*


*Figure 26. Class 0-5 with vacuum system on the left and deaerated water on the right.*

*Figure 27. Sedimentation of particles in pycnometers with distilled water.*


*Figure 28. Aggregates in pycnometers after deaeration with vacuum system.*

5. **Weighing water.** After the deaeration process is finished, the pycnometers are filled with distilled, deaerated water up to the tip of the spout, similar in step 1. Finally, they are weighed again to measure the new mass of the pycnometer containing both aggregates and water.
6. **Calculation of the density of the particles**. With all the necessary data obtained, the density of the aggregates is determined using the following formula, as specified by the the reference standard:

$$\rho_p = \frac{M_1}{V - \frac{(M_2 - M_1 - M_0)}{\rho_w}} \qquad (4.1)$$

- $M_1$ is the mass of test specimen, in grams (g);
- $M_2$ is the mass of the pycnometer, funnel, test specimen and water, in grams (g);

- $M_0$ is the mass of the pycnometer and funnel, in grams (g);
- $\rho_w$ is the density of water at the temperature recorded when $M_2$ was determined, in megagram per cubic meter ($Mg/m^3$);
- V is the volume of the pycnometer, in millilitres (ml).

$$V = \frac{M_3}{\rho_w} \qquad (4.2)$$

- $M_3$ is the mass of water filling the pycnometer and its funnel to the graduation mark, in grams (g);
- $\rho_w$ is the density of water at the temperature, in megagrams per cubic meter ($Mg/m^3$);

As previously detailed, the average of the values obtained from the two samples under investigation is defined.

Using special formula in excel, the percentage of each aggregate by weight is calculated to achieve the desired design mix, the densities are reported in the table below:

*Table 1. The density of the aggregates*

| **Aggregate class** | $\boldsymbol{\rho_{avg}}$ **[Mg/m³]** |
|---|---|
| **5-15** | 2.824 |
| **3-8** | 2.870 |
| **0-5** | 2.763 |
| **Powder** | 2.799 |
| **RA** | 2.503 |
| **$RA_{Extracted}$** | 2.770 |

### 4.2.5 Granulometric distribution

The granulometric analysis of the aggregate framework is crucial for designing mixtures, as it provides understanding into the particle size distribution of the aggregates. This procedure involves splitting and sorting the material into various granulometric categories, organized in descending order of size, by passing it through a series of sieves with gradually smaller openings.

The EN 12697-2 and EN 933-1 standards recommend two procedures: washing and subsequent sieving. However, in this thesis, reference is also made to the granulometric ranges that must be adhered to, as defined in the *Guidelines for the Construction and Maintenance of Road Pavements* (Higher Council of Public Works, 2022). These guidelines vary based on the type of layer to be used, which, in this case, is AC16 (Binder).

*Table 2. Granulometric percentage (Higher Council of Public Works, 2022)*

| Tipologia | AC32 | AC22 | AC20 | AC16 | AC12 | AC10 | PA11 | SMA11 |
|---|---|---|---|---|---|---|---|---|
| Impiego | Base | Base | Binder[1] | Binder[2] | Usura[3] | Usura[4] | Usura | Usura |
| | Granulometria | | | | | | | |
| Setacci [mm] | Passante [%] | | | | | | | |
| 63 | 100 | | | | | | | |
| 31,5 | 90-100 | 100 | | | | | | |
| 22 | | 90-100 | 100 | | | | | |
| 20 | 69-82 | - | 90-100 | 100 | | | | |
| 16 | | 55-85 | - | 90-100 | 100 | | 100 | 100 |
| 12,5 | | - | - | - | 90-100 | 100 | | - |
| 11,2 | | - | - | - | - | - | 90-100 | 90-100 |
| 10 | | - | 56-68 | 73-80 | - | 90-100 | | - |
| 8 | 45-56 | 35-60 | - | - | 70-90 | 70-90 | 20-40 | 50-65 |
| 6,3 | | - | - | - | - | - | | - |
| 5,6 | | - | - | - | - | - | | 35-45 |
| 4 | | 25-50 | 37-48 | 45-56 | 40-55 | 40-55 | | - |
| 2 | 21-31 | 20-35 | 23-33 | 28-38 | 25-38 | 25-38 | 15-25 | 20-30 |
| 0,5 | 10-17 | 6-21 | 11-17 | 14-22 | 14-20 | 14-20 | 8-16 | - |
| 0,25 | 6-12 | 4-16 | 6-12 | 7-14 | 10-15 | 10-15 | | - |
| 0,063 | 4-7 | 4-8 | 4-7 | 4-8 | 6-10 | 6-10 | 5-8 | 8-12 |
| Contenuto di legante [%] (riferito alla massa degli aggregati) | | | | | | | | |
| | 4,0-5,3 | 4,0-5,5 | 4,2-5,8 | 4,5-6,0 | 5,0-6,5 | 5,0-6,5 | 5,0-6,0 | 6,0-7,5 |

(1) per spessori compresi tra 6 e 12 cm

(2) per spessori compresi tra 4 e 6 cm

(3) per spessori uguali o superiori a 4 cm

(4) per spessori inferiori a 4 cm

1. **Washing**. Before washing, the sample to be sieved must be weighed in air to determine the amount of filler contained within the sample. Two sieves with different mesh size are prepared, with the 2 mm sieve placed on a 0.063 mm (63 µm) sieve, then the material is placed on the upper sieve and, using running water, it is washed by hand until the water passing through the lower sieve becomes clear, to remove the filler present. Lastly, the residue is dried in the oven at 105°C for a duration of 12 hours.

*Figure 29. Preparation of aggregates and sieve for washing*

*Figure 30. Washing process*

2. **Sieving**. At room temperature, the dried aggregates are separated by means of sieves arranged one above the other forming a stack of sieves with progressively decreasing mesh from top to bottom. Once the material is poured in and the column is manually shaken for a few minutes, mechanical sieving is carried out for a minimum of 20 minutes using a sieve shaker, which thanks to vibration and tilting, facilitates the full passage of the particles. Toward the end of the procedure, each sieve is individually removed from the stack and weighed on a scale, including the lower plate holding the filler, this allows to plot the granulometric curve on a semi-logarithmic scale reporting the values of percentage of progressive passage, determined by the weight of the retained material, is shown in relation to the logarithm of the opening of the sieves.

*Figure 31. Stack of sieves on mechanical sieve shaker*

*Figure 32. Post-sieving retained*

*Figure 33. Aggregate class after granulometric analysis*

The granulometric distribution are reported in the following table:

*Table 3. Granulometric analysis of aggregate classes*

| **D** | **Passante (%)** | | | | | |
|---|---|---|---|---|---|---|
| **[mm]** | **Polvere** | **0-5** | **3-8** | **5-15** | **RA** | **$RA_{Extracted}$** |
| **20** | 100.0 | 100.0 | 100.0 | 100.0 | 100.0 | 100.0 |
| **16** | 100.0 | 100.0 | 100.0 | 100.0 | 100.0 | 100.0 |
| **12.5** | 100.0 | 100.0 | 100.0 | 95.7 | 100.0 | 100.0 |
| **10** | 100.0 | 100.0 | 100.0 | 74.5 | 99.6 | 99.8 |
| **8** | 100.0 | 100.0 | 99.7 | 47.3 | 98.8 | 99.0 |
| **4** | 99.9 | 95.1 | 55.8 | 9.3 | 75.4 | 81.3 |
| **2** | 99.7 | 72.9 | 23.8 | 4.0 | 42.9 | 58.1 |
| **0.5** | 70.9 | 32.5 | 2.7 | 1.7 | 8.4 | 27.9 |
| **0.25** | 54.1 | 17.5 | 1.9 | 1.4 | 3.9 | 19.5 |
| **0.063** | 30.4 | 5.1 | 1.5 | 1.0 | 2.0 | 11.0 |

It should be noted that during the granulometric analysis, the fine milled class after ignition was examined, resulting in the extraction of only the aggregates that constitute this material (RA_extracted).

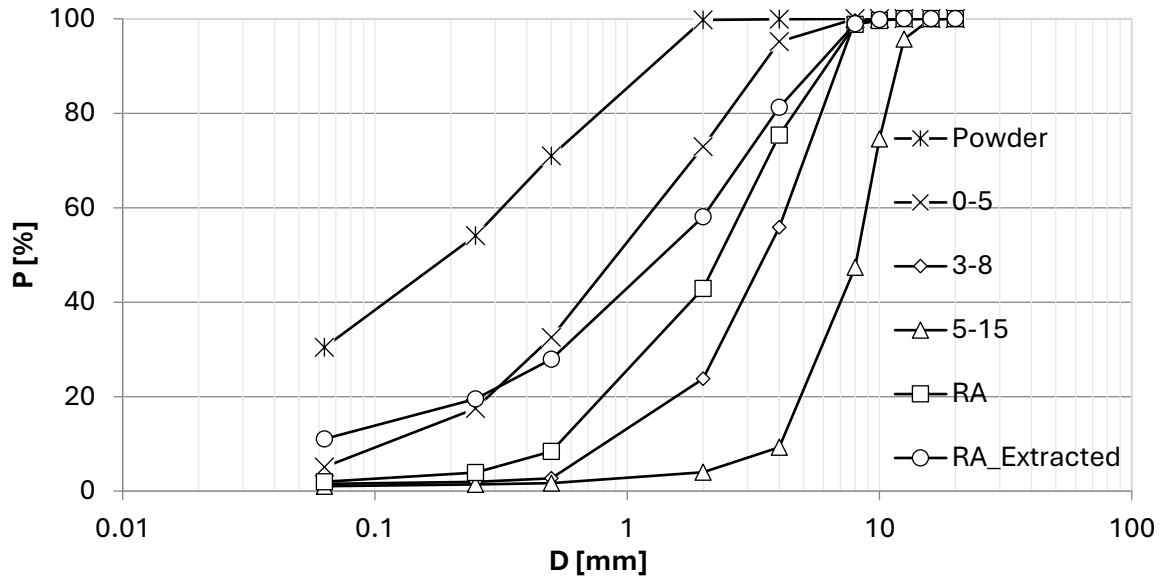


*Figure 34. Granulometry of each class of aggregates*

### 4.2.6 Bitumen

Bitumen is a viscous, dark substance obtained from the distillation of crude oil, widely used as a binding agent in road construction due to its adhesive and waterproofing properties. As an essential component in asphalt, bitumen's characteristics considerably impact the performance and endurance of paved surfaces, making it a vital material in infrastructure development.

In this particular case, 50/70 virgin bitumen from IPLOM-Busalla was used for the mix design (Sitalfa 07/22/2021).

*Figure 35. Aluminum containers containing bitumen 50/70 from IPLOM-Busalla*

The term virgin refers to bitumen that is neither recycled nor used and is obtained directly from crude oil refining; The 50/70 designation specifies the penetration range of the bitumen, indicating its consistency, i.e. the depth in tenths of a millimeter (dmm), that a standard needle

penetrates vertically into the bitumen under controlled temperature and time conditions. It evaluates the adhesion to the aggregates, guaranteeing adequate resistance to deformation and temperature variations.

A summary of the binder properties is presented in the table for reference.

*Table 4. Viscoelastic properties of bitumen 50/70 IPLOM Busalla (from Technical Data Sheet Bitumen 50/70 Iplom).*

| Prodotto | | BITUME 50-70 | | | |
|---|---|---|---|---|---|
| PROVE DI LABORATORIO | | min. | tipiche | max. | METODO |
| Penetrazione a 25°C | dmm | 50 | 62 | 70 | ASTM D 5 / UNI EN 1426 |
| Infiammabilità Cleveland | °C | 230 | >300 | | ASTM D 92 / UNI EN ISO 2592 |
| Punto Rammollimento | °C | 46,0 | 52,0 | 54,0 | ASTM D 36 / UNI EN 1427 |
| Punto Rottura Fraass | °C | | -9 | -8 | IP 80 / UNI EN 12593 |
| Volatilità a 163°C (RTFOT) | %p. | | 0,1 | 0,5 | ASTM D 2872/UNI EN 12607-1 |
| Penetrazione Residua dopo volatilità | % valore originale | 50 | 55 | | ASTM D 5 / UNI EN 1426 |
| Punto Rammollimento dopo volatilità | °C | 48 | 58 | | ASTM D 36 / UNI EN 1427 |
| Solubilità | %p. | 99 | 99,8 | | UNI EN 12592 |
| Variazione rammollimento | °C | | 6 | 11 | ASTM D 36 / UNI EN 1427 |

## 4.3 Mix design

After gathering the preliminary data of the materials, we proceeded on to the next crucial phase: the mix design of bituminous mixtures. This phase is necessary to produce the two mixtures involved, one containing the fibers from discarded tennis strings and the other without fibers, which serves as a reference or control mixture.

In the design process, the volumetric method was applied where the limits of the void values are maintained as a function of the number of gyrations of the compaction, as shown in the table below. This approach is inspired by the level 1 of the SUPERPAVE mix design, with adjustments made to the performance limits.

*Table 5. Volumetric method for mix design*

| Parametro | Normativa di riferimento | Unità di misura | Valori richiesti | | |
|---|---|---|---|---|---|
| $V_m$ a 10 rotazioni | UNI EN 12697-8 | % | 11-15 | | |
| $V_m$ a 100 rotazioni | UNI EN 12697-8 | % | 3-6 | | |
| $V_m$ a 180 rotazioni | UNI EN 12697-8 | % | ≥ 2 | | |
| | | | Base | Binder | Usura |
| Resistenza a trazione indiretta a 25°C a 100 rotazioni (*ITS*) | UNI EN 12697-23 | N/mm² | 0,95-1,65[a]<br>1,10 -1,75[b] | 0,85-1,55[a]<br>0,95-1,65[b] | 0,75-1,45[a]<br>0,85-1,55[b] |
| Coefficiente di trazione indiretta a 25°C a 100 rotazioni (*CTI*) c | - | - | ≥ 70[a]<br>≥ 80[b] | ≥ 0,70[a]<br>≥ 0,80[b] | ≥ 65[a]<br>≥ 75[b] |
| Sensibilità all'acqua (*ITSR*) | UNI EN 12697-12 | % | ≥ 80[a]<br>≥ 90[b] | ≥ 80[a]<br>≥ 90[b] | ≥ 80[a]<br>≥ 90[b] |

(a) Conglomerati prodotti con bitume normale

(b) Conglomerati prodotti con bitume modificato o polimeri di addizione

Furthermore, to attain samples capable of simulating the real behaviour during the pre-compaction phase in real construction process, the mixtures were briefly aged before compaction, following the American standard AASHTO R30-22. According to AASHTO, for aging, the materials are placed in the oven for 2 h ± 5 minutes at a temperature of 135 ± 3°C.

The proposed methodology includes phases:

1. Optimization of the aggregate framework beginning from the granulometric distribution of available aggregating pointing at getting closer to reference curve.
2. The bitumen dosage is selected at intervals of ± 0.5%.
3. Choice of fiber quantity.
4. Evaluation of volumetric properties and choice of optimal bitumen dosage.

The methods applied for mix design are described in detail below.

### 4.3.1 Preparation and hand mixing

The asphalt mixture (AC) layer implemented in the current thesis is AC16 Asphalt Concrete with maximum aggregate size of 16 mm.

With the optimal granulometric curve of the layer, materials are prepared for mixing, factoring in specific percentage of aggregate, bitumen and fibre classes. To prepare the two mixtures for the mix design, a starting point of 2.5 kg total mass of aggregates was chosen, then the available materials are proportioned with respect to the total mass of aggregates.

Afterwards, the manual mixing is performed using the appropriate mixer at the specified temperature according to the European standard EN 12697-35, using as shown in Table 6. The materials, aggregates and bitumen, are initially heated in an oven to a mixing temperature of 150°C. The bitumen remains in the oven for at least 3 hours to ensure it becomes fully liquid.

*Table 6. Reference compaction temperatures for mixtures with paving and hard paving bitumen.*

| Paving grade of bitumen | Reference compaction temperature for: °C | |
|---|---|---|
| | Mixtures of types other than mastic asphalt | Mastic asphalt mixtures |
| 10/20 to 20/30 | 180 | 230 |
| 30/45 | 175 | 220 |
| 35/50 | 165 | 210 |
| 40/60 | 155 | 200 |
| 50/70 | 150 | - |
| 70/100 | 145 | - |
| 100/150 | 140 | - |
| 160/220 | 135 | - |

The mixing procedure follows the dry method, which involves heating and drying the aggregates in an oven before being combined with hot liquid bitumen. This process eliminates

all the moisture between the aggregates, ensuring enough adhesion between the aggregates and the binder. The aggregates were first dried at 110°C in an oven for at least 12 hours.

*Figure 36. Hand mixing using heated isomantle*


*Figure 37. Mixture with different bitumen dosage*

The adopted process involves several steps:

- Aggregates are poured into the mixer at the specified temperature, starting with the coarsest grade and progressing to the finest.
- Mix for about one minute to prevent segregation and achieve the most homogeneous distribution possible.
- Optionally, add half the amount of fiber amount and mix for 30 seconds to ensure uniform distribution, as mentioned before.
- Add half the bitumen and mix for one minute to cover the aggregates as completely as possible.
- Add the remaining half of the fibres and mix for 30 seconds.
- Add the other half of bitumen and mix for one minute to accomplish a finished final mix, with a full bitumen coverage around the particles.

Once mixing is ready, the samples are placed on two plates or trays for subsequent testing.

### 4.3.2 Theoretical Maximum Density (TMD)

The first mixed sample was utilized to calculate the theoretical maximum density (TMD). This is an inherent property of the mixture, fundamental for determining the volumetric properties of the mixture. This represents the maximum density of the mixture in the absence of any voids, indicating the state of ultimate densification. From a physical point of view, it is impossible to attain this condition, for this reason this quantity is called “theoretical”.

The reference standard applied is EN 12697-5, employing with the volumetric method or pycnometer method, and with the same procedure for aggregates as outlined in paragraph 4.2.4, with changes as it is bituminous mixtures in steps 2, 4, and 6, where:

2) The materials are bituminous mixtures; therefore, samples are prepared according to the EN 12697-28 standard using quartering method. The sample, obtained from a quantity specified by the regulation depending on the maximum aggregate size, is first heated to at least 100-

110°C, ensuring it does not exceed the maximum temperature allowed by the regulation, to increase its workability. Then mixture is spread on a clean surface free of bitumen residues, where coarse particles are separated from fine particles by hand. The separated and cooled particles are then quartered, as illustrated in the figure below. The two resulting samples are poured into the pycnometers and the process proceeds to step 3, weighing in air.

*Figure 38. Spread of particles*

*Figure 39. Quartering of the mixture*

4) Since they are bituminous mixtures, the standard 4-hour waiting time is bypassed, and the mixture is deaerated using the deaerator.

*Figure 40. Deaeration process of pycnometer filler with mixture and water*

*Figure 41. Weighing pycnometer with material and deaerated water.*

6) The TMD is calculated using the formula from the EN 12697-5 standard:

$$\rho_{mv} = \frac{m_2 - m_1}{10^6 \times V_p - (m_3 - m_2)/\rho_w} \qquad (4.3)$$

Where:

- $\rho_{mv}$ is the maximum density of the bituminous mixture, as determined by the volumetric procedure, in $Mg/m^3$.
- $m_1$ is the mass of the pycnometer plus head piece and spring, in $g$.
- $m_2$ is the mass of the pycnometer plus head piece, spring and test sample, in $g$.
- $m_3$ is the mass of the pycnometer plus head piece, spring, test sample, and water or solvent, in $g$.

- $V_p$ is the volume of the pycnometer, when filled up to the reference mark, in $m^3$.
- $\rho_w$ is the density of the water, in $Mg/m^3$, equal to:

$$\rho_w = 1.00025205 + \left(\frac{7.59 \times t - 5.32 \times t^2}{10^6}\right) \qquad (4.4)$$

where t represents the water temperature in degrees Celsius (°C).

TMD is determined by calculating the average of the two subsamples.

### 4.3.3 Bitumen dosage by ignition test

Another factor related to the composition of the bituminous mixtures is the binder content that affects the mechanical characteristics of the mixture. It is possible to determine it thanks to the ignition process, considering the EN 12697-39 regulation.

This process involves completely removing the bitumen from the aggregate skeleton of the mixture inside the special oven, known as Carbolite, at a temperature of 540°C, according to the standard. The steps are:

1. **Preparation.** The Carbolite oven is preheated to the test temperature, 540°C. The sample, prepared in quantities that comply with the limits set by the regulations based on the maximum nominal size of the aggregate, is then heated to 100-110°C for proper workability.
2. **Weighing.** First, weigh the empty, oven-safe metal basket on a scale. Then after spreading the sample evenly on two levels of the basket, weigh the full basket again with the sample inside.

*Figure 42. Basket with material*


*Figure 43. Ignition oven at a 540°C temperature*

*Figure 44. Weighing full basket.*

3. **Ignition.** After obtaining the weights, the basket is placed inside the oven and the combustion process of the mixture begins with subsequent loss of mass. The process is

complete when no more weight variations are recorded, as monitored by the scale integrated into the Carbolite oven

4. **Measurement of bitumen content.** The basket containing only aggregates is cooled to room temperature and then weighed. Finally, the bitumen percentage is calculated, both in relation to the entire mixture and to the aggregates according to:

$$B_{mix} = \frac{m_{mix} - m_{agg}}{m_{mix}} \times 100 \qquad (4.5)$$

$$B_{agg} = \frac{m_{mix} - m_{agg}}{m_{agg}} \times 100 \qquad (4.6)$$

Where:

- $B_{mix}$ is the bitumen content in relation to the mixture, in %.
- $B_{agg}$ is the bitumen content relative to the aggregates, %.
- $m_{mix}$ is the mass of the mixture before ignition, in g.
- $m_{agg}$ is the mass of the post-ignition aggregate, in g.

However, the correction factor is applied to account for the presence of water in the aggregates collected from the plant (in fact these aggregates were subjected to ignition) and any potential presence of fibres was considered, so the correct bitumen content is given by:

$$B_{mix,corr} = (B_{mix} - A - F) \times 100 \qquad (4.7)$$

with A the water content of the aggregates alone, and F the fibre content in the mixture.

Therefore, the bitumen content relative to the aggregates will be:

$$B_{agg,corr} = \frac{B_{mix,corr}}{100 - B_{mix,corr}} \times 100 \qquad (4.8)$$

Granulometric distribution procedure is again done to be sure that composition for bituminous mixture is correct, it is done as explained in paragraph 4.2.5, the procedure is the same, adding the step before 1, it is written below:

**Cleaning of the aggregates after ignition**. After burning the bitumen, the mass of the aggregates before washing is known, in order to have the quantity of filler afterwards. The aggregates are removed from the basket, taking care not to lose any particles, and they are placed on a special tray before being washed.

At the end of the sieving, the granulometric curve is drawn, which is also necessary as a check with the design curve (whether they are similar or not).

*Figure 45. Cleaning aggregates from basket*

*Figure 46. washing aggregates after ignition procedure*

### 4.3.4 Gyratory compaction

To replicate the samples for simulating in the laboratory the compacting actions of the rollers in situ during the construction phase, samples are prepared using a special machine called a gyratory shear press. Developed as part of the SHRP program, replaces the traditional Marshall compaction technique and provides insights into the workability of the mix and the level of compaction, or densification, at various gyrations.

The EN 12697-31 standard describes the configuration and procedure for the gyratory technique. In this process, the bituminous mixtures are placed inside the cylindrical metal mould maintained at a constant test temperature. Compaction is achieved with two different simultaneous movements: a low static compression and the shearing action deriving from the motion of the sample (or mould) which generates a conical surface of gyration, with apex 0 and an angle of 2ϕ at the apex.

Ideally, the ends of the specimen should remain perpendicular to the axis of the conical surface.

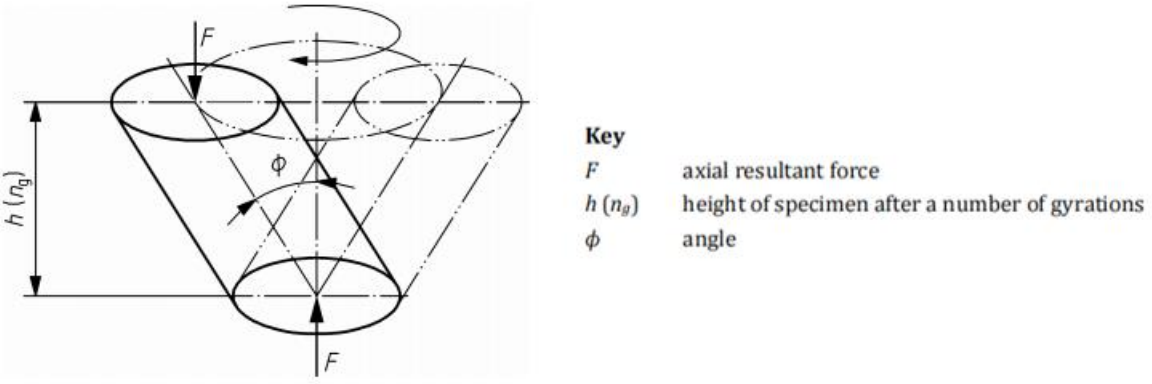


*Figure 47. Diagram of the sample's rotational movement (EN 12697-31).*

The press in the laboratory has been pre - calibrated with a constant compression force of 600 kPa, with an inclination angle of 1.25° and a rotation speed of 30 rpm. During compaction, the particles move closer together and reorganize, thanks to the combined effects of vertical compression and shear force.

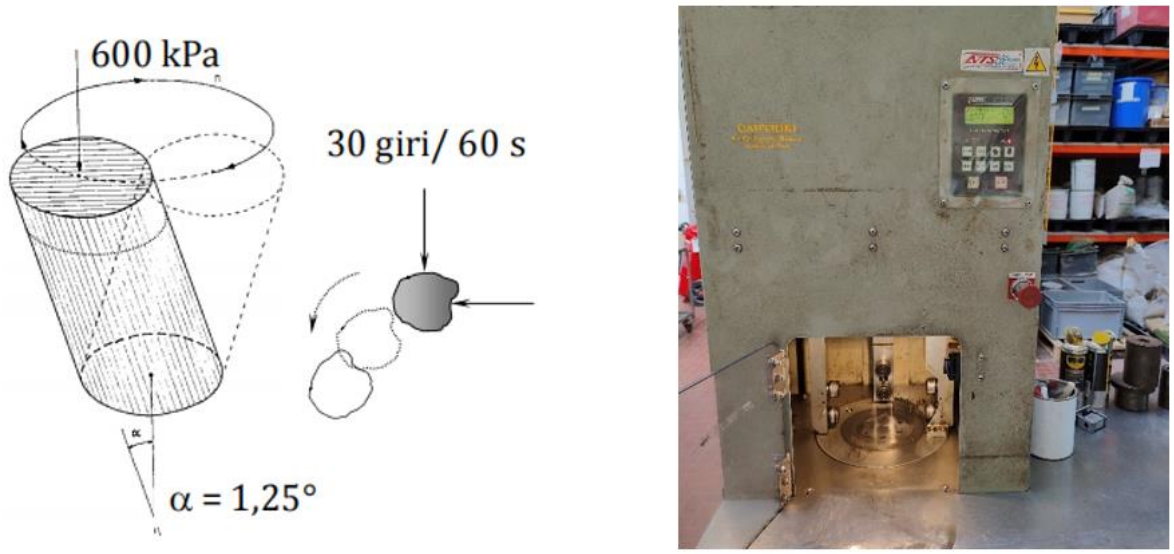


*Figure 48. Geometrical scheme of gyratory compaction (left), Gyratory compaction machine*

This machine is linked to software that records the compaction heights as the number of gyrations required to construct the workability line increases. The specimen diameter can be either 100 or 150 mm, depending on the mechanical tests to be conducted. For the mix design in this case, 100 mm specimens were chosen for the indirect tensile strength (ITS) tests, which will be explained later.

Additionally, the machine can be set based on the desired number of gyrations or height. To determine the volume, it's essential first to know the final compaction, for which the number of gyrations (180) will be considered.

The compaction process is described in detail, starting from the preparation of the test samples:

1. **Preparation of the quantity of material for the insertion into the mould**. Prior to start the actual compaction, it is crucial to determine the mass of the mixture to be inserted into the cylindrical mould. This mass is calculated through the relationship regulated by EN 12697-31 (dry mixture):

$$M = 10^{-3}\pi\frac{D^2}{4}h_{min}\rho_M \qquad (4.9)$$

Where:

- $M$ it is the mass of the mixture to be inserted into the mould, in $g$.
- $D$ is the internal diameter of the mould, in $mm$.
- $h_{min}$ is the minimum compaction height of the sample corresponding to zero void, in $mm$.
- $\rho_M$ is theoretical maximum density (TMD), obtained in 4.3.2, in $Mg/m^3$.

2. **Heating of moulds and materials.** This procedure is more time-consuming, as it requires heating the material for 2 hours in an oven at the ageing temperature of 135°C, as previously mentioned. Additionally, it involves the use of two ovens: one for short-term ageing of the samples and another for heating the mould to the target compaction temperature, 150°C. After ageing, the temperature of the material is raised to 155°C

(+20°C), which is basic for inserting it into the hot moulds with the quantity calculated from $M = 10^{-3}\pi\frac{D^2}{4}h_{min}\rho_M$ (4.9) , after placing a paper filter to separate the base of the mould from the mixture. Frequently, the temperature of the sample drops as it is being poured into the mould, so it is recommended to return the moulds into the oven until they reach the compaction temperature once more.

3. **Compaction**. Once reaching the target temperature, a second filter is added on which the steel plate that will contact the piston of the rotary press is placed. The mould is then inserted inside the machine with previous lubrication of the contact points between the disk and the piston, and the compaction is started with an initial setting of 180 rpm as input.

At the end of the test, the final sample is removed from the mould and left to cool.

*Figure 49. Pouring the material into the mould*

*Figure 50. Heating 100mm moulds in oven at 150°C.*

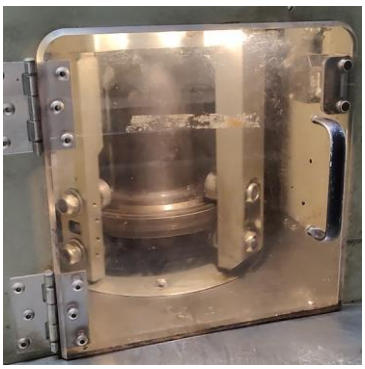

*Figure 51. Compaction process*


*Figure 52. Obtained four different Samples*

To know the final real height, measurements of the compaction height are taken at four points of the specimen, and the average of these four measurements is then calculated.

Using the data recorded by the software, compaction curves are created on a semi-logarithmic scale where the logarithms of the number of gyrations are plotted on the abscissa axis and the degree of compaction on the ordinate axis. To achieve this, it is essential to know:

- $V_x$, the geometric volume of the sample, given by:

$$V_x = \pi \frac{D^2}{4} h(n_G) \qquad (4.10)$$

  with D the diameter of the die and $h(n_G)$ the compaction height at round n.
- $C_{ux}$, the degree of compaction in which the wall effect is not considered:

$$C_{ux} = \frac{\frac{M_{eff}}{V_x}}{TMD} \cdot 100 \qquad (4.11)$$

  where $MV_{geo} = \frac{M_{eff}}{V_x}$ is the geometric density of the compacted sample, as the ratio between the effective mass of the sample and the geometric volume.
- $c$, the correction factor, as we have irregular surfaces of the cylindrical sample (therefore real volume smaller than the geometric one) and, consequently, the wall effect due to the imperfect adhesion of the sample-die is considered:

$$c = \frac{\rho_{SSD}}{M_{eff}/V_X} \qquad (4.12)$$

  with $\rho_{SSD}$ the real density, measured after compaction with the method explained in the next paragraph.
- $C_x$, the degree of compaction considering the wall effect

$$C_x = C_{ux} \cdot c \qquad (4.13)$$

The equation of the line is the following:

$$C_x(n_G) = C_1 + k\, log(n_G) \qquad (4.14)$$

Where:

- $C_x(n_G)$ it is the degree of compaction as a function of the number of gyrations, in %.
- $C_1$ is the self-compaction (intercept), that is, the degree of compaction recorded in the first gyration, in %.
- $k$ is the slope and represents the measure of workability.
- $n_G$ is the number of gyrations.

### 4.3.5 Volumetrics

The percentage of voids is a fundamental role as it affects the mechanical charactertics of the bituminous mixtures. This volumetric property is assessed based on the density of the compacted sample, according to the EN 12697-6 standard, specifically using procedure B. This methodology enables the calculation of density using a saturated sample with a dry surface (bulk density, saturated surface dry – SSD). In other words, considering the sample with a dry surface while its internal voids are entirely filled with water.

The method is quite simple:

1. Weighing in air. The sample is cooled (typically one day after compaction) to room temperature, then it is weighed on the balance.
2. Immersion and weighing in water. The sample is submerged in a water tank for at least 40 minutes, with intermittent shaking every 10 minutes, to ensure that the water fills the spaces between the particles. The sample is weighed while still in the water tank using the scale.
3. SSD Weighing. The sample is taken out of the tank, and its entire surface is dried with a damp cloth (it has not to be too wet) as fast as possible for final weighing, obtaining the mass of the saturated sample with dry surface (SSD).

At the end of the test, the temperature of the water in the tank is measured.

*Figure 53. Weighing in air m1.*

*Figure 54. Weighing in water tank, m2.*

*Figure 55. Surface drying of the sample for SSD, m3*

The bulk density $\rho_{SSD}$ (or $VM_{SSD}$) of the cylindrical sample is determined with the following formula:

$$\rho_{SSD} = \frac{m_1}{m_3 - m_2} \times \rho_w \qquad (4.15)$$

Where:

- $m_1$ is the mass of the sample in air, in $g$.
- $m_2$ is the mass of the sample in water, in $g$.
- $m_3$ is the mass of the saturated sample with dry surface, in $g$.
- $\rho_w$ is the density of water at the test temperature, in $Mg/m^3$ obtained with the same formula $\rho_w = 1.00025205 + \left(\frac{7.59 \times t - 5.32 \times t^2}{10^6}\right)$ (4.4)

Lastly, the density allows to calculate the real void content at 180 gyrations, indicative of the final compaction according to following formula:

$$v_{180} = \frac{TMD - \rho_{SSD}}{TMD} \times 100 \qquad (4.16)$$

that n turns through $C_x$, as 100's complement:

$$v_x = 100 - C_x \qquad (4.17)$$

However, changing the fiber size from 20 mm to 5mm leads to make new binder dosage, this is done according to the standard AASHTO R35-17, the change in binder dosage is determined due to volumetrics. Estimation of the binder content at 4.5 % (target void) air voids for each compacted specimen. This calculation is done in the following way:

Firstly, to determine the difference in average air void content at $N_{desgin}$ ($\Delta V_a$) of each aggregate trial blend from the target value of 4.5 % using following equation:

$$\Delta V_a = 4.5 - V_a \qquad (4.18)$$

Where:

- $V_a$ is the air void content of the aggregate trial blend $N_{desgin}$ gyrations.

Secondly, to estimate the change in binder content ($\Delta P_b$) needed to change the air void content to 4.5 % using equation below:

$$\Delta P_b = -0.4 \cdot (\Delta V_a) \qquad (4.19)$$

Afterwards, change in binder content is used for producing new specimen and volumetrics is checked. If target void percent, which is 4.5, is obtained, then the last binder dosage will be assumed for further laboratory activities.

### 4.3.6 Indirect Tensile Strength (ITS)

The cylindrical samples underwent a destructive test capable of measuring the indirect tensile strength (ITS), one of the mechanical properties of bituminous mixtures. This parameter provides information on the tensile strength and cracking behaviour of the mixtures under indirect loading conditions. It represents the maximum tensile stress derived from the peak force applied diametrically to the cylindrical sample until it fractures under certain conditions.

The test procedure is outlined in EN 12697-23, in which the specimens must be tested at the specific temperature. They are positioned in the compression machine between two metal loading plates and subjected to diametric loading along the axis of the cylinder with a constant deformation of 50 mm/min until failure occurs. The failure line at the end of the test will also be considered. Initially, the samples are stored at room temperature for 48 hours following compaction. They are then placed in a climate chamber set to the test temperature of 10°C for a minimum of 2 hours, as highlighted by the standard.

Upon completing the test, the software connected to the test equipment records the load and displacement values over time, as well as their maximum values.

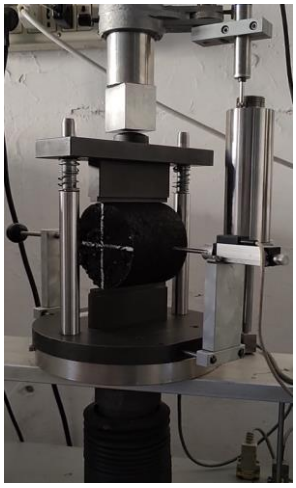

*Figure 56. Audition setup for ITS*

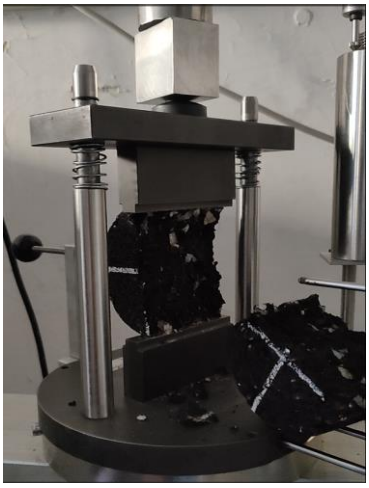

*Figure 57. ITS test specimen breakage.*

*Figure 58. Example of crack in the specimen after ITS test*

The ITS is given by:

$$ITS = \frac{2P}{\pi DH} \cdot 1000 \qquad (4.20)$$

Where:

- ITS, Indirect Tensile Strength, in $kPa$.
- $P$, is the peak load, in $N$.
- $D$, is the diameter of the sample, in $mm$.
- $H$, is the height of the sample, in $mm$.

## 4.4 Mechanical mixing and volumetric properties

With these doses obtained, we move on to mechanical mixing to obtain a greater quantity of mixtures, enough to have several samples for the next tests. Afterwards, checking its composition by volumetrics and control of binder dosage (ignition test) is completed. For mechanical mixing, in order to produce larger quantities of asphalt mixtures and perform necessary amount of compaction for mechanical testing, it was chosen to adopt 60 kg per mixture relative to the aggregates.

*Table 7. Percentage of materials for mechanical mixing*

| **Materials** | **Reference Mixture** | | **Mixture with fibers** | |
|---|---|---|---|---|
| | (kg) | (%) | (kg) | (%) |
| **5-15** | 31.8 | 53.0 | 31.8 | 53.0 |
| **0-5** | 24.0 | 40.0 | 24 | 40.0 |
| **Powder** | 4.2 | 7.0 | 4.2 | 7.0 |
| **Bitumen** | 3.06 | 5.1 | 2.94 | 4.9 |
| **Fiber** | - | - | 0.18 | 0.3 |
| **Total mass** | 63.06 | - | 63.12 | - |

### 4.4.1 Mechanical mixing

Similar to manual mixing, the materials are prepared in larger quantities.

The aggregates, fibers, and bitumen are heated in the oven at 170°C for a minimum of 3 hours. Then the machine is turned on to reach the same temperature, when it is ready for mixing, the following steps are carried out.

1. Pouring aggregates into the mechanical mixer, beginning from the coarse to the fine class grade, from 5-15 class and ending with the 0-5.
2. Mix for 30 seconds at low speed to obtain a homogeneous distribution of the aggregate skeleton.
3. Pouring 1/3 of bitumen.
4. Mix for 30 seconds at low speed to cover the bitumen aggregates as much as possible.
5. Add 1/3 of bitumen and mix slowly for 30 seconds.
6. Add 1/2 filler and mix slowly for 30 seconds.
7. Add 1/2 of fibers and mix slowly for 30 seconds.
8. Add 1/3 of bitumen and mix slowly for 30 seconds.
9. Add 1/2 filler and 1/2 fiber if needed and mix slowly for 30 seconds.
10. Mix for 3 minutes at low speed.
11. Final mixing for 1 minute at high speed.


*Figure 59. Mechanical mixer*

*Figure 60. Preparation of materials for mechanical mixing.*

*Figure 61. Mixing of aggregates only*

*Figure 62. Pouring of coarse aggregates*

*Figure 63. Pouring of virgin bitumen*

*Figure 64. Pouring of filler (powder).*

*Figure 65. Pouring of fibers*

*Figure 66. The two mixtures obtained, reference and with 0.3% Fiber*

The final mixture is placed into cardboard bags and while still hot, samples are taken and laid out on plates or trays for composition and volumetric analysis.

### 4.4.2 Composition

The measurements for bitumen percentage and granulometric curve are repeated as a control measure, the TMD is needed to evaluate the mass required for the compaction of cylindrical samples. These procedures are executed in order to check that the large mixture meets the design specifications.

The procedures are the same as explained in paragraphs 4.3.2, 4.3.3.

Upon completing big mixing, the granulometry and bitumen content are checked to ensure if they fall within the specified design range. The TMD is also measured for next stage of compaction. All these results are presented below:

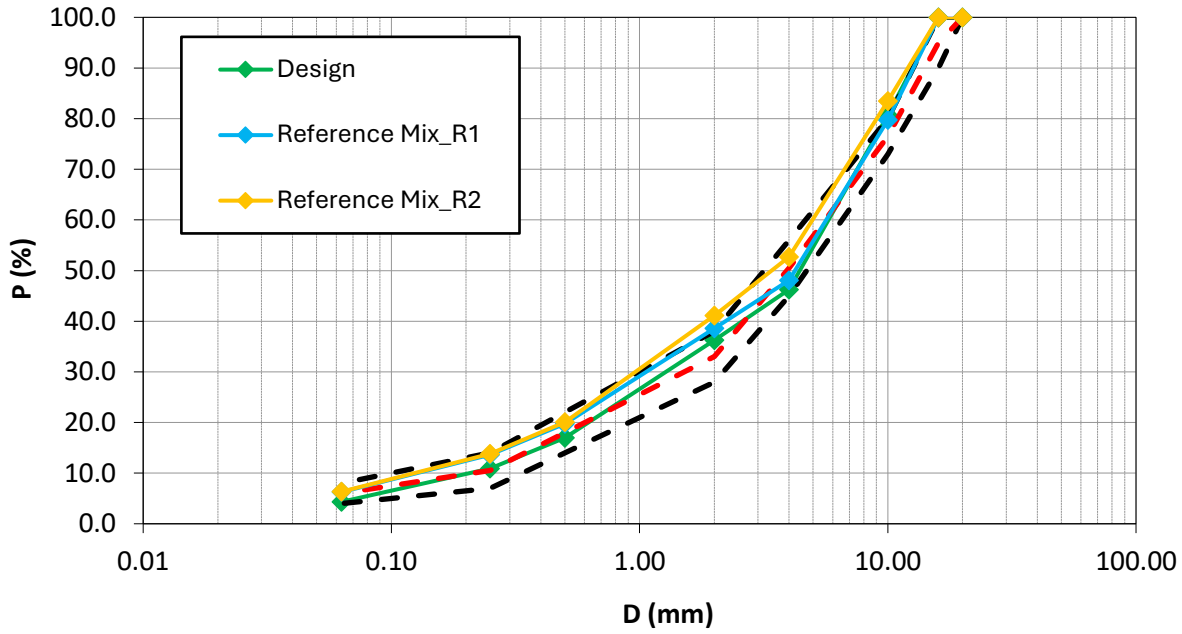


*Figure 67. Granulometric analysis of mechanical mixing (Reference mixtures)*

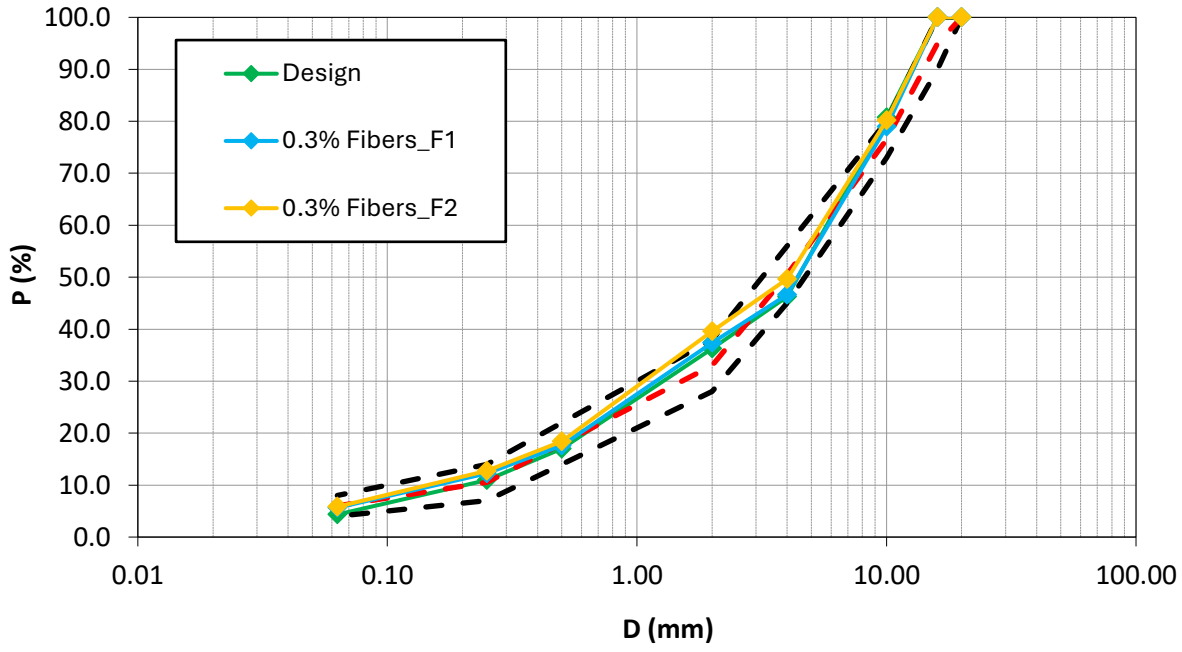


*Figure 68. Granulometric analysis of mechanical mixing (Mixtures with fibers)*

The mixtures show a deviation from the red line, which is average of design threshold. This occurred due to some inhomogeneity in the aggregate collection for mechanical mixing, as most of the aggregates were taken from the lower part of the container.

The bitumen contents of mixtures and their TMD were obtained by ignition procedure.

*Table 8. Composition of reference and mixture with 0.3% fibers*

| Mixtures | $B_{mixture}$ | $B_{aggregate}$ | TMD |
|---|---|---|---|
| | % | % | $Mg/m^3$ |
| **Reference** | 4.72 | 4.95 | 2.536 |
| **0.5% Fibers** | 4.40 | 4.61 | 2.537 |

The TMD of both mixtures is almost the same, fiber content is eliminated in bitumen content calculation of mixture with fibers due to the presence of fibres that have not been melted and therefore act as aggregates. Even though both mixes have a lower bitumen content, they are within the acceptable range referred to the AC16 binder layer in Table 2.

### 4.4.3 Compaction and volumetric properties

The samples made using a gyratory compaction press, they are cylindrical in shape, with a diameter of 100 mm, for the calculation of volume and workability, remembering however to age the material for 2 hours in an oven at 135°C, before compaction.

At the end of the compaction, with the same methodology as in paragraph 4.3.2, the volumetric properties and the void content are determined, as underlined in 4.3.5.

Initially, two cylindrical samples were prepared for each mixture to study the percentage of voids, calculated as an average. In order to obtain a certain number of samples for mechanical tests, it was decided to compact the two materials aiming for a target void percentage of 4.5%. The obtained result showed that void percentage of 0.3% fibers mixture is 4.3%, which is close to target void. However, despite efforts to achieve a uniform mixture, the achieved void percentage of reference mixture is low, which is equal to 3.5%, it is due to improper collection of aggregates and errors in pouring the bitumen to mechanical mixer. Nevertheless, during the compaction of the samples for mechanical testing, it is tried to solve this issue and at the end achieved void content is near to the target void, as shown in Table 21.

## 4.5 Mechanical testing

The aim of the current thesis is to evaluate the rutting behavior and the viscoelastic properties of the mixture. For this purpose, the following mechanical tests are carried out:

- Master Curve (Dynamic Modulus)
- Flow number (Permanent deformation)

Before starting the mechanical testing, required samples are obtained, it is explained in the following subsection.

### 4.5.1 Preparation of the sample for mechanical testing

In this section, the preparation of specific sample for further testing will be completed. Initially, compaction of samples with 150 mm in diameter and 180 mm in height will be created. Then coring and cutting are performed to achieve desired size of the sample.

According to the standard AASHTO R 84 (Master Curve by AMPT), the creation of samples with diameter 100 mm and a height of 150 mm is required. The same sample size is used for flow number test as well after the dynamic modulus test, as this test is non-destructive one. These procedures will be explained in the following steps:

1. **Gyratory compaction**. One of the main problems of compaction in the laboratory is related to the wall effect and the inhomogeneity of voids between the two extremes, upper and lower parts of the sample. Both are due to the compaction method, therefore linked to the gyratory shear press. To solve this problem, the sample size with bigger in dimension is produced than the actual size provided by standard. Its size is 150 mm in diameter and 180 mm in height, as shown in **Error! Reference source not found.**. T he mass to be inserted inside the mould is obtained as following:

$$M_{trial} = 10^{-3} \cdot \pi \cdot 180 \cdot 75^2 \cdot TMD \cdot \left(1 - \frac{(4.5\% + \Delta v\%)}{100}\right) \qquad (4.21)$$

Where:

- $\Delta v\%$ is the difference between the bulk void and real void of the cored sample.

*Figure 69. Compacted samples for dynamic modulus*

2. **Core drilling and cutting of the bases.** Afterwards obtaining the big samples. The next step is to create sample with size of diameter 100mm to height 150 mm. To produce such a sample, the core drill machine and cutting machines are used. The first is used to reduce the diameter from 150 mm to 100 mm. It is equipped with a support on which the sample is placed, with the base of the compacted sample facing downwards, and the core drill itself equipped with a diamond blade. The core drill is set in motion and by rotating and lowering manually at a constant speed using a crank, while pouring water inside of core drill to reduce friction created by metal core and sample. Subsequently, a sample of 100 mm in diameter and 180 mm in height is created. The internal diameter measured is approximately 94 mm.

*Figure 70. Coring process*

*Figure 71. Cutting the two sides of the sample in sawing machine*

Once this has been done, the bases are cut using a cutter, a circular saw with a diamond blade. Once the sample is positioned in the test configuration, the machine consisting of the rotating blade placed at the level of the cut and cutting is started. Also in this case, the water is poured by system of cutting machine to reduce heat generated due to friction between saw and material, also to eliminate dust coming from sample. The cuts made on the two bases have different depths, this is to consider the lower compaction of the sample head. Therefore, a 35 mm cut is made at the upper end and a 15 mm cut at the lower end.

3. **Volumetrics.** The next step is to verify the target void content. If this is not respected, it will be necessary to proceed with the processing of a new quantity of mass to be inserted into the mould with subsequent compaction, coring and cutting. The cored samples are placed in the climatic chamber at 35 °C for 3 days until all the water evaporates, after 3 days the mass variability is checked in the following way: when, after at least two hours, the weight varies by only 1%, then it is considered completely dry.

4. **Attaching the special clamps to the samples.** The final manual step involves gluing of the cubes that will hold the clamps, which in turn the transducers (LVDT) for measuring axial deformation will be mounted. A system with three adjustable arms is employed for gluing: a bar is mounted on these arms, onto which the cubes are screwed, spaced vertically at 75 mm from each other. The sample is positioned at the center of the three arms, by applying the epoxy glue (two-component adhesive made by combining glue and hardener, with ultra-fast bonding) and activating the compressed air system, the ultimate result will be achieved. After that, it will be sufficient disassembling the system, so that only the cubes remain attached to the sample.

*Figure 72. Device to attach the clamps*

*Figure 73. Attaching the clamps on samples.*

### 4.5.2 Dynamic modulus

A dynamic modulus master curve is a graphical representation used to describe the viscoelastic behaviour of materials, primarily polymers and asphalt mixtures, over a wide range of temperatures and loading frequencies. This curve is constructed using the principle of time-temperature superposition, which allows data collected at various temperatures to be shifted along the time or frequency axis to form a single, smooth curve.

The master curve typically includes parameters such as the dynamic modulus (which measures the material's stiffness) and the phase angle (which reveals the lag between applied stress and resulting strain). These parameters help in understanding the material's relaxation characteristics and overall dynamic properties, furthermore master curve is used for characterizing asphalt concrete for pavement thickness design and performance analysis.

In this context, this refers to the dynamic modulus, defined as the norm of the complex modulus E*. As mentioned earlier, bituminous mixtures exhibit a linear viscoelastic behaviour that varies with temperature. For this reason, the complex modulus consists of two components: the real component E1, which represents the elastic properties of the material, and the component E2, which instead summarizes its viscous characteristics. The value of E* is given as:

$$E^* = \sqrt{E_1^2 + E_2^2} \qquad (4.22)$$

The dynamic modulus increases as temperature decreases and increasing loading frequency, showing an elastic behaviour of the mixture. Conversely, as temperature rises and the loading frequency decreases, the complex modulus decreases, reflecting the material's viscous behaviour. In the process of determining of the dynamic modulus, the samples are subjected to a controlled sinusoidal uniaxial compressive stress, at many frequencies. The mixtures were assessed at 4°C, 20°C and 40°C. The applied stress is combined with the measured axial strain,

as a function of time, to calculate both the dynamic modulus and the phase angle. This test can be performed under confined or unconfined pressure conditions.

## Running the test

The test is performed in the unconfined regime with the same machine used for the definition of the stiffness in the indirect traction configuration and cylindrical sample, i.e. AMPT, in accordance with standard AASHTO R 84 (Master Curve by AMPT). The test follows these steps:

1. Sample is prepared by gluing the LVDT transducers, the sample is positioned between two cylindrical supports, so that it is not in direct contact with the actuator during the test.

*Figure 74. Dynamic modulus test: LVDT*

After that, the system is positioned inside the AMPT climatic chamber (which is at the sample conditioning temperature) at the centre of the crosspiece and with the upper cylindrical support exactly vertical to the actuator. The latex is put bottom and upper parts of the sample, technical oil is put between the two latexes. So, this will prevent extra friction between the sample and support. Ensuring good application loading.

2. Software settings

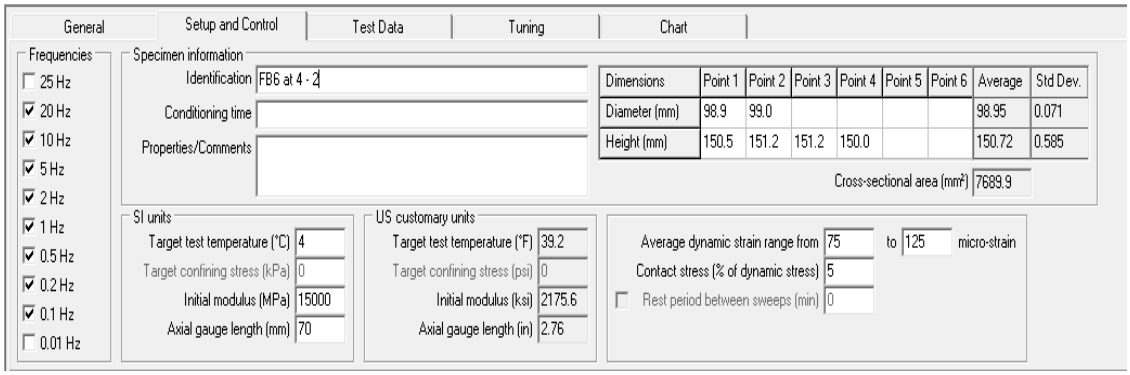


*Figure 75. Settings of dynamic modulus at 4 °C*

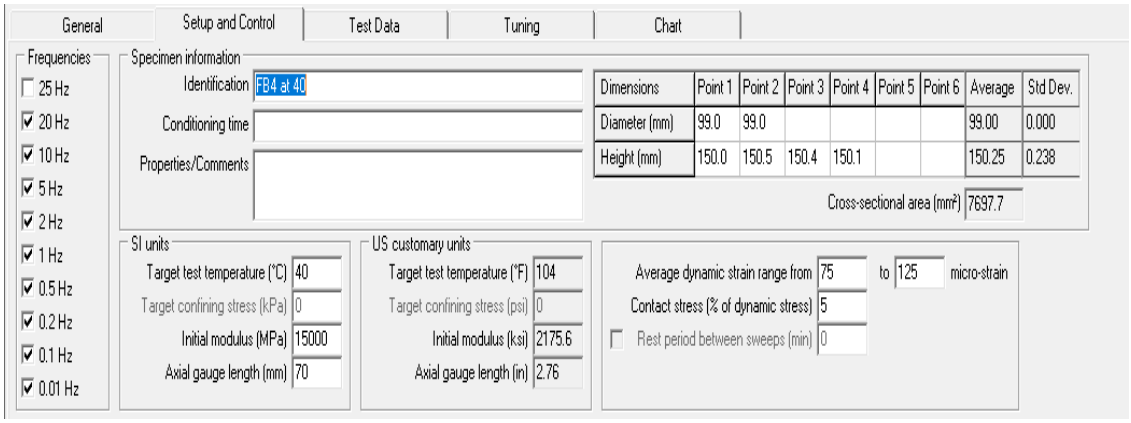


*Figure 76. Settings of dynamic modulus at 40 °C*

Figure 75 shows some of the main settings to be inserted into the software. In general, the dimensions of each individual sample must be inserted in terms of height and diameter, but also the test temperature and the frequencies at which to test the sample. These are defined by the regulations and in the case in question are the following table:

*Table 9. Frequencies at different temperatures*

| **Temperature, °C** | **Frequancy, Hz** | **Temperature, °C** | **Frequancy, Hz** | **Temperature, °C** | **Frequancy, Hz** |
|---|---|---|---|---|---|
| 4 °C | 20 | 20 °C | 20 | 40 °C | 20 |
| | 10 | | 10 | | 10 |
| | 5 | | 5 | | 5 |
| | 2 | | 2 | | 2 |
| | 1 | | 1 | | 1 |
| | 0.5 | | 0.5 | | 0.5 |
| | 0.2 | | 0.2 | | 0.2 |
| | 0.1 | | 0.1 | | 0.1 |
| | - | | - | | 0.01 |

3. Test execution

   At this stage, the test is initiated by pressing the start button in the software. The actuator applies a sinusoidal compression load at different frequencies as shown in Table 9, from the highest to the lowest one and for each frequency there are ten load cycles. Prior to applying the load and at each frequency, the machine performs ten calibration pulses, to ensure that a certain deformation remain within threshold between 75 and 125 micro strains. The test is carried out without confining pressure and is non-destructive: in fact, the applied load is such that the samples have a visco-elastic behaviour. Further, the samples will be used in flow number test.

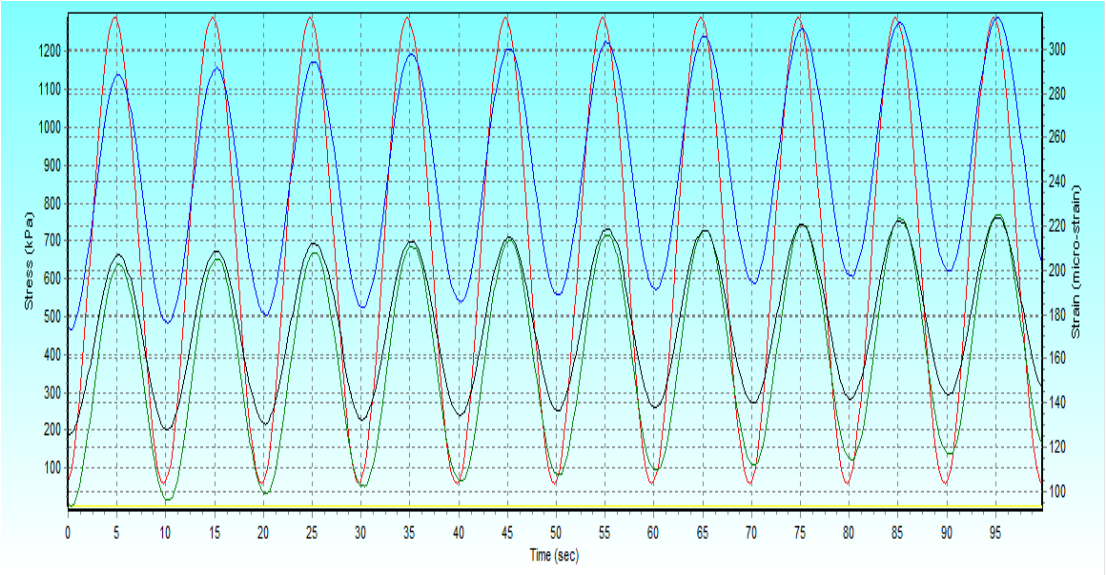


*Figure 77. Graph of dynamic modulus*

During the test, the software calculates in real time the dynamic modulus and the phase angle for each load frequency. As a control method during the test, it is confirmed that the modulus value decreases with the frequency decreasing, while the phase angle increases. Two other controls are the load standard error, which must not exceed 10%, and the sinusoidal curves generated on the screen, which must be continuous and smooth, it indicates that the transducers are not accurately measuring deformations, likely due to improper mounting on the supports.

After obtaining the dynamic modulus values at different frequencies and temperatures, it is appropriate to represent them in a graph, known as a master curve. Its construction uses the principle of time-temperature equivalence, which links the frequency and time of loading to the response of the sample. As mentioned earlier, the stiffness of the bituminous mixtures depends on these parameters. Specifically, as the temperature rises and the frequency decreases, the modulus decreases, and the mixture behaves more viscously. Conversely, as the temperature drops and the frequency increases, the dynamic modulus rises, leading to rigid behaviour of the mixture.

Commonly, the reference temperature for the master curves is set at 20°C, which was also used in the thesis under review. For the modelling process, reference is made to the AASHTO R 84 standard, which in turn refers to the modelling approach outlined in the Mechanistic Empirical Pavement Design Guide (MEPDG). These guidelines enable to obtain the master curve using a sigmoidal model, evaluating the moduli as a function of a reduced frequency, defined as the frequency referred to the reference temperature equivalent to the actual load frequency of the test for a certain temperature.

## Data analysis

$$log|E^*| = \delta + \frac{(Max - \delta)}{1 + e^{\beta + \gamma log f_r}} \qquad (4.23)$$

Where:

- |E*| is the dynamic modulus.
- Max is the logarithm of the value of the glass asymptote |E*|max.
- γ is a parameter that represents the slope of the curve at its inflection point.
- β is a parameter that represents the reduced frequency value for the inflection point of the curve.
- δ is the intercept of the curve with the y-axis.

$$log f_r = log f + \frac{\Delta E_a}{19.14714}\left(\frac{1}{T} - \frac{1}{T_r}\right) \qquad (4.24)$$

Where:

- $\Delta E_a$ is the activation energy (treated as a fitting parameter).
- $f_r$ is the reduced frequency at the reference temperature, Hz.
- $f$ is the loading frequency at the test temperature, Hz.
- $T$ is the test temperature, °K.
- $T_r$ is the reference temperature, °K.

$$log[a(T)] = \frac{\Delta E_a}{19.14714}\left(\frac{1}{T} - \frac{1}{T_r}\right) \qquad (4.25)$$

Where:

- $a(T)$ is the shift factor at temperature $T$.
  *other parameters are given above.*

The model parameters were calculated through numerical optimization using Excel's solver, it uses the principle of least squares. This approach recognizes the combination that minimizes the sum of squared differences between the test results of the dynamic modulus and the values predicted by the sigmoidal function. In this analysis, it was considered applicable to evaluate and define the upper horizontal asymptote as a model parameter and subsequently determined using the solver. Alternatively, the Hirsch model could be employed, which calculates the value of |E*|max with a relationship involving VMA and VFA. Finally, the master curve can be plotted.

### 4.5.3 Flow number

Rutting is one of the key phenomena in structural degradation, where grooves appear on the surface of the pavement and gradually worsen due to the continuous passage of vehicles. The grooves are generated from the buildup of permanent deformations, as the bituminous mixtures is a material with viscoelastic behaviour influenced by temperature. This effect becomes significant when temperatures rise to higher levels.

For the evaluation of permanent deformations was based on a uniaxial cyclic compression test, called flow number test, from which a parameter called flow number is obtained. This test, which is destructive as it leads to the sample's failure, the cumulative permanent deformations are evaluated as a function of the load cycles and, at the same time, the deformation rate as shown in Figure 10

The load applied is uniaxial, repeated in a load cycle with 0.1 seconds of loading followed by 0.9 seconds of unloading at a frequency of 1 Hz. This setup allows to evaluate the cumulative permanent deformations while simultaneously allowing to observe the results on a graph. The outcomes display a behaviour categorized by three distinct regions:

- Initially, the deformation rate decreases rapidly with the increasing number of cycles (region 1).
- This phase is followed by a period, with a highly variable number of cycles, where the deformation rate remains nearly constant (region 2).
- The final phase is characterized by an increasing deformation rate, leading the material to rapidly reach failure (region 3).

The flow number represents the number of cycles that defines the transition zone between secondary and tertiary creep and is determined by locating the minimum point of the strain rate.

The test was conducted on the samples used for the determination of the dynamic modulus and construction of the master curves, with the only precaution of removing the transducer holder nuts previously attached. The test is carried out in the same machine used for master curve, in accordance with the standard AASHTO T378 (E and Flow Number by AMPT). The steps of the test are following:

1. Sample preparation
   In this test, the sample configuration is straightforward, because it is enough to place it in the center of the upper and lower containment plates, separated by lattice disks. So that the actuator is in the center of the upper plate. The samples were conditioned at a temperature of 58°C for 12 hours. The cell reaches 58°C within 20 minutes.

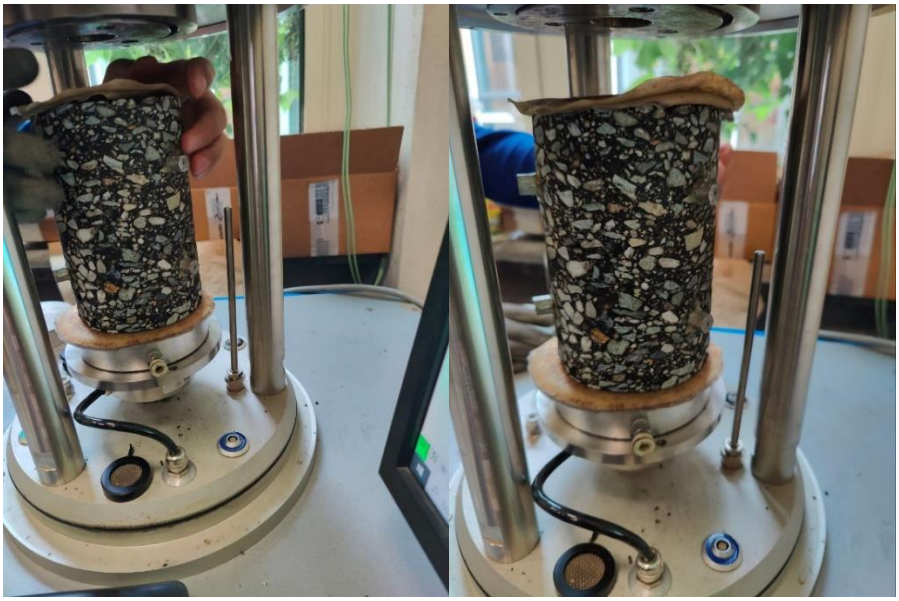

*Figure 78. Preparing the sample for testing*

2. Parameter setting

   The test is conducted using a software within which it is necessary to set a series of parameters defined by the AASHTO T 378-17 standard:

- Specimen size in terms of height and diameter at four points.
- Test temperature of 58°C.
- Repeated axial stress intensity of 600 kPa.
- Contact stress equal to 5% of the axial stress equal to 30 kPa.
- Maximum allowable permanent axial deformation of 100000 micro strain.
- Maximum allowable number of load cycles equal to 20000

3. Test execution
   After setting all the parameters, the test is initiated. Since the test is a destructive type and for this reason, upon completion, a reduction in height with a lateral bulging is typically observed. If the sample does not decrease in height but only bulges, then the failure is not attributed to permanent deformations.

*Figure 79. Flow number test under execution*

The flow number value can be determined from the increment of permanent deformation using the Francken model, which is defined by the coupling of a power law and an exponential function:

$$\varepsilon_p = A \cdot n^B + C \cdot (e^{D \cdot n} - 1) \qquad (4.26)$$

Where:

- $\varepsilon_p$ is the permanent axial deformation.
- n is the number of load cycles.
- A, B, C, D of the control parameters.

The flow number is calculated by imposing the second derivative to the Francken model to zero, after determining the control parameters through a numerical optimization process.

# 5. Results

The primary aim of this research was to analyse the effect of fibers to mixture performance. Experimental results are reported and analysed, from the tests carried out on the mixture in question, comparing it with the control one. The samples are labelled as “R” for reference mixture and “F” for mixtures containing fibers, with a fiber content of 0.3%. The results are presented in order, beginning with the aggregates and concluding with the mechanical testing.

## 5.1 Mix design

Mix design in pavement construction is a fundamental process aimed at identifying the optimal combination of materials to ensure that the pavement can withstand the loads and environmental conditions it will face over its lifespan. The outcome of this analysis is provided below.

### 5.1.1 Optimization AC16

The reference line, which is red line, is average of threshold from the standard, as shown in Table 2. Optimization is achieved by utilizing sieve analysis results for each available aggregate. The formula is applied to ensure that the design percentage for each sieve remains within the target gradation range. Obtained optimal percentage of aggregates for optimization is shown in Table 11.

*Table 10. Granulometric distribution of Optimization AC16*

| **D** | **Passante [%]** | | | |
|---|---|---|---|---|
| **[mm]** | **Powder** | **0-5** | **5-15** | **Design** |
| **20** | 100.0 | 100.0 | 100.0 | 100.0 |
| **16** | 100.0 | 100.0 | 99.7 | 99.8 |
| **10** | 100.0 | 100.0 | 61.3 | 79.2 |
| **4** | 99.7 | 92.7 | 6.2 | 46.7 |
| **2** | 99.3 | 70.8 | 3.9 | 36.7 |
| **0.5** | 71.9 | 28.1 | 1.9 | 16.9 |
| **0.25** | 52.8 | 16.3 | 1.5 | 10.8 |
| **0.063** | 26.5 | 4.6 | 1.0 | 4.1 |

*Table 11. Percentage of aggregates in the mixture*

| **Aggregate class** | **%** |
|---|---|
| **5-15** | 5.0 |
| **0-5** | 39.0 |
| **powder** | 56.0 |

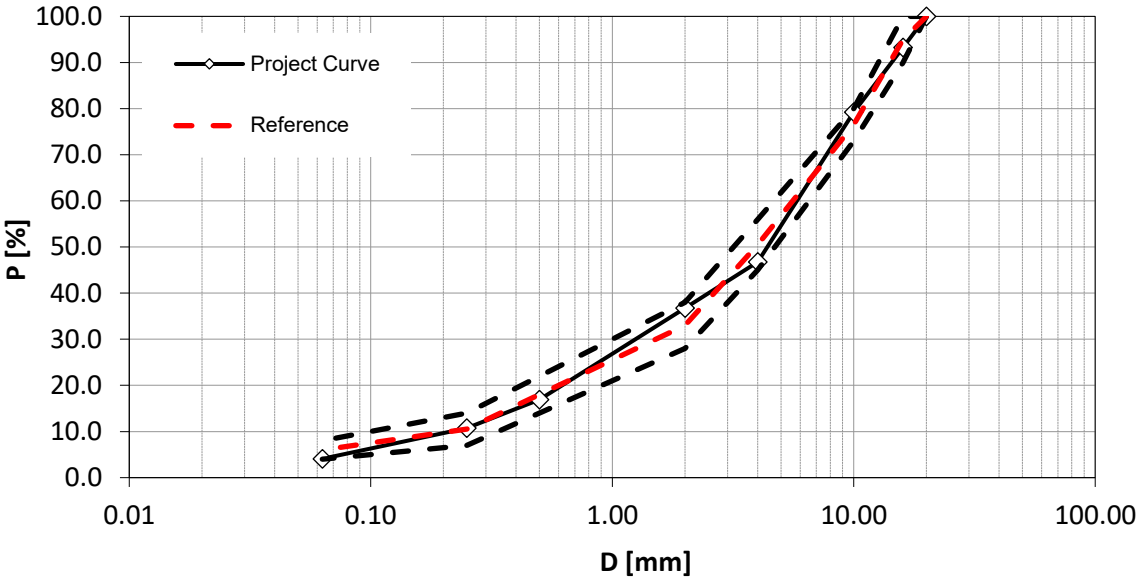


*Figure 80. The Optimization of layer AC16*

### 5.1.2 Bitumen content

During the mix design process, manual mixing was performed using certain quantities of aggregates. Four mixtures were created with different fiber content relative to the mass of the aggregates, 1.0%, 0.5% and 0.3%, and one mixture without fibers, as a reference. Each asphalt mixture has different bitumen dosage ranging from 4.5% to 6.0%, with increment of 0.5%.

The mixtures were compacted at 180 gyrations to analyse the volumetric properties, obtaining cylindrical samples with a minimum height of 70 mm and a diameter of 100 mm, following the volumetric method of mix design (as shown in Table 5). Specifically, the results of the void content at 100 gyrations are presented, while the data for 10 and 180 gyrations will be included in the appendices.

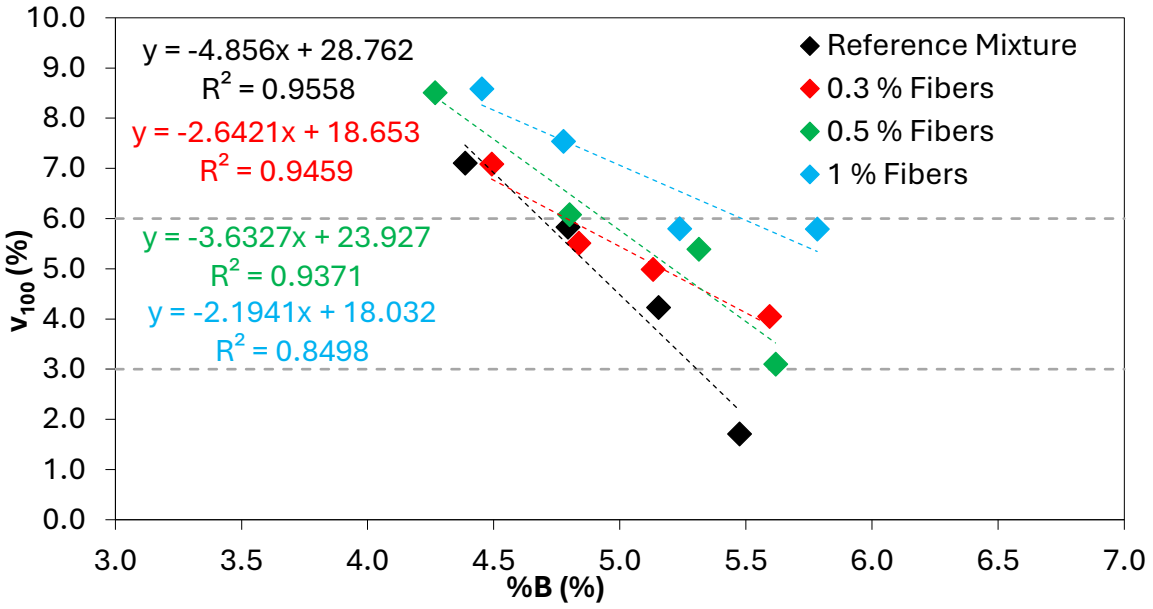


*Figure 81. Void content at 100 gyrations in mix design*

A certain degree of inhomogeneity of the mixtures with fibres can be observed, due to the difficulty of manual mixing. Additionally, during the compaction phase, the material may have reached a point where further compaction was no longer possible.

The experimental results from the ITS test are also summarized below:

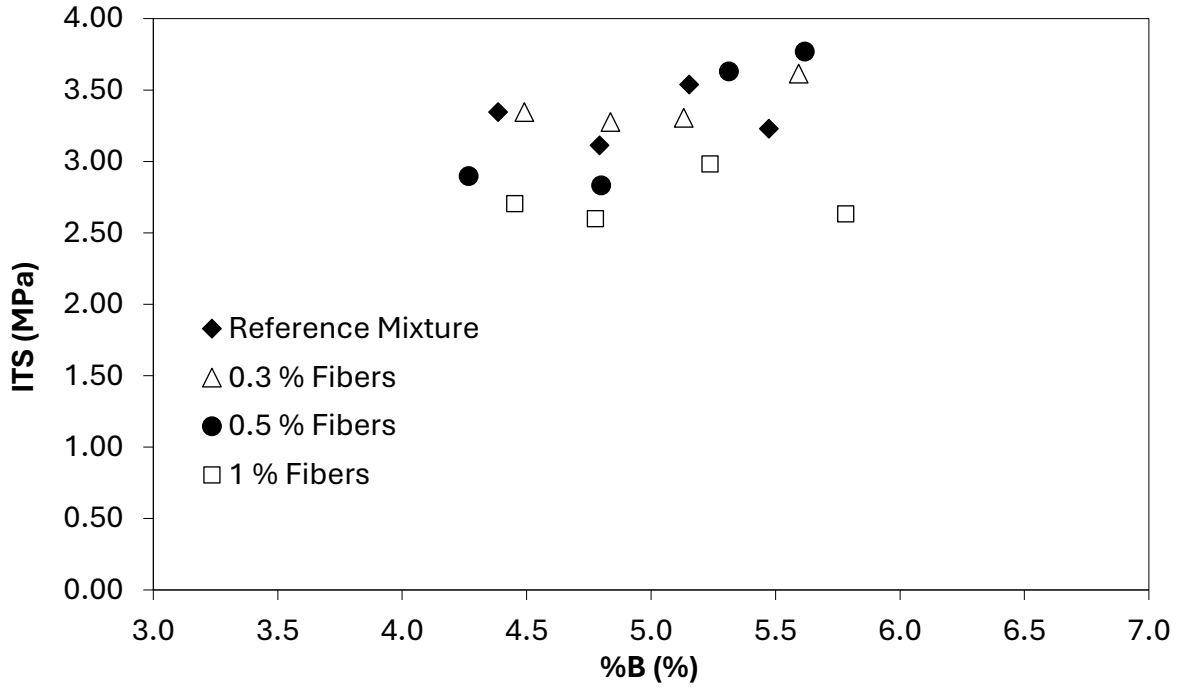


*Figure 82. ITS values at 10°C of different mixtures.*

The optimum bitumen content corresponding to the average value of the void content limits at 100 turns, i.e. 4.5%, will be taken:

*Table 12. Dosage of optimum bitumen content*

| Mixture | %B |
|---|---|
| **Reference mixture** | 5.0 |
| **1% Fibers** | 6.2 |
| **0.5% fibers** | 5.3 |
| **0.3% fibers** | 5.4 |

After compaction, an extension in height of the cylindrical sample containing fibres was observed, also with an insignificant expansion in diameter. As the fibre content increased during compaction, the material could no longer compress further despite the increase in binder dosage. Consequently, the mixture with 1% fibers was excluded. Among the other two contents for fibers with 20 mm length, 0.5% was selected with respect to the aggregates to maximize the dose of the fibers. Therefore, this corresponds to 5.3% of optimal bitumen content for mixture with fibers, while for the reference mixture, 5.0% will be adopted.

Following this analysis, it was decided to use 5mm of fibers instead of 20 mm, due to this change, initial binder content is assumend to be as just above described. To verify these binder content with 5mm of fibers, a new analysis is performed, aiming to maintain a target void content of 4.5% using fibers of 5 mm in lengths. The analysis revealed a binder content of 4.9% for mixtures containing 0.3% of fibers and 5.1% for reference mixtures. This new calculation is outlined at the end of the paragraph 4.3.5.

## 5.2 Mechanical test

### 5.2.1 Dynamic modulus

To assess the thermo-visco-elastic behaviour of the mixtures under study, reference is made to the dynamic modulus. Fundamentally, each specimen undergoes a uniaxial load applied at varying frequencies and conditioning temperature, as indicated in Table 9, to replicate the vehicular load effect and the climate conditions that the pavement experiences on-site conditions.

The AMPT was used to record deformation values with three transducers after applying the load, determining the complex modulus (E*) and phase angle. Using E* values across various temperatures and frequencies, a master curve is created. Shift factors, calculated using formula $log[a(T)] = \frac{\Delta E_a}{19.14714}\left(\frac{1}{T} - \frac{1}{T_r}\right)$ (4.25), adjust the real frequency range to a reduced frequency range at a reference temperature of 20°C. This results in a single curve combining data from three experimental curves, aligning dynamic modulus values to the reference temperature.

Initially, three separate curves are obtained, each showing different modulus values at different temperatures for the same frequencies. Modulus values at high temperatures are shifted left, and those at low temperatures are shifted right relative to the reference temperature, as shown in Figure 83 and Figure 84.

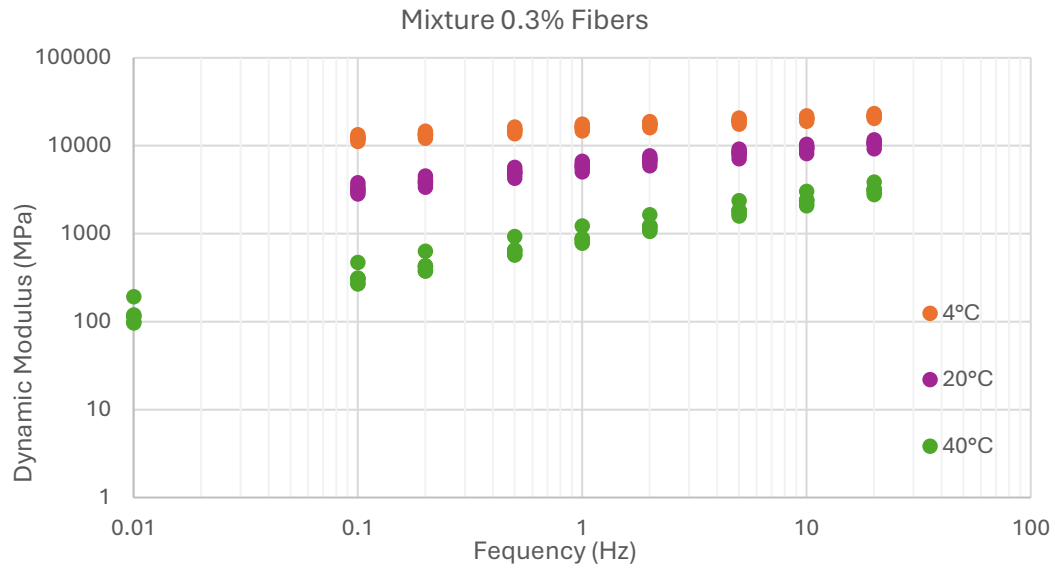


*Figure 83. Master curve before applying shift factor (Raw data)*

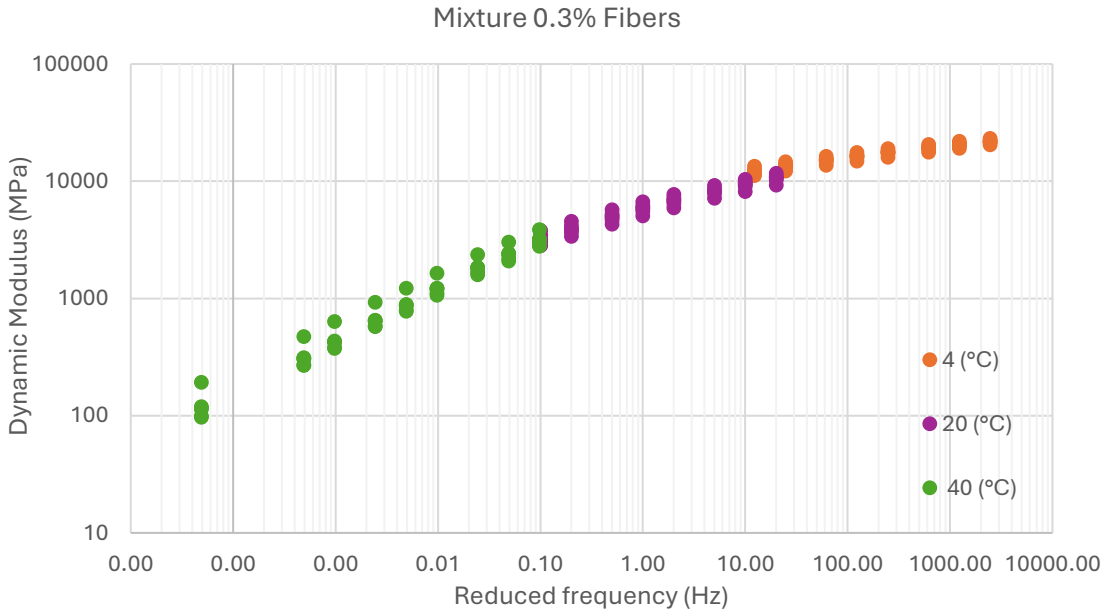


*Figure 84. Master curve after applying shift factor*

The raw experimentally obtained data were modelled according to MEPDG guidelines, with some modifications, resulting in a sigmoid curve. The recommended values for master curve calculation are assumed as follows: δ = 0.5, β = -1.0, γ = -0.5, and $\Delta E_a$ = 200 000. Initially, using these recommended parameters and formula $log|E^*| = \delta + \frac{(Max-\delta)}{1+e^{\beta+\gamma log fr}}$ (4.23), the predicted dynamic modulus is calculated. Then, Excel solver is applied to minimise the difference between measured and predicted dynamic modulus. Finally, the adjusted values of the fitting parameters γ, β, δ as well as the glassy asymptote $|E^*|_{max}$ are determined.

The fitting parameters δ, β, and γ are part of a mathematical model commonly used to describe the master curve for the viscoelastic properties (like the dynamic modulus, |E*|) of bituminous mixtures. These parameters are essential in constructing the curve because they define the shape and characteristics of the stiffness-frequency relationship.

Here's what each parameter represents in detail:

Parameter δ (Delta)

- δ defines the asymptote or baseline modulus of the curve, it represents the stiffness at extremely low frequencies or very high temperatures (where the material behaves more fluidly, and the modulus is low). In practical terms, δ is indicative of the minimum stiffness the material can have, which is crucial for understanding behaviour under long loading times or high temperatures.

- The results showed that the δ (Delta) in the fiber mixture is slightly higher than in the reference mixture, with values of 3.36 and 3.27, respectively. This indicates that the material has a higher minimum stiffness.

Parameter β (Beta)

- β is a horizontal shift factor that controls the position of the curve along the frequency axis (x-axis). Changing β shifts the curve left or right along the frequency axis. This parameter is crucial for aligning the curve at a specific reference temperature and adjusting it to fit the measured data points. β essentially helps calibrate the curve to align with real-world observations.

- The β (Beta) parameter in the reference mixture is -1.26, while in the fiber mixture it is -1.74. The more negative β shifts the curve to the left, allowing the fiber mixture to reach higher stiffness at lower frequencies than the reference. The fibers contribute to a faster stiffness response, potentially improving resistance to deformation under heavy, slow-moving loads.

Parameter γ (Gamma)

- γ controls the slope or steepness of the curve in the transition region between high and low stiffness. γ affects how quickly the stiffness changes between the low- and high-frequency regions. A larger γ results in a steeper transition, while a smaller γ makes for a more gradual change. This parameter is important for capturing the rate at which the material stiffness changes with frequency. It essentially defines the sensitivity of the material to loading rates, which is critical for accurately predicting performance under varied traffic speeds.

- The γ (Gamma) parameter in the reference mixture is -0.5, while in the fiber mixture it is -0.61, indicating that the transition from low to high stiffness occurs more sharply for the fiber mixture.

By fitting δ, β, γ to experimental data, engineers can create a master curve that accurately describes how a bituminous mixture will respond to different traffic loading frequencies and environmental conditions, which is essential for designing durable pavements.

The master curve for the reference mixture and with fibers are reported below.

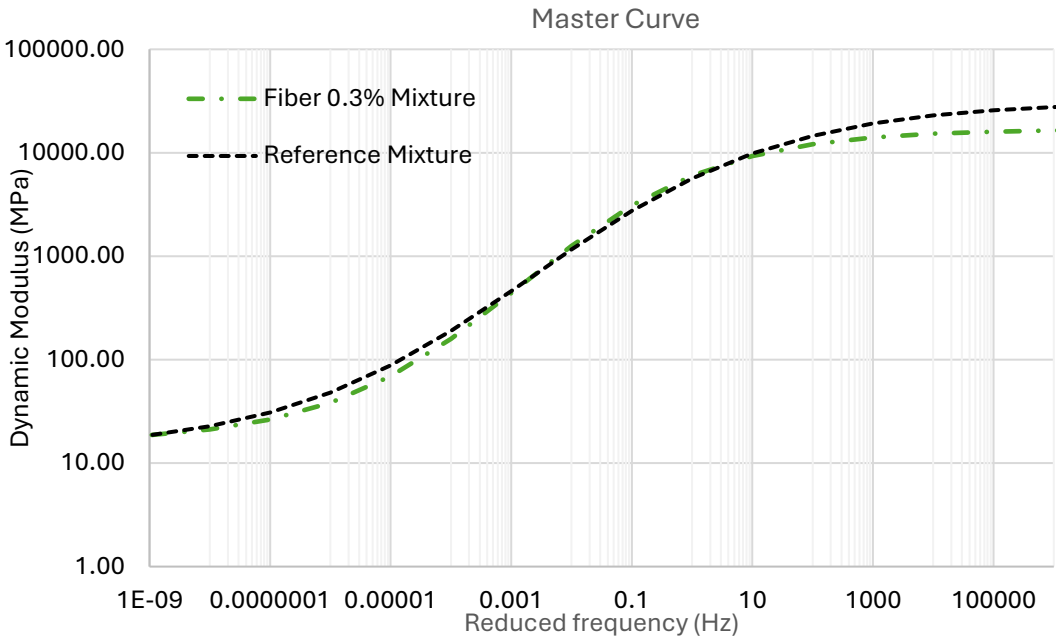


*Figure 85. Master curve results*

The graph shows that both mixtures exhibit the expected S-shape trend in the master curve, with gradual increase in modulus from low to high frequencies. At low frequencies (left side of the graph), the mixtures have lower modulus values, meaning they are less stiff. This is because, under slower loading (or high temperatures), bituminous materials tend to behave more like viscous fluids. At high frequencies (right side of the graph), the modulus values are higher, indicating greater stiffness. This is typical under fast loading (or low temperatures), where the material behaves more elastically, providing better resistance to deformation.

At low temperatures (or high frequencies), the reference mixture has higher dynamic modulus than mixture with fibers, it can be due to aggregate interlocking, the fiber is added in dry condition, which may not interact well with entire aggregate skeleton. This may decrease overall dynamic modulus. This could imply that the addition of 0.3% fiber does not necessarily improve stiffness at low temperatures, and may even slightly reduce it, as in this case.

As the frequency increases, both mixtures show an increase in dynamic modulus, indicating increased stiffness. This transition zone is where the material behaviour shifts from more flexible to more rigid. In this zone, dynamic modulus of both mixtures overlaps each other, indicating similar performance.

High temperature (or low frequencies) performance, the fiber-reinforced mixture (green line) still shows a slightly reduced values in dynamic modulus at low frequencies compared to the reference mixture, but they converge at end point. This suggests that the fiber modification may not significantly help the material maintain some stiffness under slow-loading or high-temperature conditions. There is no evidence to suggest that fiber modification can enhance rutting resistance. A conclusion can only be drawn after conducting the flow number test, which evaluates rutting behaviour of the mixture.

### 5.2.2 Flow number

The same dynamic modulus samples are used to qualify their resistance to permanent deformations employing a destructive uniaxial cyclic compression test known as flow number test. The test is intended to compare reference mixture with fiber-reinforced mixture, examining whether fibers enhance the performance of the asphalt mixture against permanent deformation.

The samples were conditioned at a temperature of 58°C, as defined by the Specifications, and the obtained results are presented in Figure 86.

The test provides a more accurate representation of field conditions compared to traditional tests, making it an essential tool for designing durable asphalt pavements, especially for high-traffic areas or warm climates where rutting is a significant issue. During the test, the deformation of the sample is measured continuously. The cumulative axial strain, representing the sample's deformation over time, is recorded for each load cycle.

As earlier explained in paragraph 4.5.3. There are three regions which related to phases of deformation. It is explained below:

1. Primary (initial) deformation, the sample shows a rapid increase in deformation as it adjusts to the applied load. This phase is characterized by a relatively high rate of strain accumulation.
2. Secondary (steady-State) deformation, this occurs at a slower, nearly constant rate. This phase indicates that the material is adjusting and distributing the load with minimal permanent deformation.
3. Tertiary (failure) deformation, eventually, the deformation rate increases sharply, leading to failure. This phase represents a breakdown of the internal structure of the mixture under repeated loading.

The FN is defined as the load cycle number at the beginning of the tertiary phase, where deformation rapidly increases. It marks the point at which the mixture can no longer effectively resist further permanent deformation.

In Figure 86, the set of lines represent two different mixtures, one with the mixture modified with 0.3% fibers (green lines) and another with the reference mixture (black lines), the fiber-reinforced samples show a delayed sharp increase in strain, indicating a higher resistance to permanent deformation and a longer life under repeated loading.

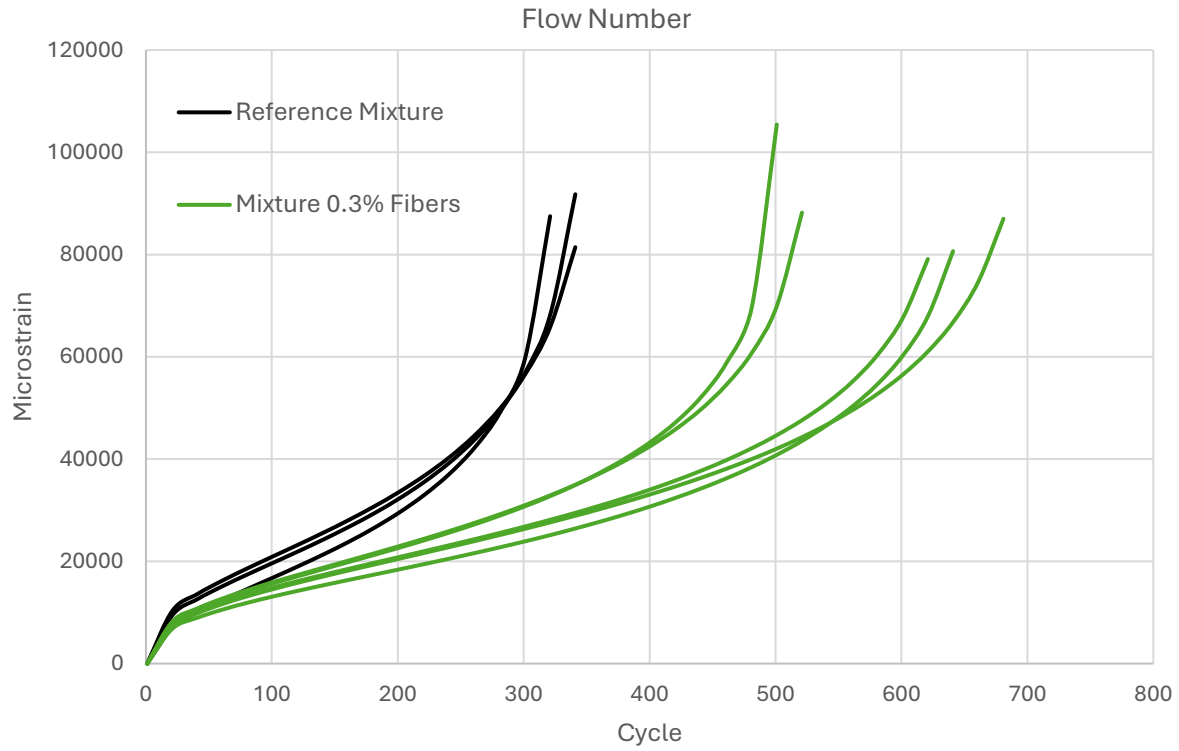


*Figure 86. Flow number results*

In the initial phase of both mixtures, there's a rapid increase in strain as the material adjusts to the applied load. This phase represents the initial consolidation of the material, where it undergoes some permanent deformation but at a relatively stable rate.

In the secondary phase, both the reference and fiber-reinforced mixtures show a slower, almost linear increase in strain with each cycle. This is a critical phase as it indicates the mixture's ability to resist further permanent deformation. The fiber-reinforced mixture maintains a lower strain rate compared to the reference mixture, showing better resistance to deformation.

In the tertiary phase, the fiber-reinforced mixture reaches the tertiary phase much later, at a higher number of cycles. The green curves continue further in the x-direction, meaning the mixture can withstand more cycles before reaching a critical level of permanent deformation. While the reference mixture reaches the tertiary phase sooner, where the strain increases sharply, indicating a rapid breakdown of the mixture under repeated loading. This early failure suggests lower rutting resistance.

Although, the mixture with fibers demonstrated less dynamic modulus at low temperatures, it achieved high values of flow number values in this test. This indicates that despite its lower dynamic modulus, the fiber-reinforced mixture, outperformed the reference mixture. This improvement is likely due to the fibers strengthening the internal structure and distributing the stress more efficiently, which reduces the material's tendency to deform under load. This higher flow number suggests that the fiber-reinforced mixture has a longer lifespan in terms of rutting resistance, making it more suitable for high-traffic pavements or areas susceptible to rutting.

# 6. Conclusion

This investigation is carried out for comparing the reference and modified fiber (tennis string) mixture under dynamic modulus and flow number.

Concerning aggregates, several classes of aggregates were collected from the Brillada plant (Borgaro Torinese - Torino), which were subsequently tested in the laboratory to determine the particle density and particle size distribution. The bitumen was characterised as 50/70 by Iplom Busalla. Specifically, experimental observation was made on the fibres through their thermal behaviour, they are polyester materials with a high melting temperature (around 275°C). The addition of the fibers was as separate aggregate.

The mix design of bituminous mixtures was carried out by applying the volumetric approach. Initially, tennis strings were cut to an average length of less than 20 mm, with this length bitumen content is determined, further according to the available literature review on fibers were cut at around 5 mm and binder dosage of previous analysis is adopted, consequently new analysis to find bitumen dosage is carried out. A total of 16 mixes (4 mixes and 4 doses of binder) were mixed using the dry method, with the aim of obtaining the optimum bitumen content for the mechanical tests. During the mix design, cylindrical samples were created by compaction to determine the composition, volumetry and indirect tensile strength (ITS). In fact, fibers remained intact and did not undergo softening processes at mixing and compaction temperatures.

Upon completing the mix design, large-scale batches of 60 kg each were prepared for both the reference mixture and the mixture incorporating 0.3% fiber content. Specimens for mechanical testing were subsequently fabricated using gyratory compaction, yielding a total of 11 specimens for analysis.

The analysis of both the master curve and flow number test results provides insights into the performance of the fiber-reinforced mixture compared to the reference mixture. The master curve graph shows that the fiber-reinforced mixture has a slightly lower dynamic modulus at high frequencies (low temperatures) and only a modest improvement across most of the frequency range. This suggests that the addition of fibers does not significantly enhance stiffness under varying temperature conditions.

However, the flow number test reveals a different aspect of performance. The fiber-reinforced mixture demonstrated a substantially higher flow number, indicating a much better resistance to permanent deformation (rutting) under repeated loading. This improvement is likely due to the fibers strengthening the internal structure and more effectively distributing stress within the mixture, which reduces its susceptibility to deformation under load.

In summary, while the fiber reinforcement may not greatly increase the stiffness (as shown by the dynamic modulus), it significantly enhances the mixture’s resistance to rutting, as evidenced by the higher flow number. The mixture containing 0.3% fibers demonstrated a 65% improvement in rutting resistance compared to the reference mixture. This makes the fiber-reinforced mixture a more durable option for high-traffic pavements or areas prone to rutting, where long-term performance and reduced maintenance are essential.

For a comprehensive evaluation of fiber-reinforced asphalt mixtures, especially considering thermal cracking, fatigue resistance, and the effect of different fiber sizes and dosages, several laboratory tests can be recommended.

Recommendations:

- Study different fiber dosages beyond the 0.3% used in this test to assess if higher or lower concentrations provide optimal performance across both stiffness and rutting resistance.
- Perform standard volumetric and compaction tests to understand how different fiber sizes and dosages affect air voids and compaction properties. Fibers can influence the mixture's density and air void distribution, impacting performance.
- Implement four point bending test to assess the mixture’s resistance to fatigue cracking by repeatedly loading a beam specimen until failure. It’s useful for evaluating how fibers influence the material’s endurance under cyclic loading and whether they can extend the mixture’s fatigue life.
- Conduct French Rutting Tester to provide additional validation of rutting resistance by simulating repeated loading. It can be used to confirm the performance improvements seen in the flow number test and assess the effects of different fiber sizes and dosages on rutting resistance.
- Perform the test for measuring the material’s resistance to thermal cracking by subjecting a restrained specimen to decreasing temperature.

# References


Pasetto, Marco, et al. "Dry addition of recycled waste polyethylene in asphalt mixtures: A laboratory study." *Materials* 15.14 (2022): 4739.

Ma, Jianmin, and Simon AM Hesp. "Effect of recycled polyethylene terephthalate (PET) fiber on the fracture resistance of asphalt mixtures." *Construction and Building Materials* 342 (2022): 127944.

Saharia, Mitali, and Kh Lakshman Singh. "Effect of plastics in applications of bituminous pavement: A laboratory study." *Materials Today: Proceedings* 65 (2022): 3362-3368.

Ballester-Ramos, Mireia, et al. "Second Life for Plastic Fibre Waste Difficult to Recover: Partial Replacement of the Binder in Asphalt Concrete Mixtures by Dry Incorporation." *Materials* 16.3 (2023): 948.

McDaniel, Rebecca S. *Fiber additives in asphalt mixtures*. No. Project 20-05 (Topic 45-15). 2015.

National Academies of Sciences, Engineering, and Medicine. *Recycled plastics in infrastructure: Current practices, understanding, and opportunities*. 2023.

Alnadish, Adham Mohammed, Narinderjit Singh Sawaran Singh, and Aawag Mohsen Alawag. "Applications of synthetic, natural, and waste fibers in asphalt mixtures: A citation-based review." *Polymers* 15.4 (2023): 1004.

Poulikakos, Lily D., et al. "RILEM interlaboratory study on the mechanical properties of asphalt mixtures modified with polyethylene waste." *Journal of Cleaner Production* 375 (2022): 134124.

Tušar, Marjan, et al. "RILEM TC 279 WMR round robin study on waste polyethylene modified bituminous binders: advantages and challenges." *Road Materials and Pavement Design* 24.2 (2023): 311-339.

Dokl, Monika, et al. "Global projections of plastic use, end-of-life fate and potential changes in consumption, reduction, recycling and replacement with bioplastics to 2050." *Sustainable Production and Consumption* (2024).

The British Standard Institution (2022). *BS EN 1097-6:2022 Tests for mechanical and physical properties of aggregates Part 6: Determination of particle density and water absorption.*

The British Standard Institution (2012). *BS EN 933-1:2012 Test for geometrical properties of aggregates Part 1: Determination of particle size distribution - Sieving method.*

The British Standard Institution (2020). *BS EN 12697-28:2020 Bituminous Mixtures – Test Methods Part 28: Preparation of samples for determining binder content, water content and grading.*

The British Standard Institution (2015+A1). *BS EN 12697-2:2015+A1:2019 Bituminous Mixtures – Test Methods Part 2: Determination of particle size distribution.*

The British Standard Institution (2016). *BS EN 12697-35:2016 Bituminous Mixtures – Test Methods Part 35: Laboratory Mixing.*

The British Standard Institution (2020). *BS EN 12697-39:2020 Bituminous Mixtures – Test Methods Part 39: Binder content by ignition.*

The British Standard Institution (2018). *BS EN 12697-5:2018 Bituminous mixtures – Test methods Part 5: Determination of the maximum density.*

American Association of State Highway and Transportation Officials. *AASHTO Designation R 30-22 Standard Practice for Laboratory Conditioning of Asphalt Mixtures.*

The British Standard Institution (2019). *BS EN 12697-31:2019 Bituminous mixtures – Test methods Part 31: Specimen preparation by gyratory compactor.*

The British Standard Institution (2020). *BS EN 12697-6:2020 Bituminous mixtures – Test methods Part 6: Determination of bulk density of bituminous specimens.*

The British Standard Institution (2017). *BS EN 12697-23:2017 Bituminous mixtures – Test methods Part 23: Determination of the indirect tensile strength of bituminous specimens.*

American Association of State Highway and Transportation Officials. *AASHTO Designation R 84 – 17 Developing Dynamic Modulus Master Curves for Asphalt Mixtures Using the Asphalt Mixture Performance Tester (AMPT)*

American Association of State Highway and Transportation Officials. *AASHTO Designation T 378 – 17 Determining the Dynamic Modulus and Flow Number for Asphalt Mixtures Using the Asphalt Mixture Performance Tester (AMPT)*

12 Countries Have Built Roads Out of Plastic – And They Can Perform As Well or Better Than Asphalt, https://www.goodnewsnetwork.org/paving-with-plastic-dent-global-waste-problem-yale/ (Published on Mar 26, 2021)

Understanding the Differences Between Primary, Secondary, and Tertiary Recycling, https://recyclenation.com/2021/10/understanding-the-differences-between-primary-secondary-and-tertiary-recycling/ (Published on Oct 26, 2021)

Tennis Strings Explained https://www.tenniswarehouse-europe.com/Learning_Center/Gear_Guides/Tennis_String/Tennis_Strings_Explained.html

Is String Biodegradable? https://www.ablison.com/is-string-biodegradable/#wpaicg-the-environmental-impact-of-non-biodegradable-strings

How to Choose a Tennis String https://www.wilson.com/en-us/blog/tennis/how-tos/how-choose-tennis-string (Published on Jan 18, 2024)

Tennis Racket String Patterns Explained – Our Full Guide https://tennispursuits.com/tennis-racket-string-patterns-explained-our-full-guide/

The global apparel industry is a significant yet overlooked source of plastic leakage https://www.nature.com/articles/s41467-024-49441-4 (Published on Jun 12, 2024)

Plastic pollution is growing relentlessly as waste management and recycling fall short, says OECD https://www.oecd.org/en/about/news/press-releases/2022/02/plastic-pollution-is-growing-relentlessly-as-waste-management-and-recycling-fall-short.html (Published on Feb 22, 2022)

How is Plastic Recycled: Complete Plastics Recycling Process https://energytheory.com/plastic-recycling-process/ (Published on Apr 1, 2024)

Everything you need to know about plastic pollution https://www.unep.org/news-and-stories/story/everything-you-need-know-about-plastic-pollution (Published on Apr 25, 2023)

The world's plastic pollution crisis, explained https://www.nationalgeographic.com/environment/ article/plastic-pollution (Published on Sep 23, 2024)

Plastic recycling: A panacea or environmental pollution problem https://www.nature.com/articles/s44296-024-00024-w (Published on Aug 01, 2024)

Ocean plastic pollution an overview: data and statistics https://oceanliteracy.unesco.org/plastic-pollution-ocean/ (Published on May 09, 2022)

# Appendix A. Mix design

*Table 13. Design curve of AC16 layer*

| D | Passing percentage [%] | | | |
|---|---|---|---|---|
| **[mm]** | **5-15** | **0-5** | **Powder** | **Design** |
| **20** | 100.0 | 100.0 | 100.0 | 100.0 |
| **16** | 100.0 | 100.0 | 100.0 | 100.0 |
| **10** | 61.9 | 100.0 | 100.0 | 78.6 |
| **4** | 10.0 | 93.7 | 99.9 | 47.0 |
| **2** | 7.1 | 70.9 | 99.7 | 36.5 |
| **0.5** | 3.8 | 31.2 | 68.0 | 17.6 |
| **0.25** | 3.0 | 15.8 | 51.3 | 10.3 |
| **0.063** | 1.8 | 3.0 | 28.3 | 3.6 |

*Table 14. Bitumen dosage for each mixture and thier TMD*

| | **Bitumen dosage** | **$\rho_{mv}$** |
|---|---|---|
| | **(%)** | **(Mg/m$^3$)** |
| **Reference** | 4.39 | 2.585 |
| | 4.79 | 2.555 |
| | 5.15 | 2.547 |
| | 5.47 | 2.512 |
| **1.0%F** | 4.45 | 2.548 |
| | 4.78 | 2.530 |
| | 5.24 | 2.507 |
| | 5.78 | 2.494 |
| **0.5%F** | 4.27 | 2.572 |
| | 4.80 | 2.538 |
| | 5.31 | 2.533 |
| | 5.62 | 2.514 |
| **0.3%F** | 4.49 | 2.572 |
| | 4.84 | 2.551 |
| | 5.13 | 2.532 |
| | 5.59 | 2.514 |

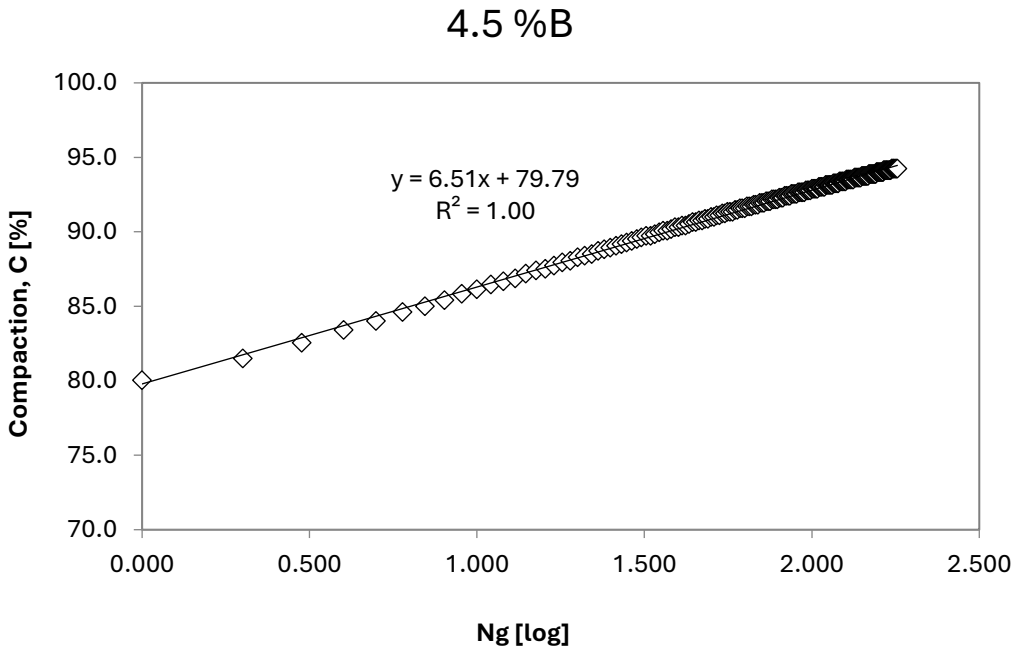


*Figure 87. Workability of the reference mixture with 4.5%B.*

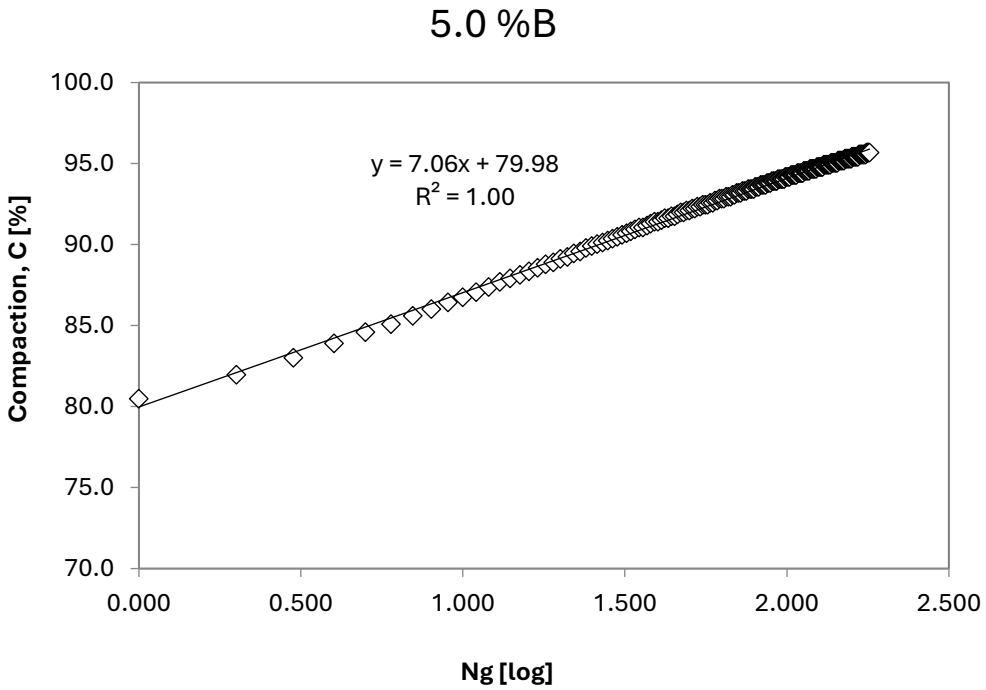


*Figure 88. Workability of the reference mixture with 5.0%B*

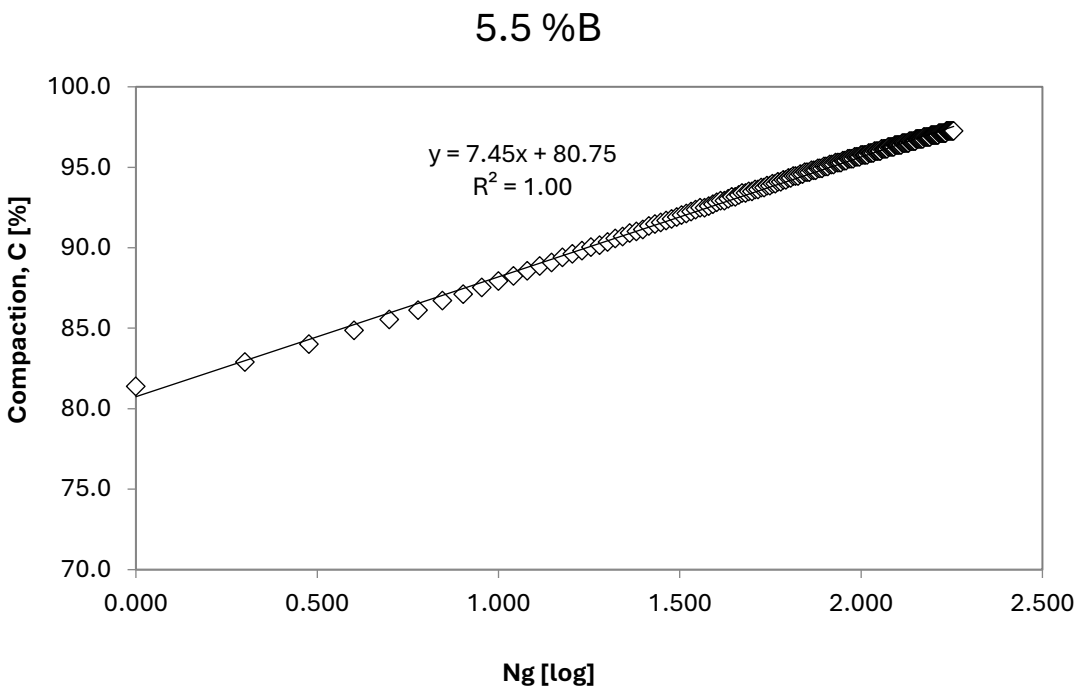


*Figure 89. Workability of the reference mixture with 5.5%B*

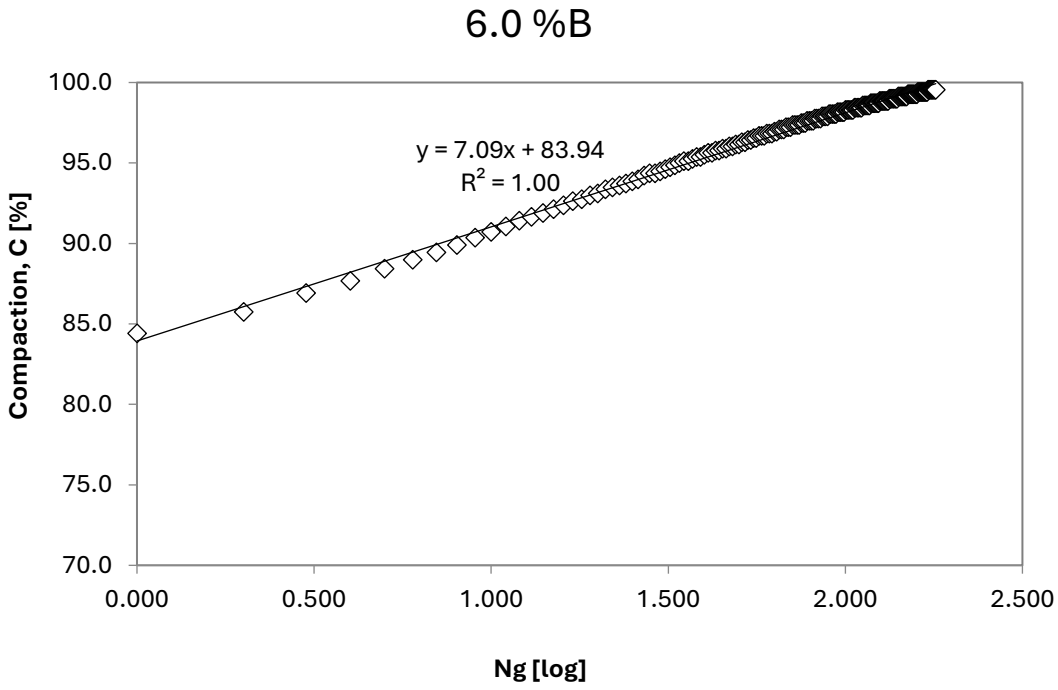


*Figure 90. Workability of the reference mixture with 6.0%B*

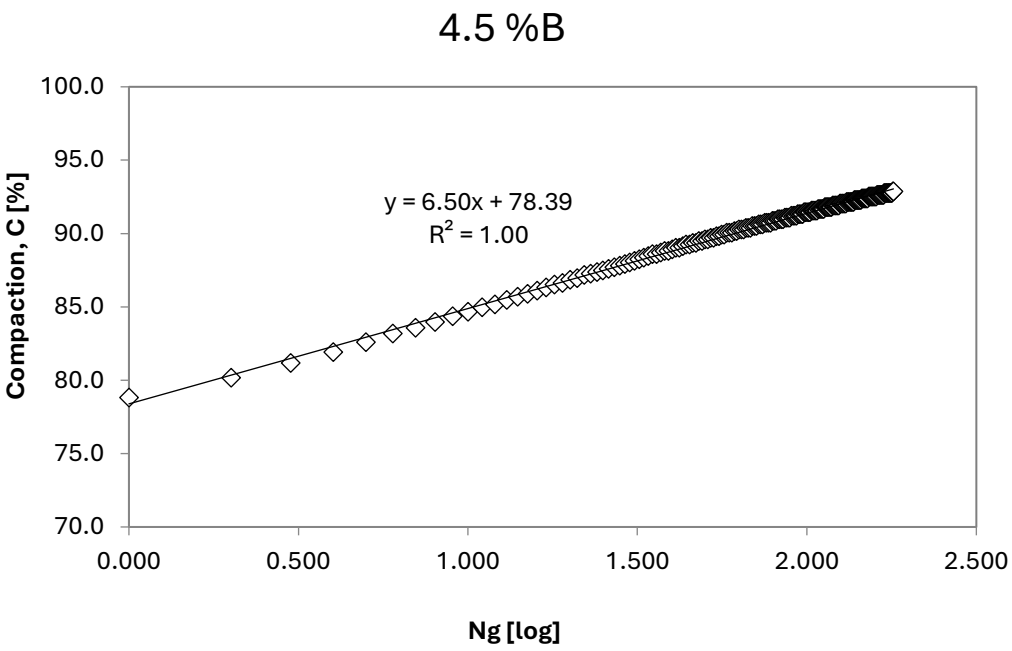


*Figure 91. Workability of the mixture 1.0% Fiber with 4.5%B*

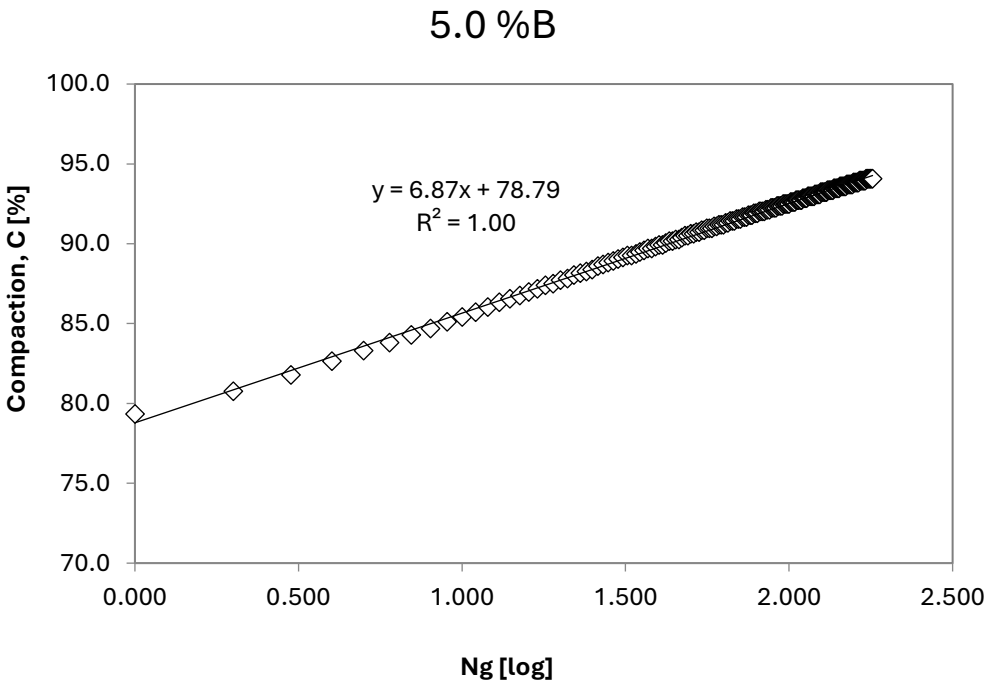


*Figure 92. Workability of the mixture 1.0% Fiber with 5.0%B*

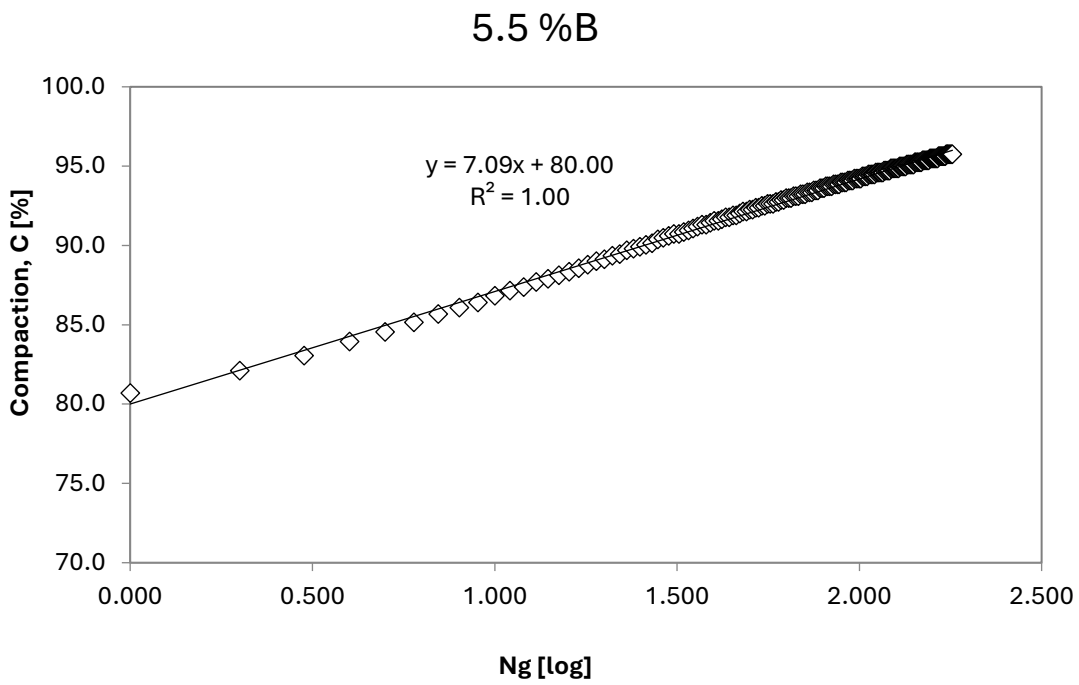


*Figure 93. Workability of the mixture 1.0% Fiber with 5.5%B*

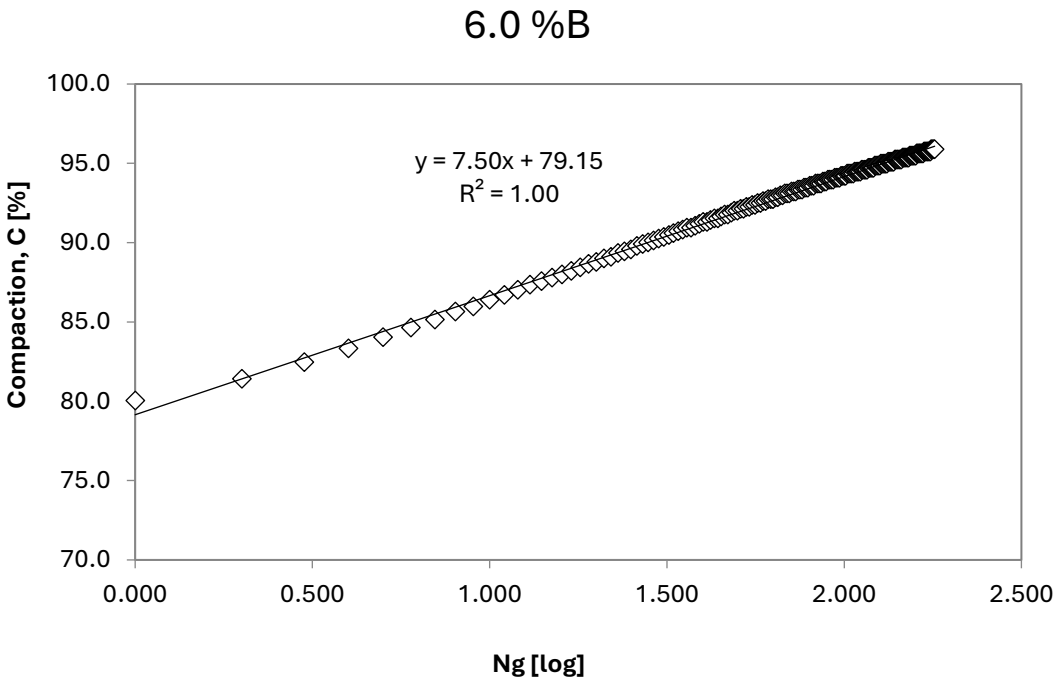


*Figure 94. Workability of the mixture 1.0% Fiber with 6.0%B*

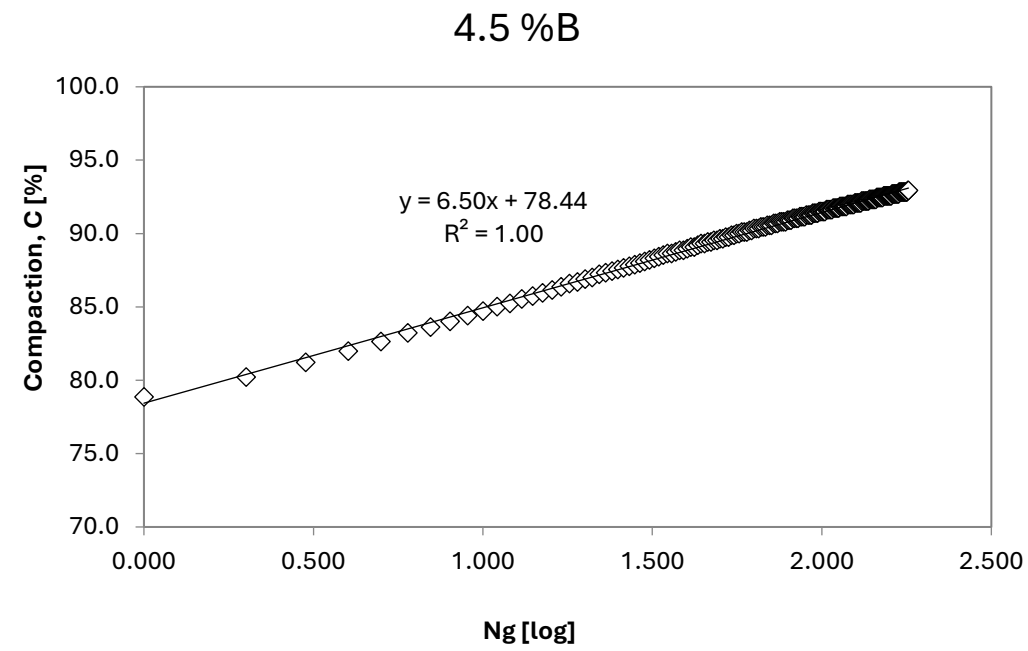


*Figure 95. Workability of the mixture 0.5% Fiber with 4.5%B*

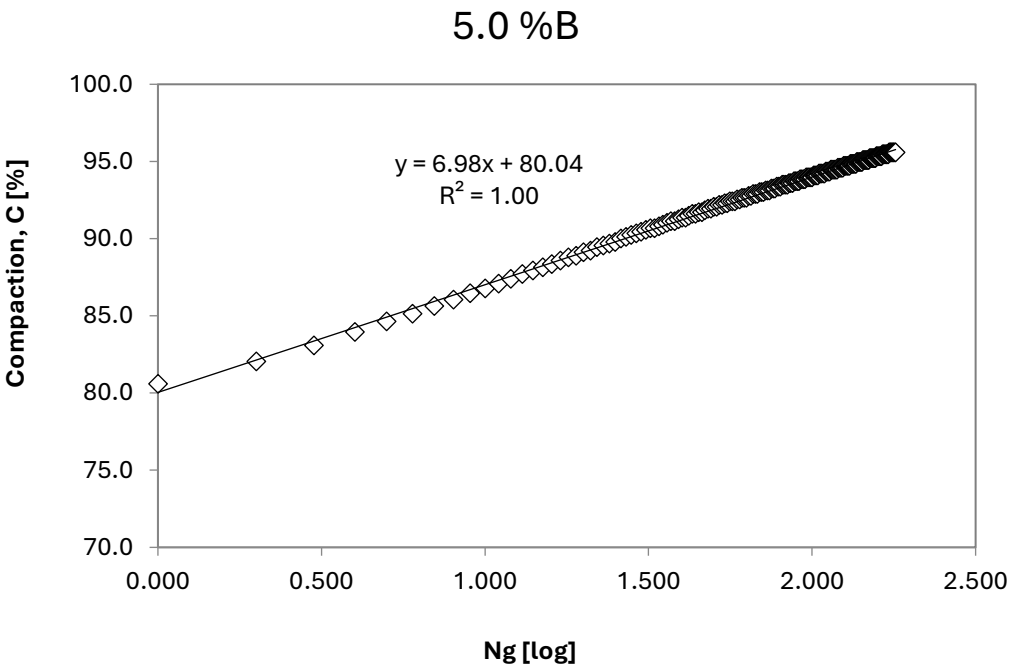


*Figure 96. Workability of the mixture 0.5% Fiber with 5.0%B*

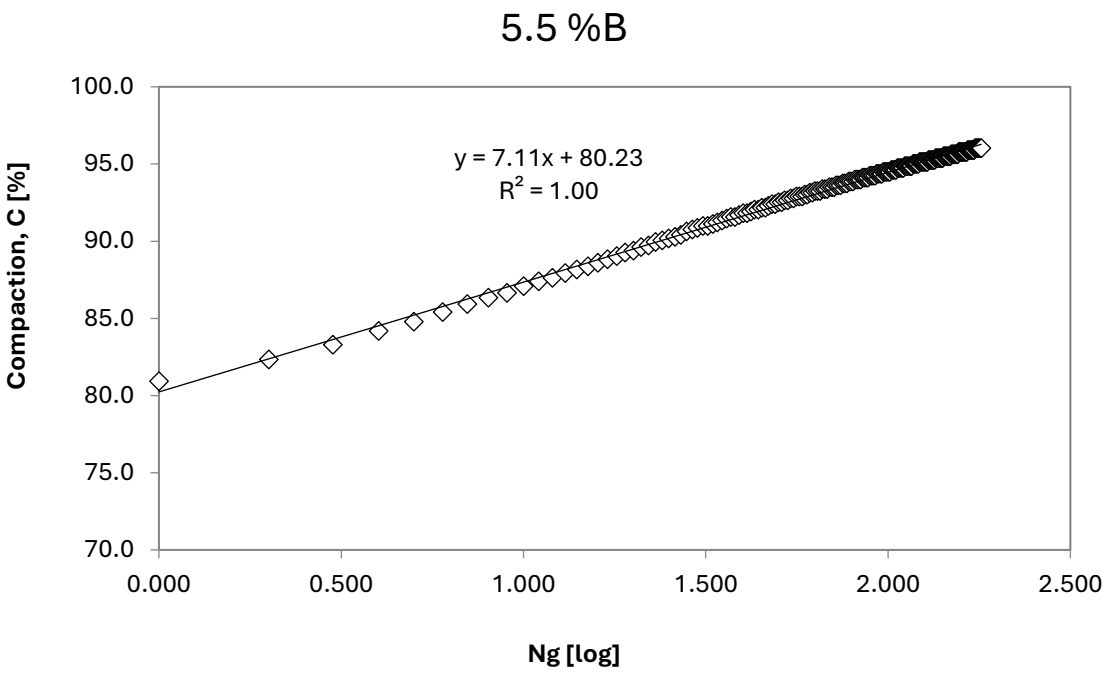


*Figure 97. Workability of the mixture 0.5% Fiber with 5.5%B*

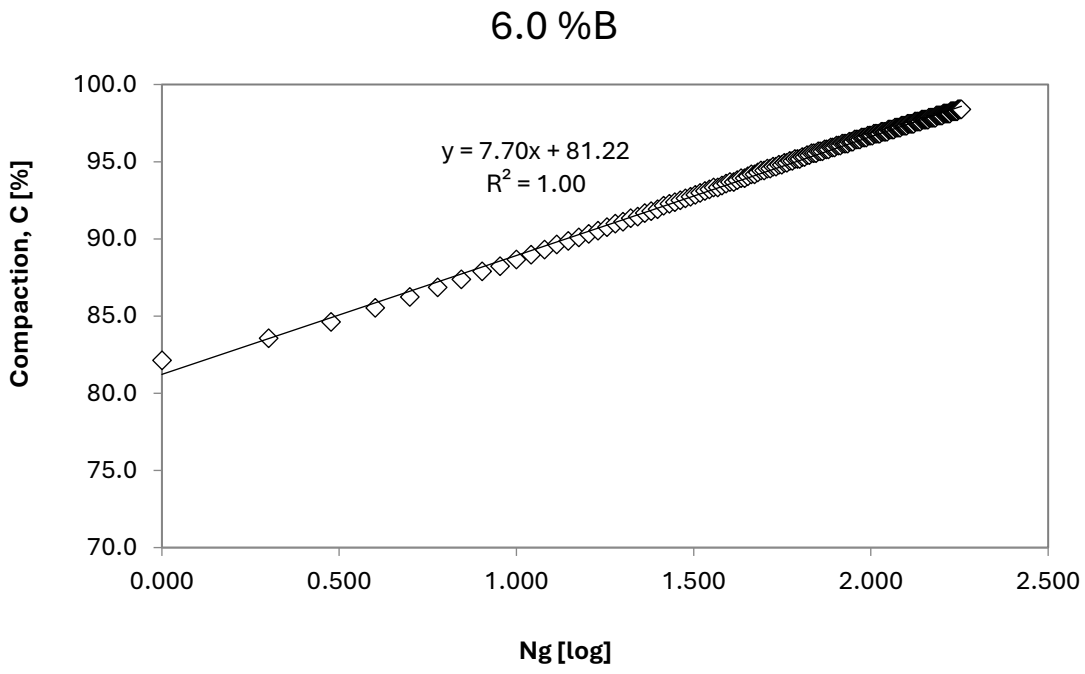


*Figure 98. Workability of the mixture 0.5% Fiber with 6.0%B*

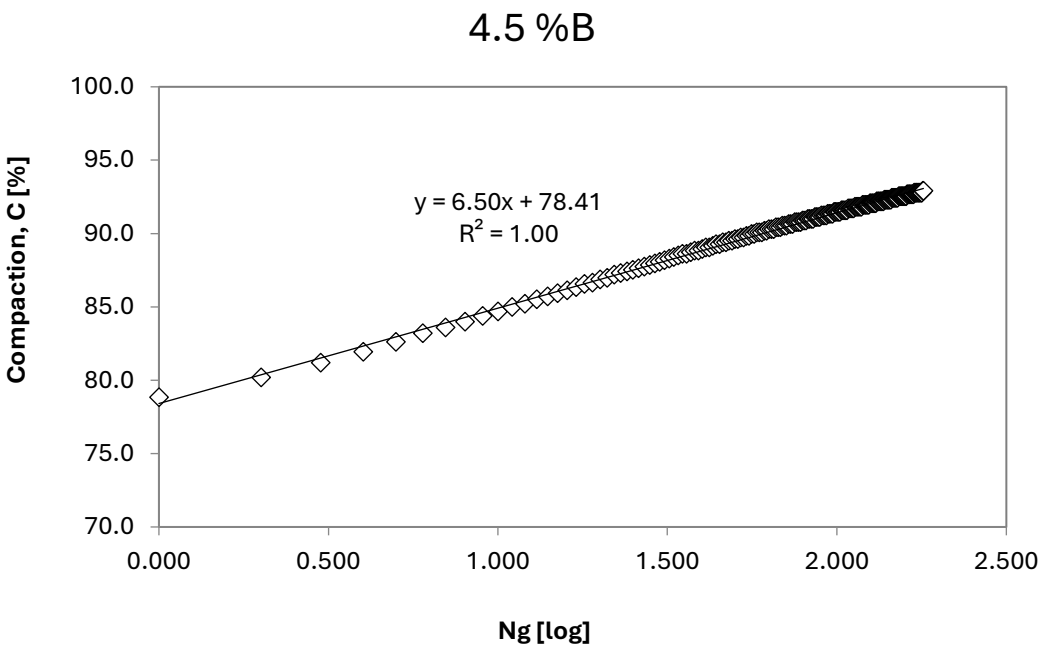


*Figure 99. Workability of the mixture 0.3% Fiber with 4.5%B*

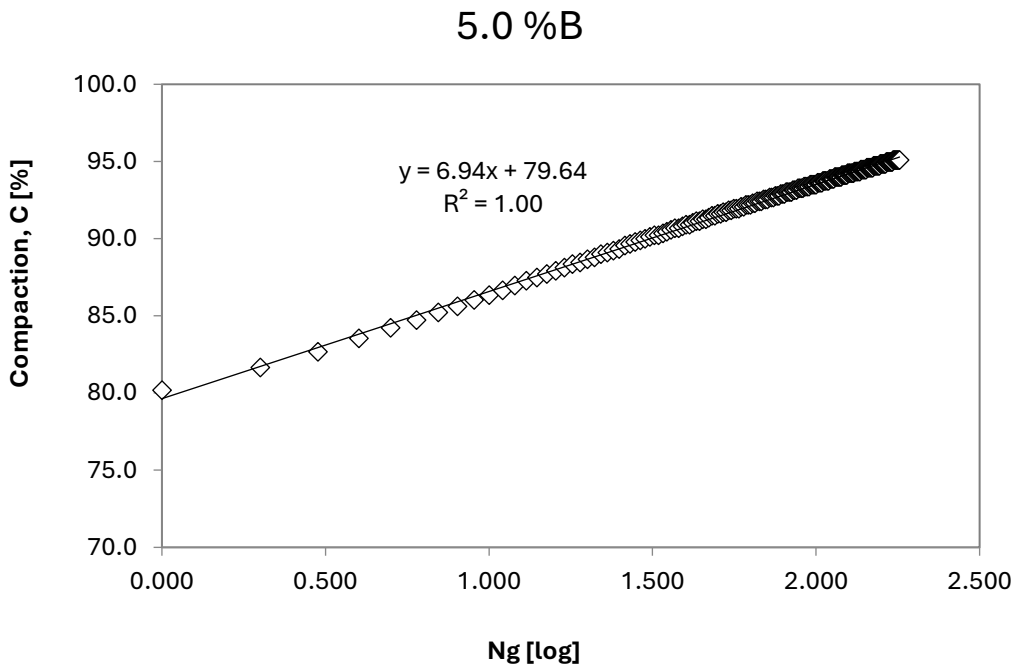


*Figure 100. Workability of the mixture 0.3% Fiber with 5.0%B*

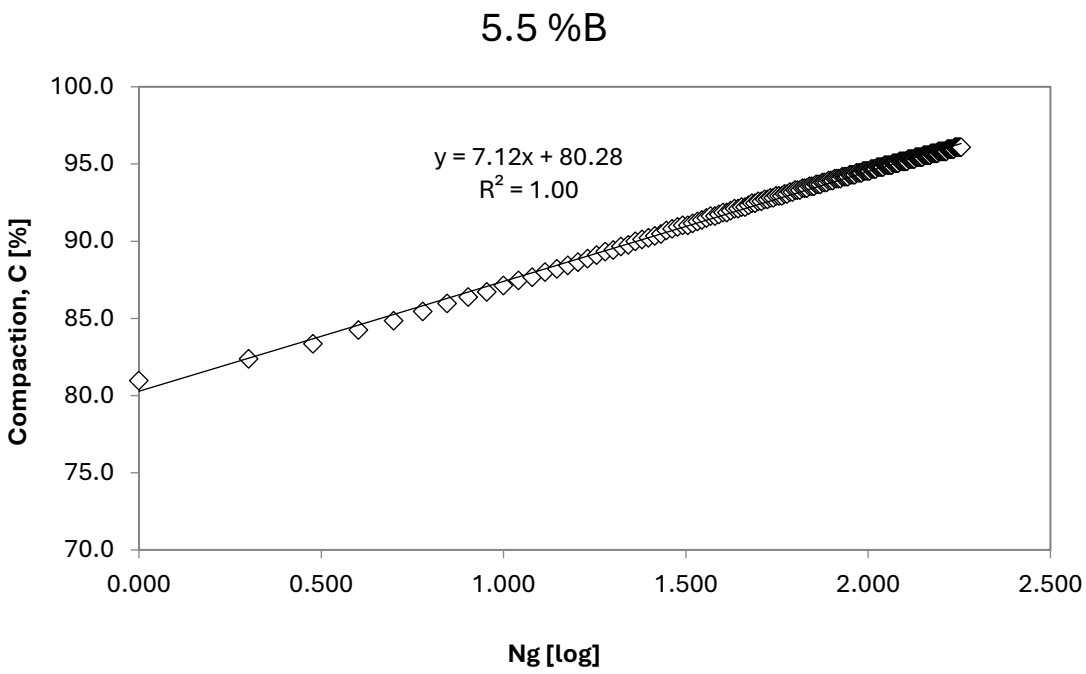


*Figure 101. Workability of the mixture 0.3% Fiber with 5.5%B*

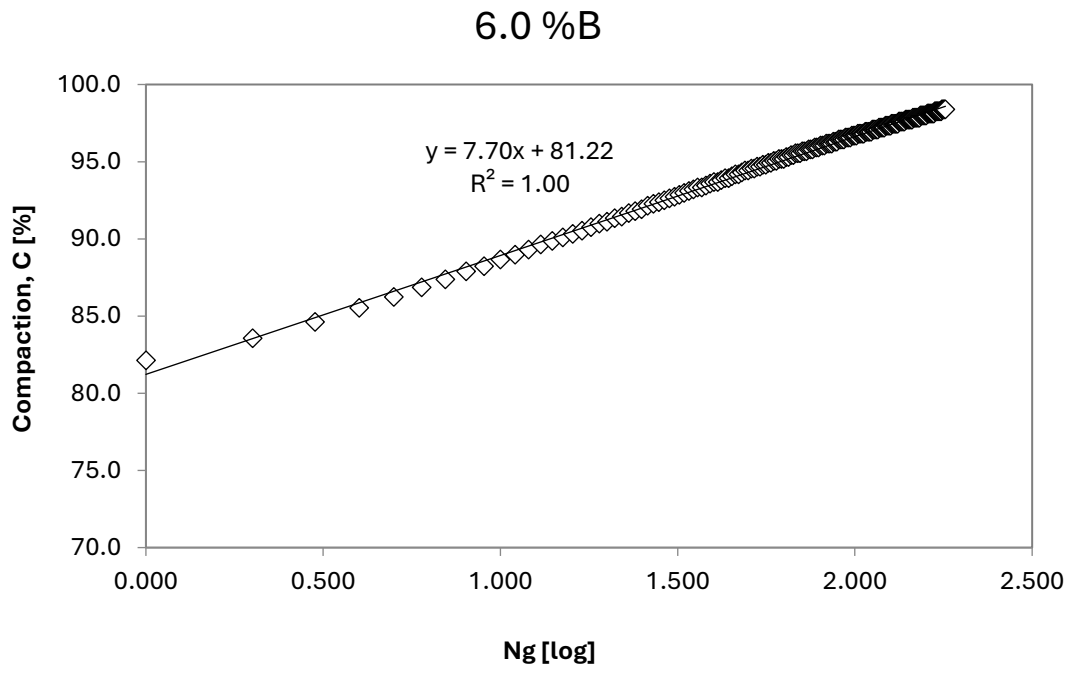


*Figure 102. Workability of the mixture 0.3% Fiber with 6.0%B*

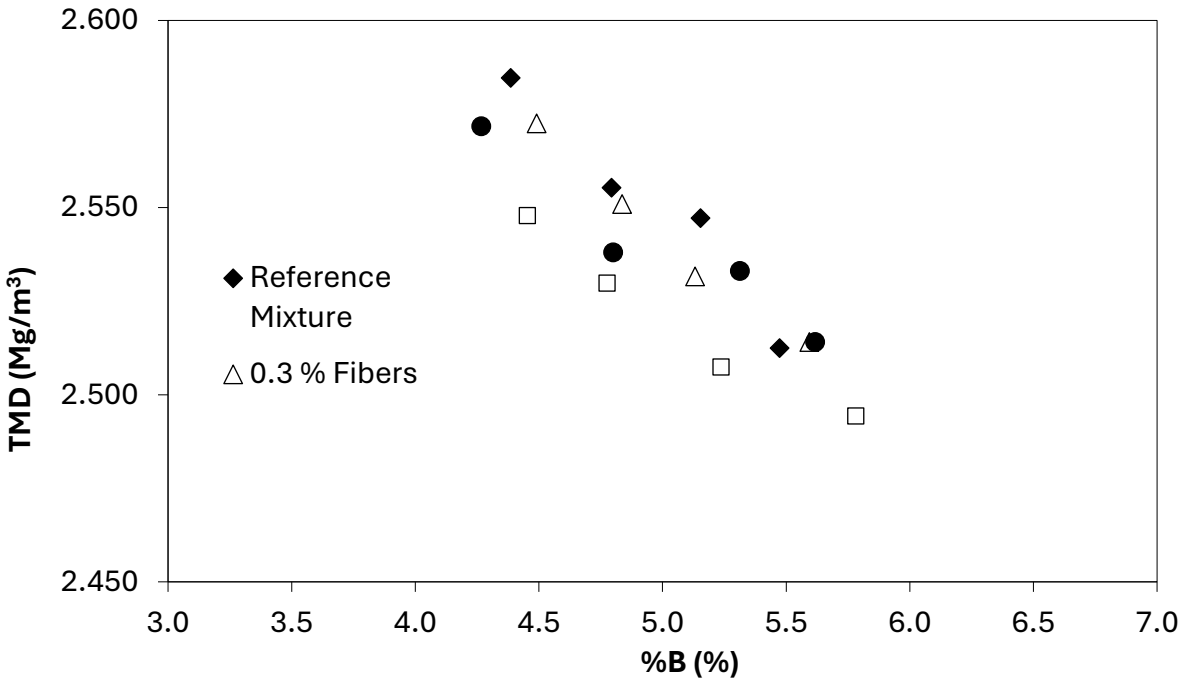


*Figure 103. TMD of mixtures as a function of %B*

*Table 15. Void content of the mixtures at 3 different gyrations.*

| Mixture | Bitumen dosage | $v_{180}$ | $v_{100}$ | $v_{10}$ |
|---|---|---|---|---|
| | (%) | (%) | (%) | (%) |
| Reference | 4.39 | 5.7 | 7.1 | 13.9 |
| | 4.79 | 4.3 | 5.8 | 13.3 |
| | 5.15 | 2.7 | 4.2 | 12.1 |
| | 5.47 | 0.5 | 1.7 | 9.3 |
| 1.0%F | 4.45 | 7.1 | 8.6 | 15.5 |
| | 4.78 | 5.9 | 7.5 | 14.7 |
| | 5.24 | 4.2 | 5.8 | 13.3 |
| | 5.78 | 4.1 | 5.8 | 13.7 |
| 0.5%F | 4.27 | 7.1 | 8.5 | 14.9 |
| | 4.80 | 4.4 | 6.1 | 13.4 |
| | 5.31 | 4.0 | 5.4 | 12.5 |
| | 5.62 | 1.6 | 3.1 | 10.7 |
| 0.3%F | 4.49 | 5.7 | 7.1 | 14.1 |
| | 4.84 | 4.0 | 5.5 | 13.1 |
| | 5.13 | 3.4 | 5.0 | 12.5 |
| | 5.59 | 2.5 | 4.1 | 11.5 |

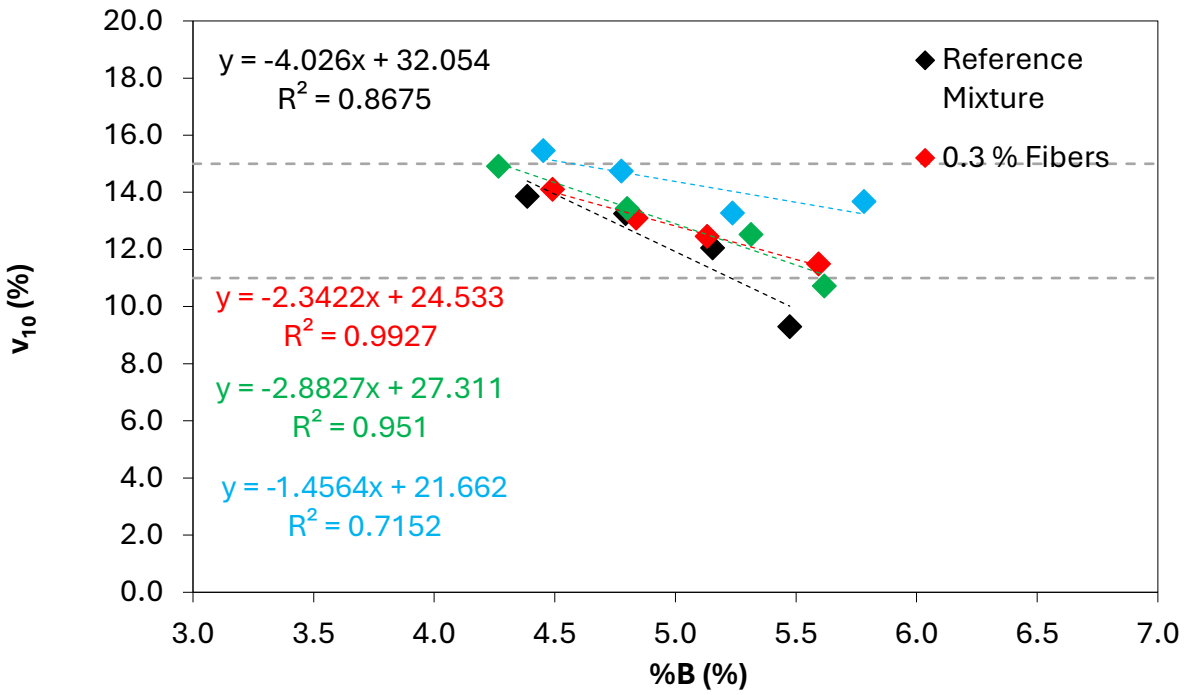


*Figure 104. Void content at 10 gyrations ($N_{ini}$) of the mixtures*

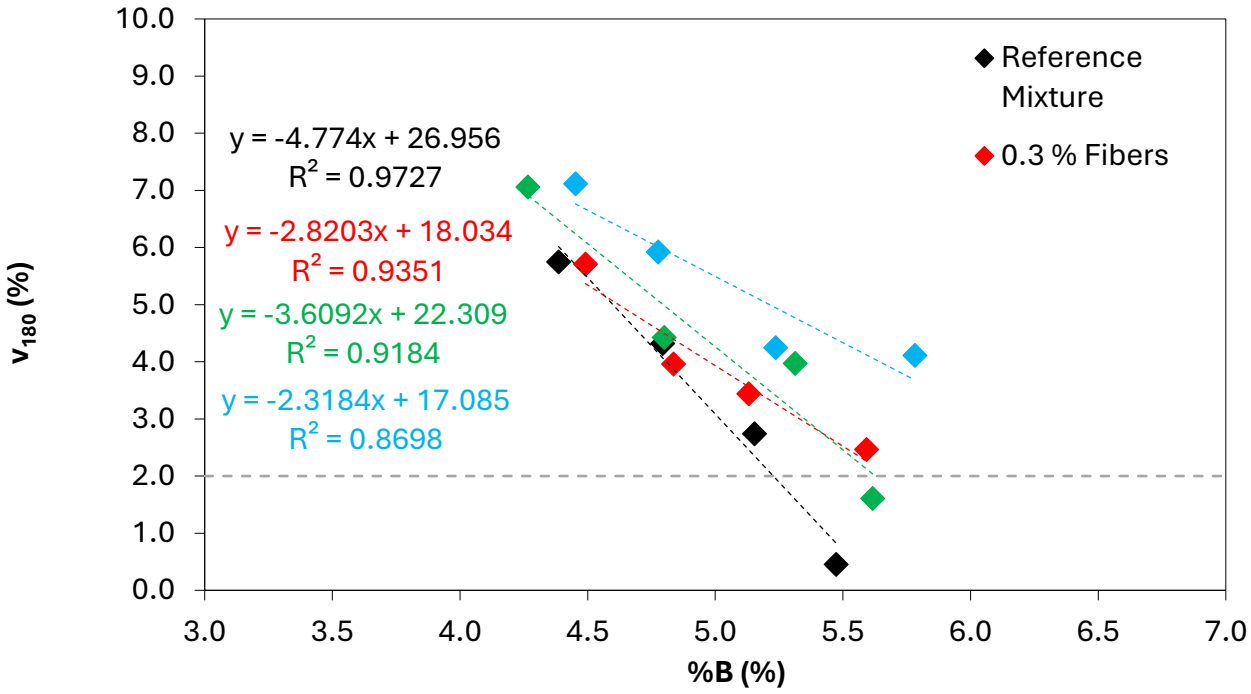


*Figure 105. Void content at 10 gyrations ($N_{fin}$) of the mixtures*

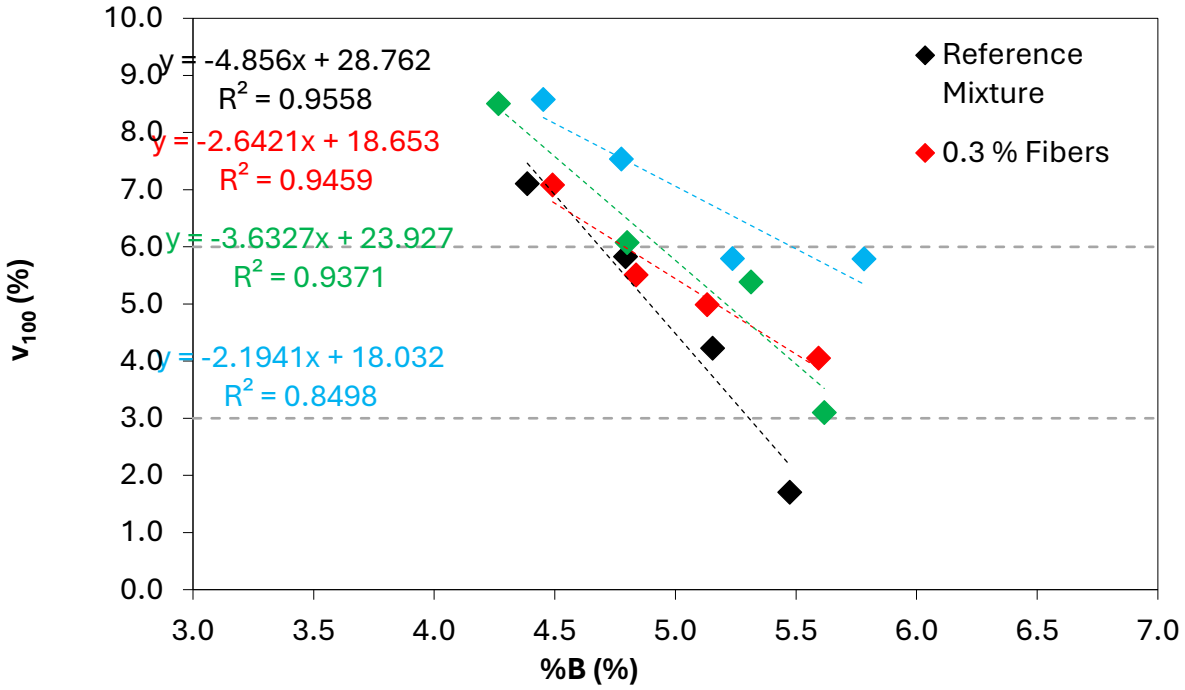


*Figure 106. Void content at 100 gyrations ($N_{design}$) of the mixtures*

*Table 16. ITS results of the mixtures*

| Mixture | Bitumen dosage | RTI | CTI | $S_V$ |
|---|---|---|---|---|
| | (%) | (MPa) | (MPa) | (mm) |
| Reference | 4.39 | 3.35 | 397.8 | 1.32 |
| | 4.79 | 3.11 | 249.6 | 1.96 |
| | 5.15 | 3.54 | 376.2 | 1.48 |
| | 5.47 | 3.23 | 378.5 | 1.34 |
| 1.0%F | 4.45 | 2.71 | 312.3 | 1.36 |
| | 4.78 | 2.60 | 255.4 | 1.60 |
| | 5.24 | 2.98 | 247.5 | 1.89 |
| | 5.78 | 2.63 | 239.5 | 1.73 |
| 0.5%F | 4.27 | 2.90 | 331.9 | 1.37 |
| | 4.80 | 2.83 | 279.8 | 1.59 |
| | 5.31 | 3.63 | 363.2 | 1.57 |
| | 5.62 | 3.77 | 469.8 | 1.26 |
| 0.3%F | 4.49 | 3.35 | 505.7 | 1.04 |
| | 4.84 | 3.28 | 430.6 | 1.20 |
| | 5.13 | 3.31 | 703.9 | 0.74 |
| | 5.59 | 3.62 | 367.4 | 1.55 |

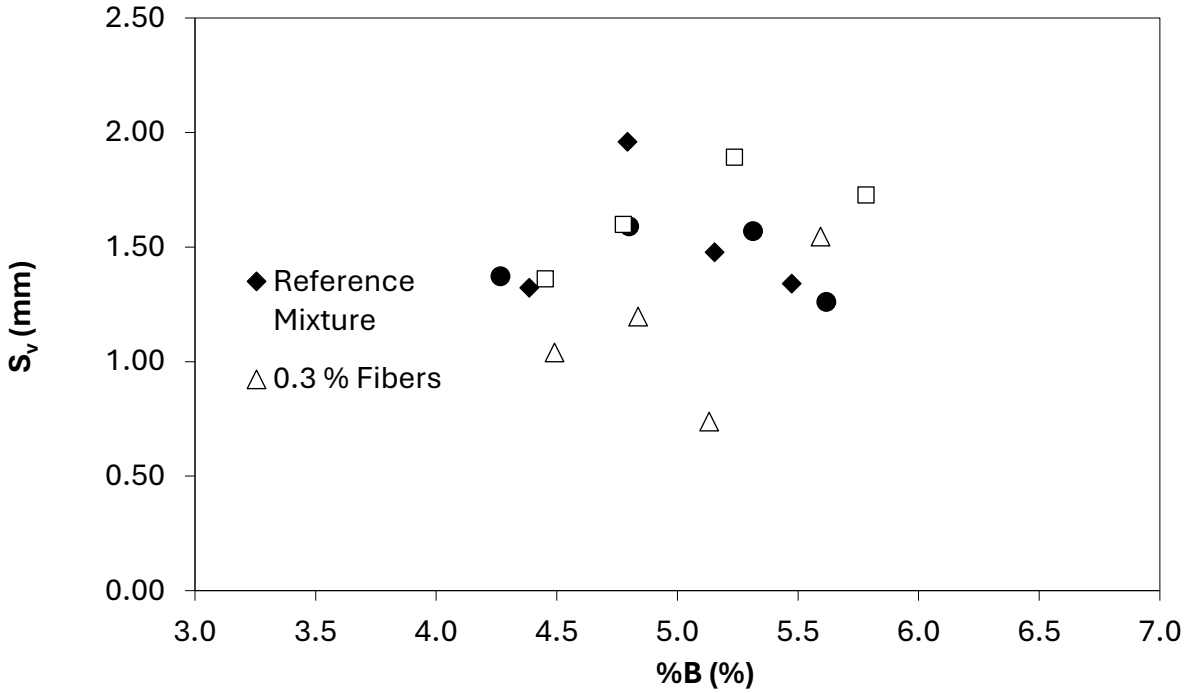


*Figure 107. Vertical displacements from ITS of the mixtures*

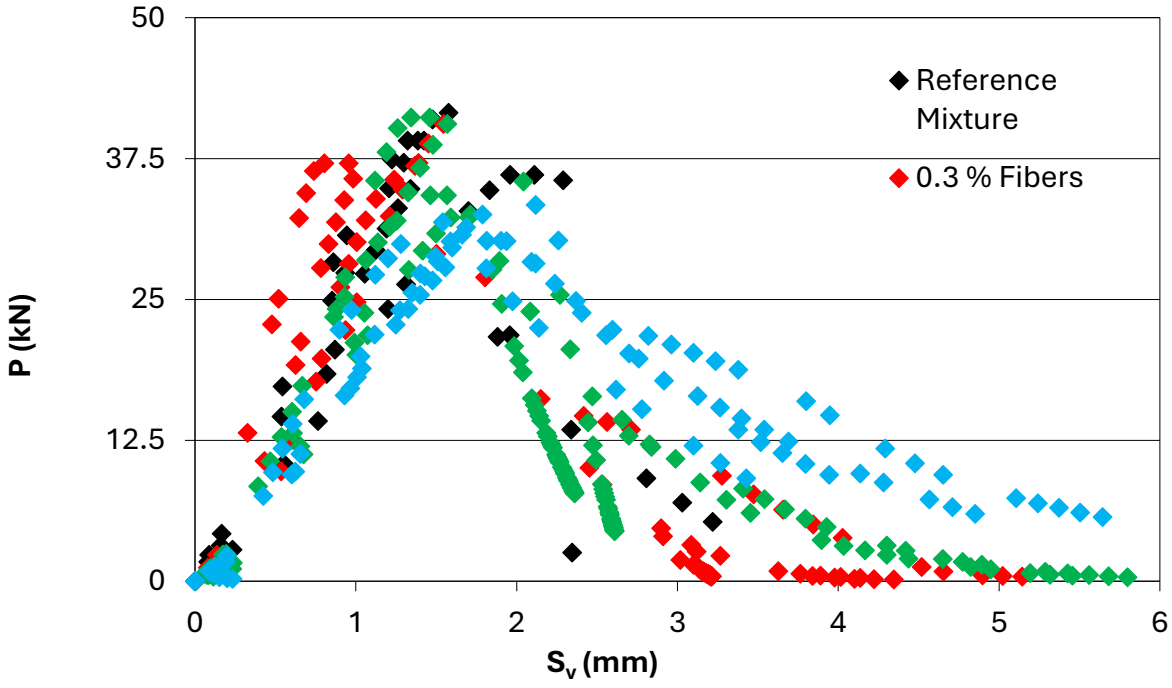


*Figure 108. Load-displacement curve from ITS of the mixtures*

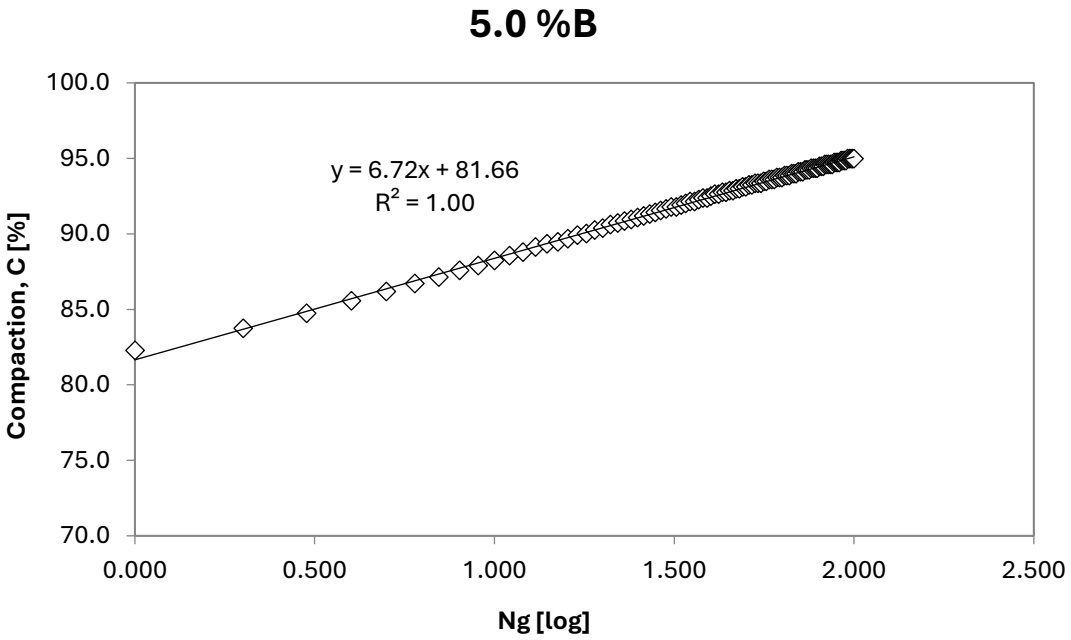


*Figure 109. Workability of the reference mixture with 5.0%B*

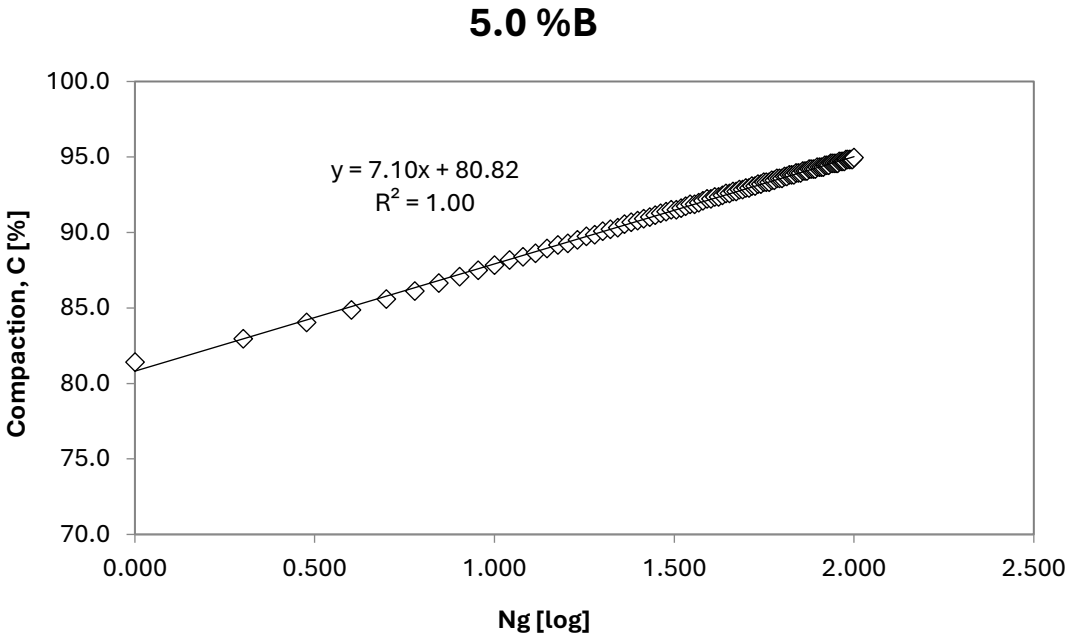


*Figure 110. Workability of the mixture 0.5% Fiber with 5.0%B*

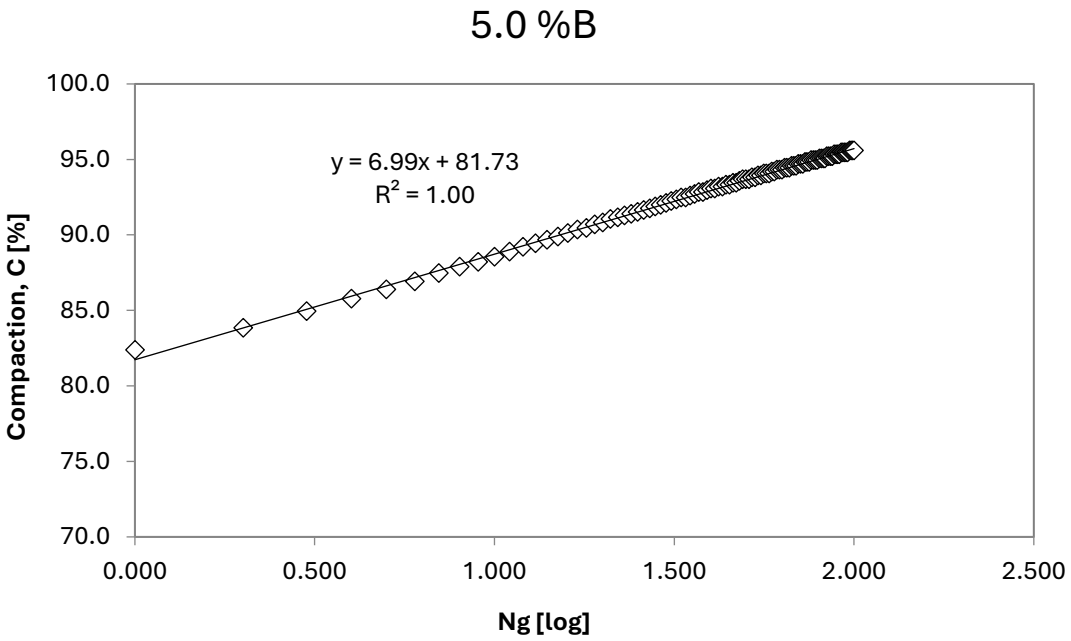


*Figure 111. Workability of the mixture 0.3% Fiber with 5.0%B*

# Appendix B. Compaction and volumetrics

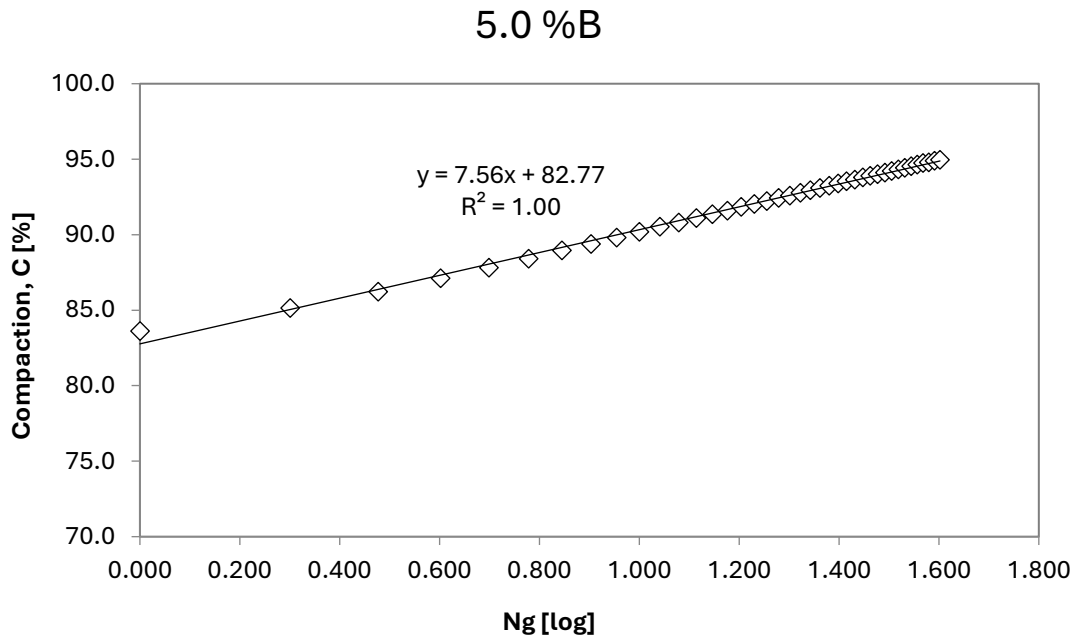


*Figure 112. Workability of the reference mixture RA2 with 5.0%B*

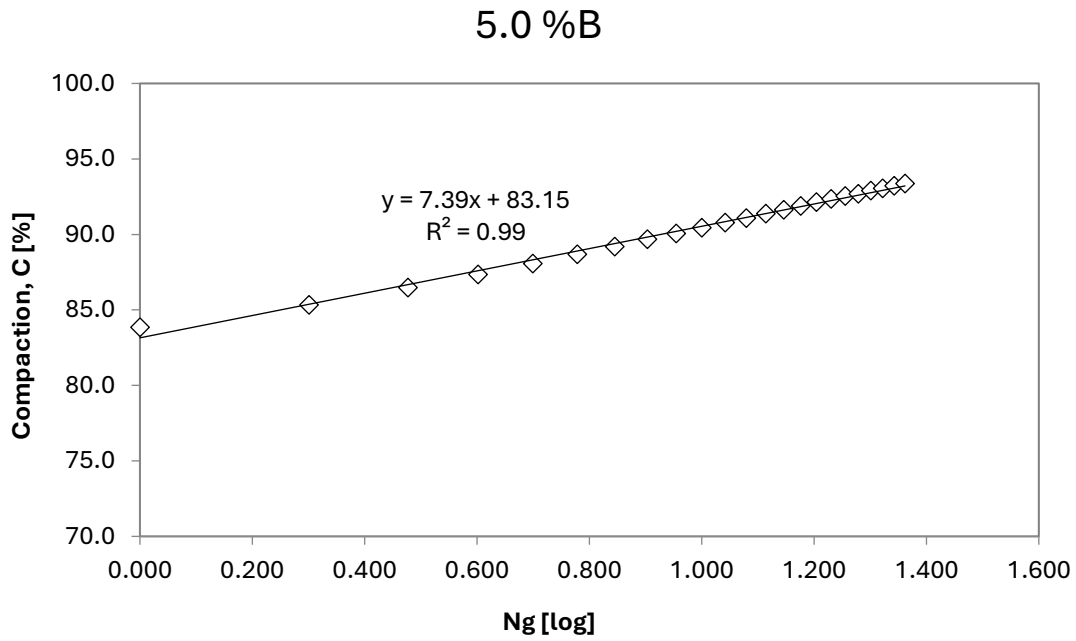


*Figure 113. Workability of the reference mixture RA3 with 5.0%B*

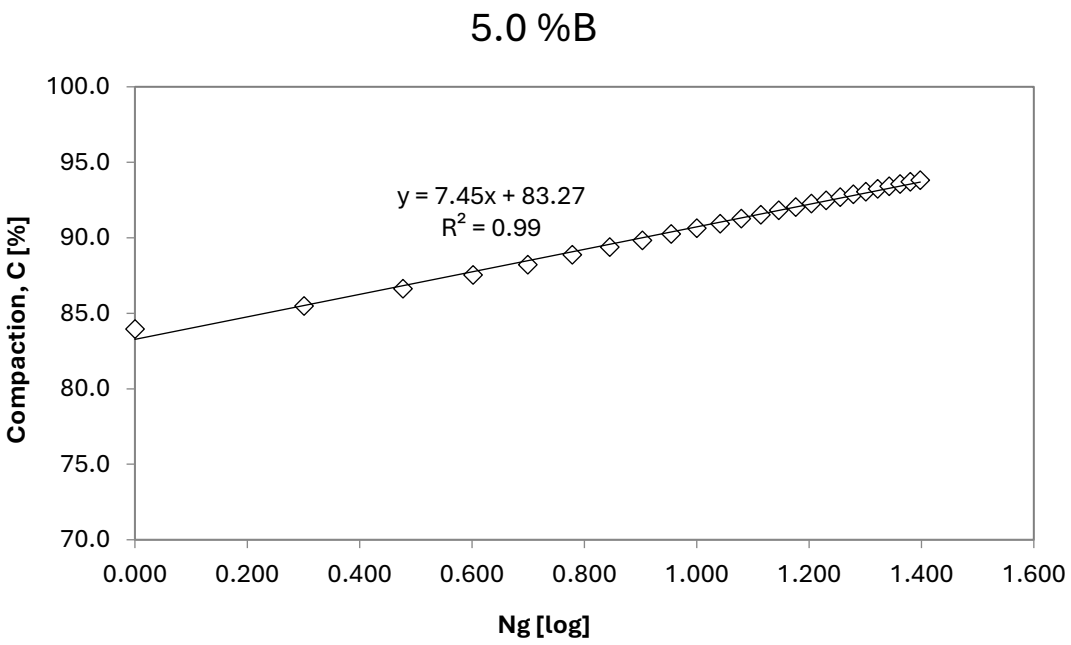


*Figure 114. Workability of the reference mixture RA4 with 5.0%B*

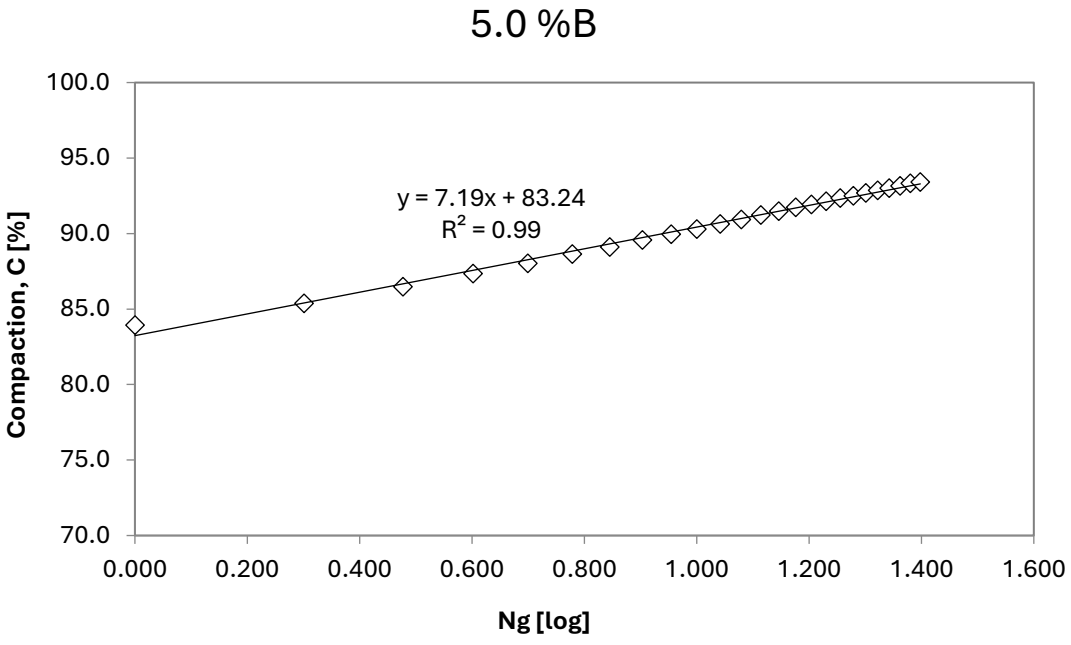


*Figure 115. Workability of the reference mixture RA5 with 5.0%B*

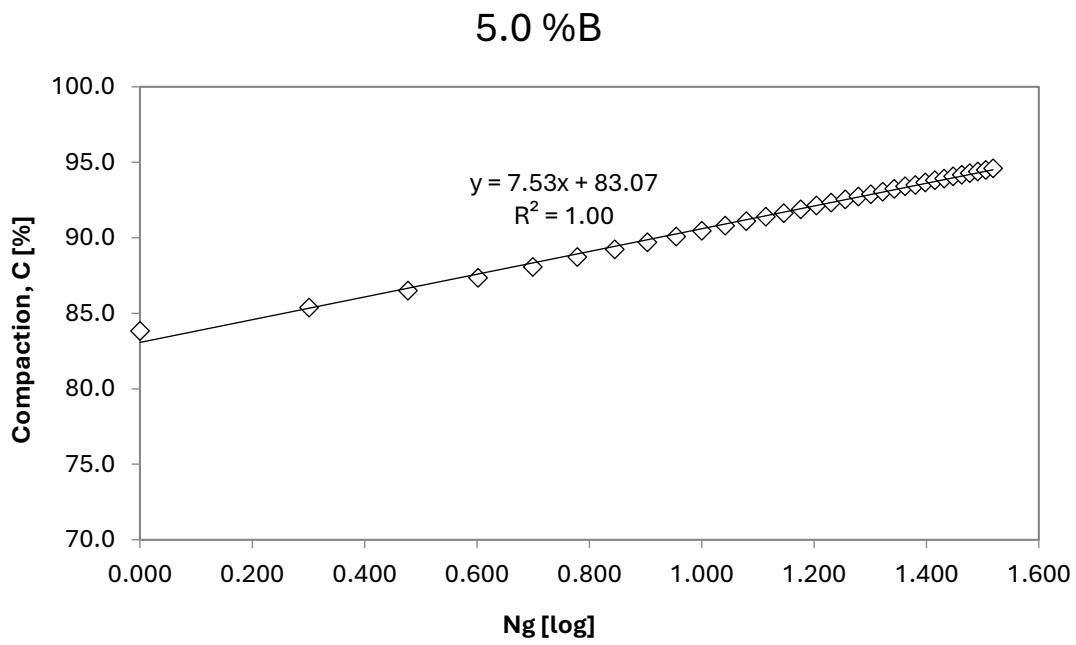


*Figure 116. Workability of the reference mixture RA6 with 5.0%B*

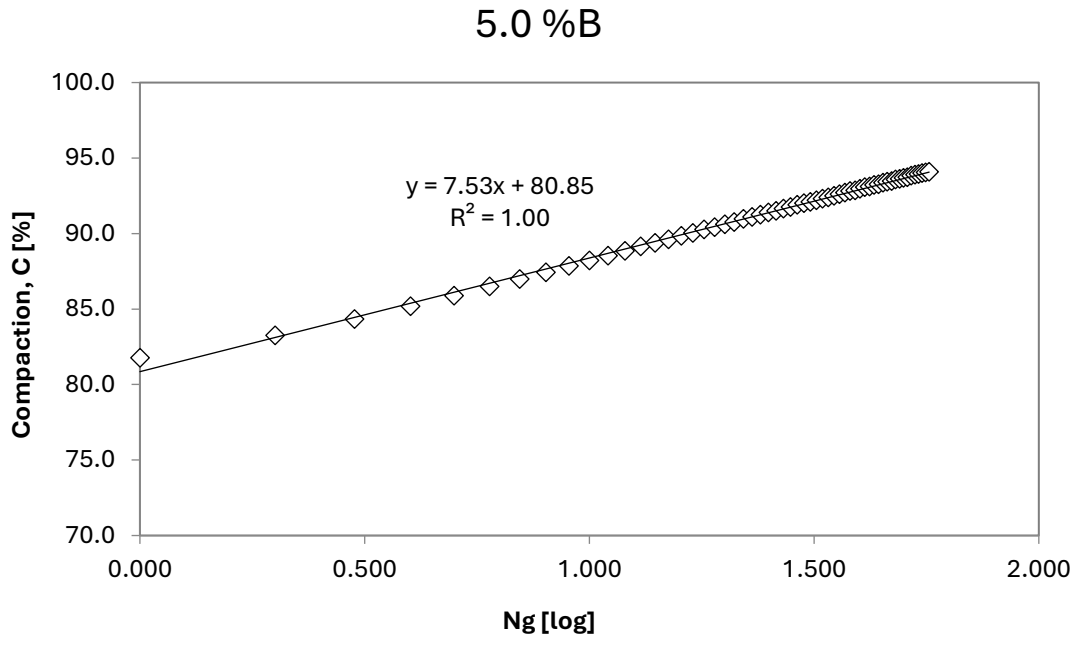


*Figure 117. Workability of the mixture FB1 0.3% Fibers with 5.0%B*

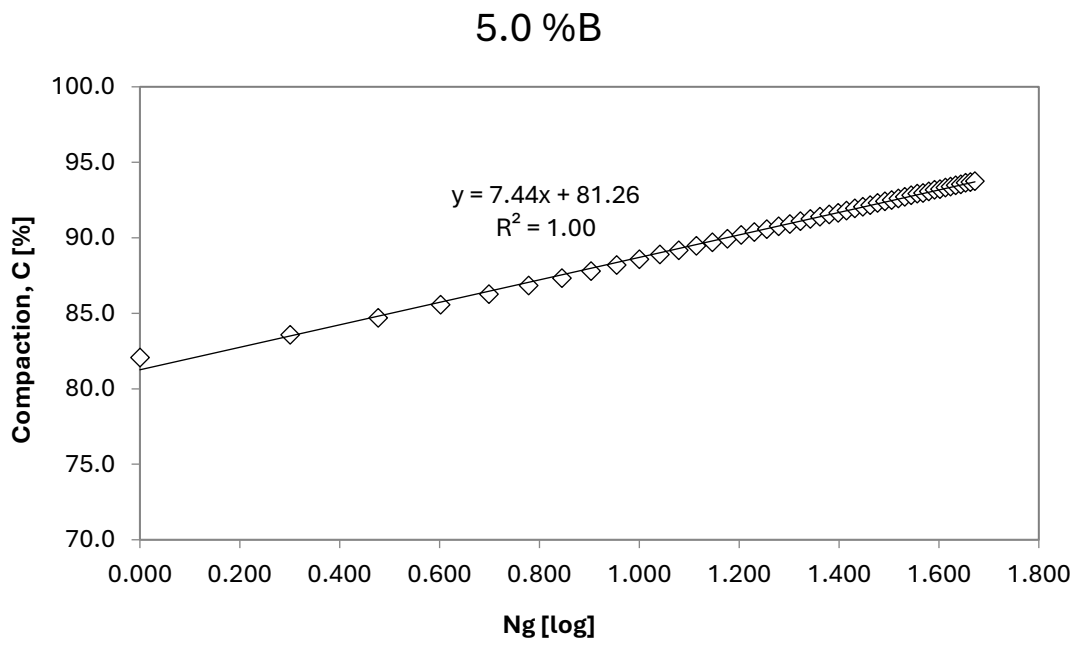


*Figure 118. Workability of the mixture FB2 0.3% Fibers with 5.0%B*

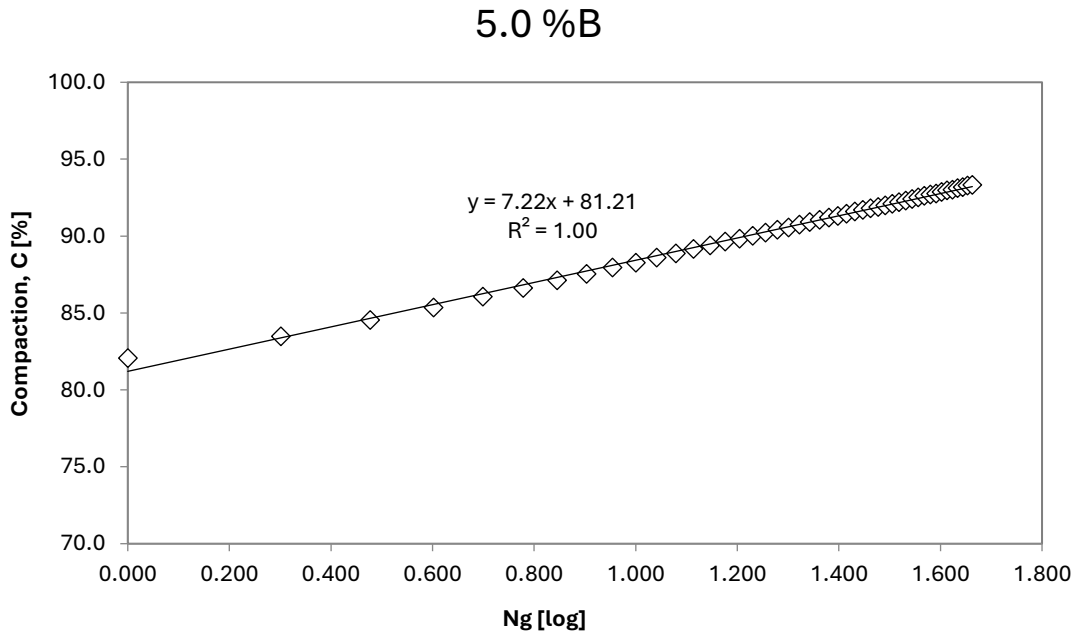


*Figure 119. Workability of the mixture FB3 0.3% Fibers with 5.0%B*

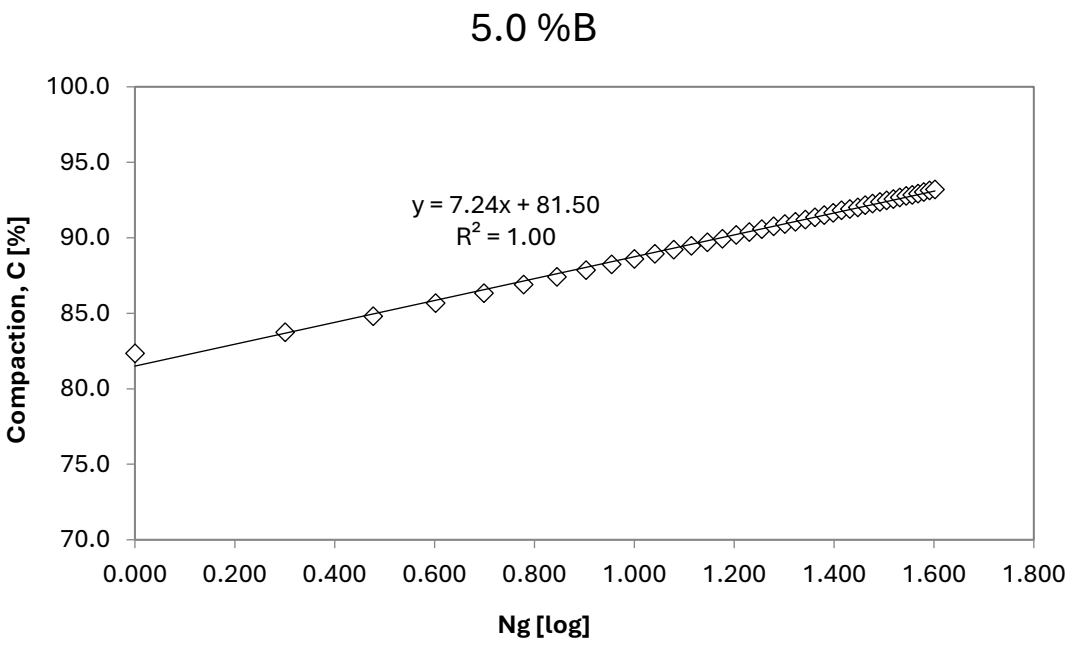


*Figure 120. Workability of the mixture FB4 0.3% Fibers with 5.0%B*

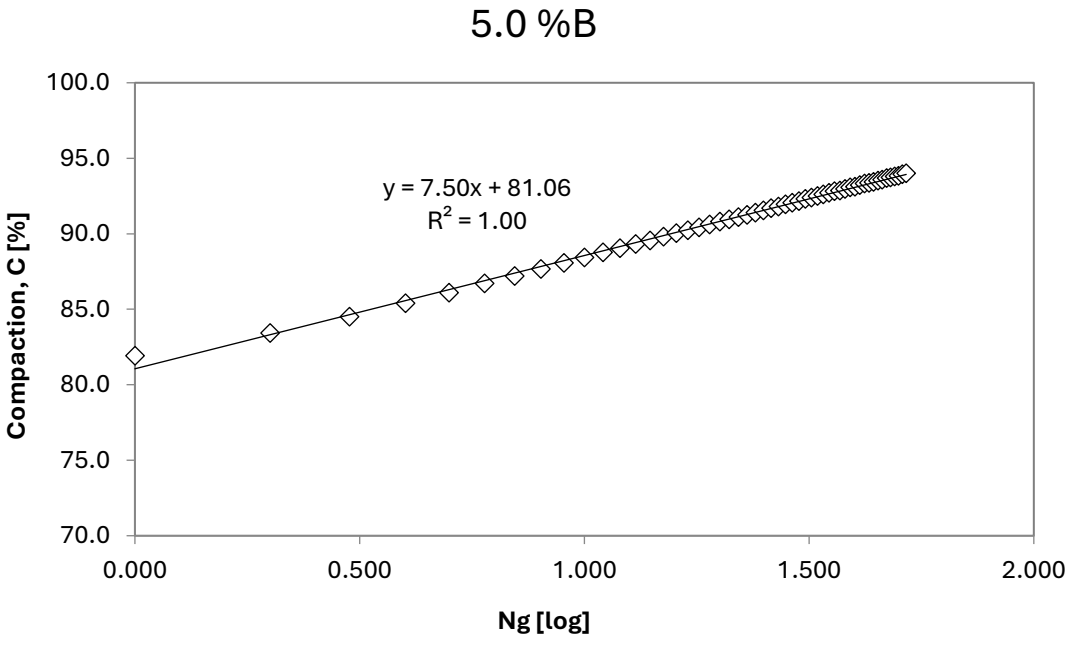


*Figure 121. Workability of the mixture FB5 0.3% Fibers with 5.0%B*

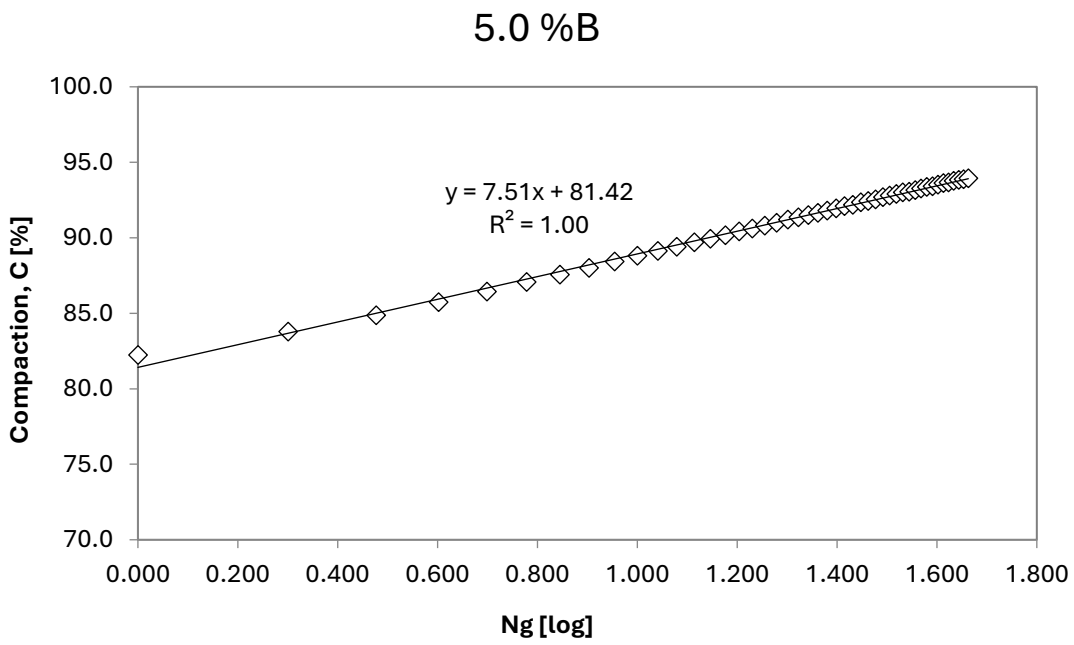


*Figure 122. Workability of the mixture FB6 0.3% Fibers with 5.0%*

*Table 17. Void content of 180x150 mm Samples (Reference Mixture)*

| ID | $M_{air}$ | $M_{H2O}$ | $M_{SSD}$ | T | v |
|---|---|---|---|---|---|
| (-) | (g) | (g) | (g) | (°C) | (%) |
| **RA2** | 7495.3 | 4442.5 | 7544.6 | 27.2 | 5.05 |
| **RA3** | 7343.3 | 4335.3 | 7426.6 | 26.6 | 6.64 |
| **RA4** | 7343.3 | 4365.7 | 7463.5 | 27.5 | 6.18 |
| **RA5** | 7395.3 | 4345.0 | 7455.8 | 27.2 | 6.58 |
| **RA6** | 7474.8 | 4416.0 | 7521.8 | 26.3 | 5.40 |

*Table 18. Void content of 180x150 mm Samples (Mixture with 0.3% Fibers)*

| ID | $M_{air}$ | $M_{H2O}$ | $M_{SSD}$ | T | v |
|---|---|---|---|---|---|
| (-) | (g) | (g) | (g) | (°C) | (%) |
| **FB1** | 7509.4 | 4445.2 | 7580.1 | 27.0 | 5.90 |
| **FB2** | 7467.2 | 4412.3 | 7541.6 | 26.6 | 6.25 |
| **FB3** | 7461.4 | 4385.9 | 7526.0 | 27.5 | 6.67 |
| **FB4** | 7466.2 | 4394.9 | 7539.8 | 27.2 | 6.75 |
| **FB5** | 7465.8 | 4403.4 | 7524.3 | 26.3 | 6.01 |
| **FB6** | 7466.5 | 4412.6 | 7534.0 | 26.3 | 6.02 |

# Appendix C. Master Curve

*Table 19. Master Curve data and fitting parameters (Reference Mixture)*

| Conditions | | RA2 | | RA3 | | RA4 | | RA5 | | RA6 | | | | |
|---|---|---|---|---|---|---|---|---|---|---|---|---|---|---|
| Temperature [°C] | Frequency [Hz] | Dynamic modulus [Mpa] | Phase angle [Degrees] | Dynamic modulus [Mpa] | Phase angle [Degrees] | Dynamic modulus [Mpa] | Phase angle [Degrees] | Dynamic modulus [Mpa] | Phase angle [Degrees] | Dynamic modulus [Mpa] | Phase angle [Degrees] | Average Dynamic Modulus [Mpa] | Dynamic Modulus CV,% | Average Phase Angle [Degrees] | Phase Angle CV,% |
| 4 | 20 | 22291 | 7.26 | 20334 | 8.94 | 19949 | 8.7 | 22342 | 9.17 | 22350 | 8.11 | 21453 | 5.62 | 8.44 | 0.77 |
| 4 | 10 | 21051 | 7.72 | 18489 | 9.19 | 18664 | 8.78 | 20263 | 9.46 | 21027 | 8.56 | 19899 | 6.28 | 8.74 | 0.67 |
| 4 | 5 | 19815 | 8.38 | 17194 | 9.48 | 17489 | 9.41 | 18750 | 9.79 | 19756 | 9.15 | 18601 | 6.61 | 9.24 | 0.53 |
| 4 | 2 | 18170 | 9.32 | 15789 | 10.5 | 15930 | 10.44 | 17035 | 10.85 | 18064 | 10.12 | 16998 | 6.65 | 10.25 | 0.58 |
| 4 | 1 | 16925 | 10.13 | 14819 | 11.23 | 14774 | 11.5 | 15737 | 11.79 | 16823 | 10.93 | 15816 | 6.58 | 11.12 | 0.64 |
| 4 | 0.5 | 15653 | 11.11 | 13722 | 12.28 | 13585 | 12.83 | 14462 | 12.82 | 15552 | 11.89 | 14595 | 6.71 | 12.19 | 0.72 |
| 4 | 0.2 | 13958 | 12.52 | 12228 | 13.75 | 12078 | 13.88 | 12827 | 14.38 | 13859 | 13.32 | 12990 | 6.81 | 13.57 | 0.70 |
| 4 | 0.1 | 12755 | 13.63 | 11169 | 14.93 | 10952 | 15.07 | 11606 | 15.6 | 12614 | 14.47 | 11819 | 6.99 | 14.74 | 0.74 |
| 20 | 20 | 10941 | 17.1 | 8936 | 17.41 | 9950 | 18.16 | 10088 | 18.6 | 10563 | 17.5 | 10096 | 7.51 | 17.75 | 0.61 |
| 20 | 10 | 9673 | 18.4 | 7902 | 19.01 | 8566 | 19.47 | 8874 | 20.16 | 9304 | 19.11 | 8864 | 7.70 | 19.23 | 0.65 |
| 20 | 5 | 8471 | 19.72 | 6913 | 20.55 | 7428 | 21 | 7724 | 21.55 | 8148 | 20.72 | 7737 | 7.87 | 20.71 | 0.67 |
| 20 | 2 | 7006 | 21.5 | 5707 | 22.66 | 6089 | 23.24 | 6300 | 23.44 | 6722 | 22.83 | 6365 | 8.06 | 22.73 | 0.76 |
| 20 | 1 | 5960 | 22.84 | 4871 | 24.21 | 5171 | 24.79 | 5311 | 24.8 | 5761 | 24.25 | 5415 | 8.17 | 24.18 | 0.80 |
| 20 | 0.5 | 4988 | 24.39 | 4095 | 25.77 | 4325 | 26.4 | 4409 | 26.3 | 4856 | 25.84 | 4535 | 8.26 | 25.74 | 0.80 |
| 20 | 0.2 | 3849 | 26.42 | 3191 | 27.86 | 3336 | 28.73 | 3344 | 28.23 | 3768 | 27.85 | 3498 | 8.34 | 27.82 | 0.86 |
| 20 | 0.1 | 3121 | 27.68 | 2615 | 28.92 | 2711 | 29.71 | 2683 | 29.22 | 3070 | 28.89 | 2840 | 8.33 | 28.88 | 0.75 |
| 40 | 20 | 3600 | 30.47 | 2796 | 31.1 | 2663 | 31.92 | 2793 | 31.96 | 2927 | 31.95 | 2956 | 12.59 | 31.48 | 0.67 |
| 40 | 10 | 2742 | 32.38 | 1990 | 34.1 | 1867 | 35.05 | 2010 | 34.61 | 2162 | 34.01 | 2154 | 16.01 | 34.03 | 1.01 |
| 40 | 5 | 2099 | 33.1 | 1465 | 35.02 | 1365 | 36.03 | 1495 | 35.24 | 1624 | 34.29 | 1610 | 17.94 | 34.74 | 1.11 |
| 40 | 2 | 1430 | 33.82 | 948.5 | 35.77 | 880.3 | 36.63 | 968.8 | 35.84 | 1075 | 34.6 | 1061 | 20.56 | 35.33 | 1.11 |
| 40 | 1 | 1056 | 34.15 | 692.1 | 35.49 | 651.1 | 35.76 | 720.7 | 35.02 | 784.3 | 34.4 | 781 | 20.66 | 34.96 | 0.69 |
| 40 | 0.5 | 798.8 | 33.74 | 519.8 | 34.77 | 489.6 | 34.6 | 535.7 | 34.14 | 591.4 | 33.33 | 587 | 21.12 | 34.12 | 0.60 |
| 40 | 0.2 | 563.7 | 32.01 | 356.7 | 33.45 | 343.7 | 32.98 | 369.4 | 32.54 | 407.4 | 31.93 | 408 | 22.08 | 32.58 | 0.65 |
| 40 | 0.1 | 437.1 | 30.85 | 272.3 | 32.2 | 263.7 | 31.44 | 279.4 | 31.6 | 309.1 | 30.6 | 312 | 22.99 | 31.34 | 0.63 |
| 40 | 0.01 | 213.1 | 24.85 | 125.3 | 26.86 | 129.5 | 25.83 | 129.3 | 26.52 | 142.4 | 25.72 | 148 | 25.01 | 25.96 | 0.78 |

| | |
|---|---|
| VMA | 12.83 |
| VFA | 69.16 |
| Pc | 0.8839 |
| Emax (psi) | 3,431,937.30 |
| log Emax | 6.66 |

6.535539

| T (°C) | T (k) | aT |
|---|---|---|
| 4 | 277.15 | 148.03 |
| 20 | 293.15 | 1.00 |
| 40 | 313.15 | 0.00 |

| | |
|---|---|
| $\Delta E_a$ | **211016.2253** |
| δ | **3.274562687** |
| β | **-1.264063865** |
| γ | **-0.477050232** |

recommended: $\delta = 0.5$, $\beta = -1.0$, $\gamma = -0.5$, and $\Delta E_a = 200\,000$.

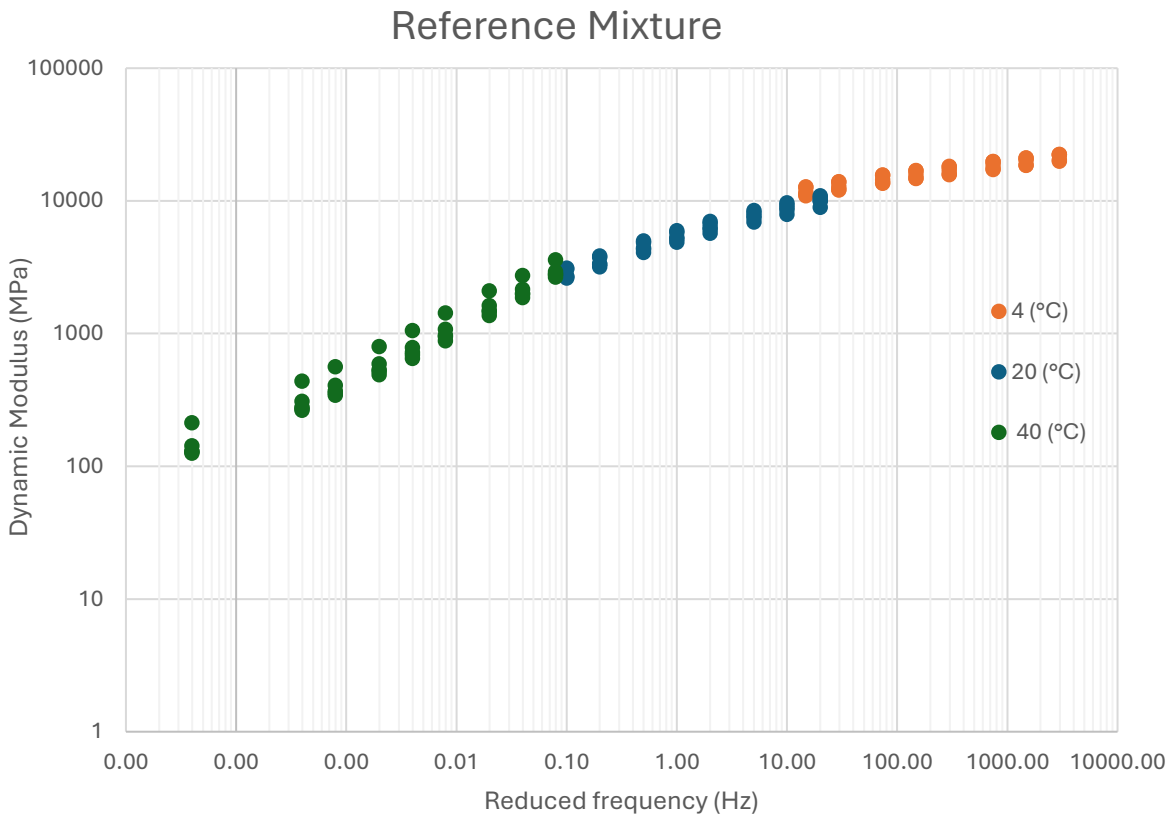


*Figure 123. Measured Master Curve*

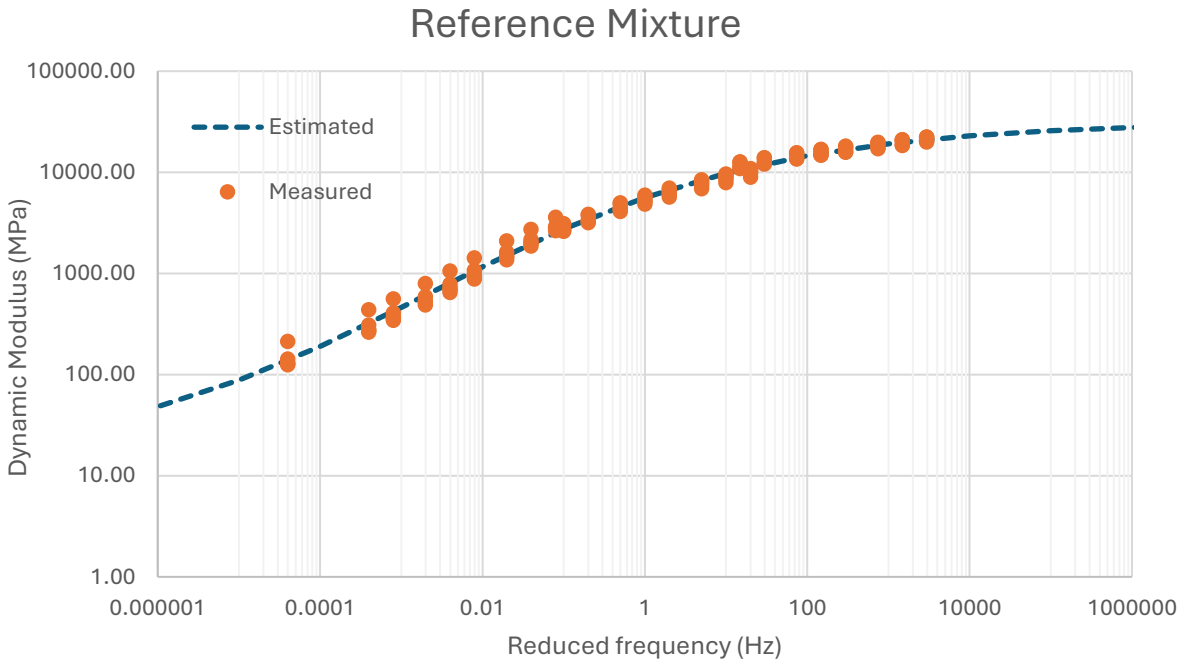


*Figure 124. Measured and Estimated Master Curve*

*Table 20. Master Curve data and fitting parameters (Fibers 0.3%)*

| Conditions | | FB1 | | FB2 | | FB3 | | FB4 | | FB5 | | FB6 | | Average Dynamic Modulus [Mpa] | Dynamic Modulus CV,% | Average Phase Angle [Degrees] | Phase Angle CV,% |
|---|---|---|---|---|---|---|---|---|---|---|---|---|---|---|---|---|---|
| Temperature [°C] | Frequency [Hz] | Dynamic modulus [Mpa] | Phase angle [Degrees] | Dynamic modulus [Mpa] | Phase angle [Degrees] | Dynamic modulus [Mpa] | Phase angle [Degrees] | Dynamic modulus [Mpa] | Phase angle [Degrees] | Dynamic modulus [Mpa] | Phase angle [Degrees] | Dynamic modulus [Mpa] | Phase angle [Degrees] | | | | |
| 4 | 20 | 23150 | 7.05 | 21889 | 7.91 | 21523 | 8.15 | 20472 | 8.17 | 22105 | 7.97 | 21563 | 8.27 | 21784 | 4.01 | 8 | 5.64 |
| 4 | 10 | 21861 | 7.49 | 20664 | 8.38 | 20237 | 8.72 | 19026 | 8.71 | 20831 | 8.57 | 20342 | 8.57 | 20494 | 4.50 | 8 | 5.54 |
| 4 | 5 | 20585 | 8.09 | 19407 | 8.86 | 18928 | 9.36 | 17645 | 9.19 | 19481 | 9.13 | 19119 | 9.12 | 19194 | 4.96 | 9 | 5.08 |
| 4 | 2 | 18877 | 9 | 17742 | 9.74 | 17217 | 10.39 | 16002 | 10.05 | 17754 | 10.06 | 17543 | 10.06 | 17523 | 5.32 | 10 | 4.85 |
| 4 | 1 | 17580 | 9.79 | 16486 | 10.53 | 15902 | 11.22 | 14794 | 10.78 | 16505 | 10.75 | 16316 | 10.85 | 16264 | 5.59 | 11 | 4.49 |
| 4 | 0.5 | 16321 | 10.71 | 15243 | 11.45 | 14609 | 12.2 | 13649 | 11.62 | 15268 | 11.74 | 15079 | 11.82 | 15028 | 5.84 | 12 | 4.30 |
| 4 | 0.2 | 14650 | 12.02 | 13618 | 12.83 | 12977 | 13.68 | 12169 | 12.97 | 13579 | 13.03 | 13437 | 13.13 | 13405 | 6.09 | 13 | 4.16 |
| 4 | 0.1 | 13373 | 13.09 | 12413 | 14 | 11797 | 14.86 | 11154 | 14.04 | 12336 | 14.32 | 12223 | 14.32 | 12216 | 6.01 | 14 | 4.14 |
| 20 | 20 | 11629 | 15.86 | 11030 | 16.52 | 10252 | 17.39 | 9239 | 17.46 | 10638 | 16.8 | 10819 | 16.86 | 10601 | 7.62 | 17 | 3.52 |
| 20 | 10 | 10352 | 17.26 | 9799 | 17.96 | 8998 | 18.82 | 8164 | 18.92 | 9350 | 18.27 | 9538 | 18.42 | 9367 | 7.95 | 18 | 3.34 |
| 20 | 5 | 9169 | 18.64 | 8596 | 19.36 | 7857 | 20.31 | 7143 | 20.36 | 8198 | 19.8 | 8348 | 19.85 | 8219 | 8.34 | 20 | 3.27 |
| 20 | 2 | 7683 | 20.5 | 7170 | 21.33 | 6471 | 22.34 | 5913 | 22.4 | 6793 | 21.86 | 6922 | 21.86 | 6825 | 8.85 | 22 | 3.27 |
| 20 | 1 | 6655 | 21.92 | 6184 | 22.78 | 5536 | 23.8 | 5068 | 23.88 | 5818 | 23.31 | 5940 | 23.35 | 5867 | 9.26 | 23 | 3.15 |
| 20 | 0.5 | 5680 | 23.5 | 5249 | 24.35 | 4677 | 25.44 | 4285 | 25.5 | 4923 | 24.9 | 5013 | 24.9 | 4971 | 9.61 | 25 | 3.02 |
| 20 | 0.2 | 4537 | 25.5 | 4157 | 26.42 | 3674 | 27.48 | 3389 | 27.63 | 3860 | 26.96 | 3930 | 27.04 | 3925 | 10.08 | 27 | 2.91 |
| 20 | 0.1 | 3786 | 26.74 | 3454 | 27.65 | 3039 | 28.7 | 2820 | 28.66 | 3168 | 28.15 | 3231 | 28.3 | 3250 | 10.35 | 28 | 2.64 |
| 40 | 20 | 3859 | 29.94 | 3208 | 31.44 | 2940 | 31.73 | 2775 | 32.11 | 3164 | 31.38 | 3171 | 31.65 | 3186 | 11.60 | 31 | 2.39 |
| 40 | 10 | 3020 | 31.44 | 2419 | 33.66 | 2192 | 33.96 | 2083 | 34.22 | 2386 | 33.56 | 2390 | 33.54 | 2415 | 13.45 | 33 | 2.98 |
| 40 | 5 | 2368 | 32.09 | 1840 | 34.4 | 1668 | 34.6 | 1592 | 34.75 | 1819 | 34.33 | 1820 | 34.18 | 1851 | 14.69 | 34 | 2.89 |
| 40 | 2 | 1645 | 32.87 | 1223 | 35.4 | 1109 | 35.44 | 1063 | 35.42 | 1206 | 35.19 | 1214 | 34.87 | 1243 | 16.66 | 35 | 2.87 |
| 40 | 1 | 1223 | 33.3 | 883.1 | 35.95 | 797.5 | 35.82 | 776.8 | 35.43 | 865.2 | 35.7 | 879 | 35.24 | 904 | 17.96 | 35 | 2.80 |
| 40 | 0.5 | 926.4 | 33.07 | 645.5 | 35.81 | 582.8 | 35.66 | 572 | 35.18 | 637.3 | 35.4 | 650.9 | 34.9 | 669 | 19.48 | 35 | 2.86 |
| 40 | 0.2 | 634 | 32.79 | 423.3 | 35.8 | 380.2 | 35.69 | 374.3 | 35.09 | 423.4 | 34.68 | 432.1 | 34.65 | 445 | 21.58 | 35 | 3.14 |
| 40 | 0.1 | 471.5 | 32.79 | 304.7 | 35.53 | 270.5 | 35.52 | 268.5 | 34.76 | 308.7 | 34.26 | 311.8 | 34.52 | 323 | 23.38 | 35 | 2.93 |
| 40 | 0.01 | 192 | 29.61 | 113.5 | 33.05 | 96.9 | 32.9 | 99 | 31.9 | 119.1 | 30.44 | 116.9 | 31.48 | 123 | 28.56 | 32 | 4.30 |

| | | |
|---|---|---|
| VMA | 13.28 | |
| VFA | 66.00 | |
| Pc | 0.8790 | |
| Emax (psi) | 3,394,158.15 | |
| log Emax | 6.39 | 6.53 |

| T (°C) | T (k) | **aT** |
|---|---|---|
| 4 | 277.15 | 123.08 |
| 20 | 293.15 | 1.00 |
| 40 | 313.15 | 0.00 |

| | |
|---|---|
| $\Delta E_a$ | **203224.4937** |
| $\delta$ | **3.364431502** |
| $\beta$ | **-1.746240843** |
| $\gamma$ | **-0.614111297** |

recommended: $\delta = 0.5$, $\beta = -1.0$, $\gamma = -0.5$, and $\Delta E_a = 200\,000$.

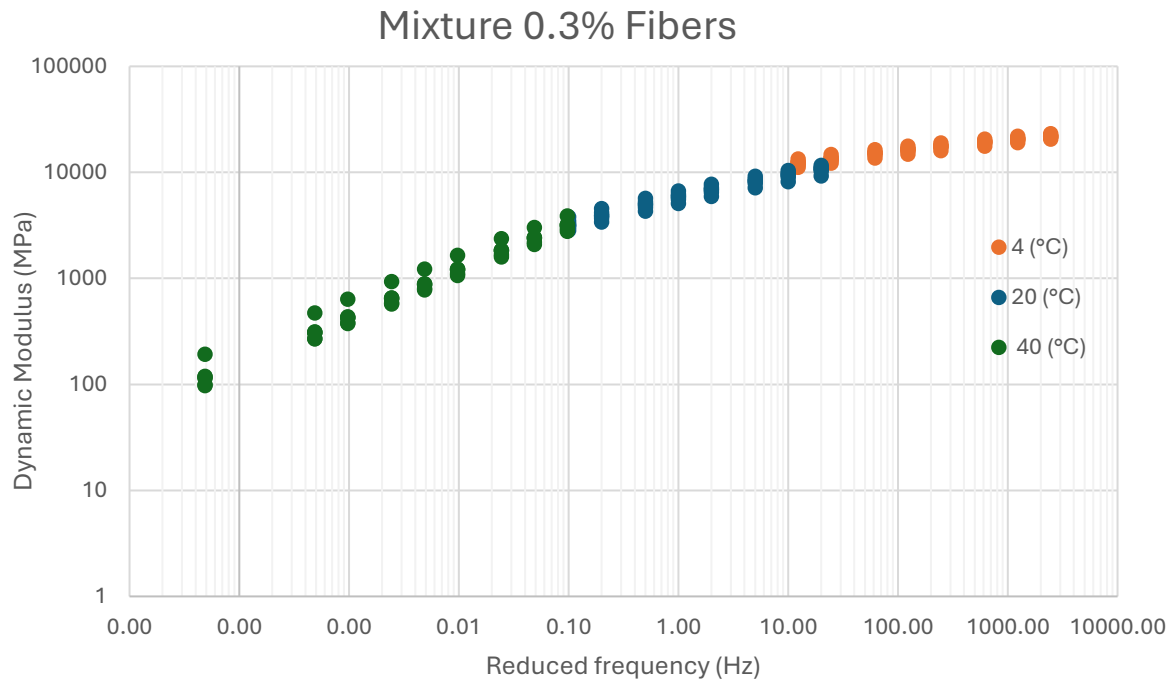


*Figure 125. Measured Master Curve*

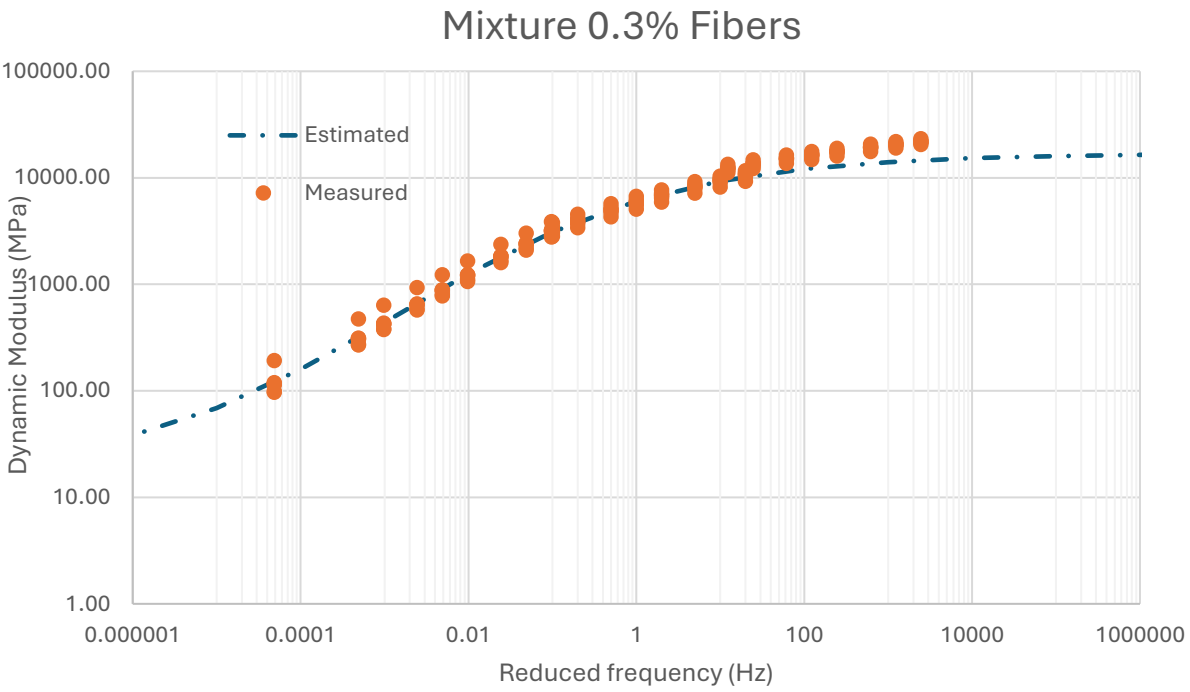


*Figure 126. Measured and Estimated Master Curve*

# Appendix D. Flow number

*Table 21. Core Sample voids of Reference Mixture*

| ID | $M_{air}$ | $M_{H2O}$ | $M_{SSD}$ | T | $\rho_w$ | $\rho_{SSD}$ | $\rho_{mv}$ | v |
|---|---|---|---|---|---|---|---|---|
| (-) | (g) | (g) | (g) | (°C) | ($Mg/m^3$) | ($Mg/m^3$) | ($Mg/m^3$) | (%) |
| **RA2** | 2796.2 | 1664.1 | 2802.7 | 27.2 | 0.997 | 2.447 | 2.536 | 3.50 |
| **RA3** | 2718.0 | 1603.3 | 2728.0 | 26.4 | 0.997 | 2.409 | 2.536 | 5.01 |
| **RA4** | 2787.5 | 1648.4 | 2795.2 | 27.4 | 0.996 | 2.422 | 2.536 | 4.49 |
| **RA5** | 2772.3 | 1636.6 | 2779.3 | 27.4 | 0.996 | 2.418 | 2.536 | 4.67 |
| **RA6** | 2773.6 | 1647.2 | 2777.9 | 26.5 | 0.997 | 2.445 | 2.536 | 3.59 |

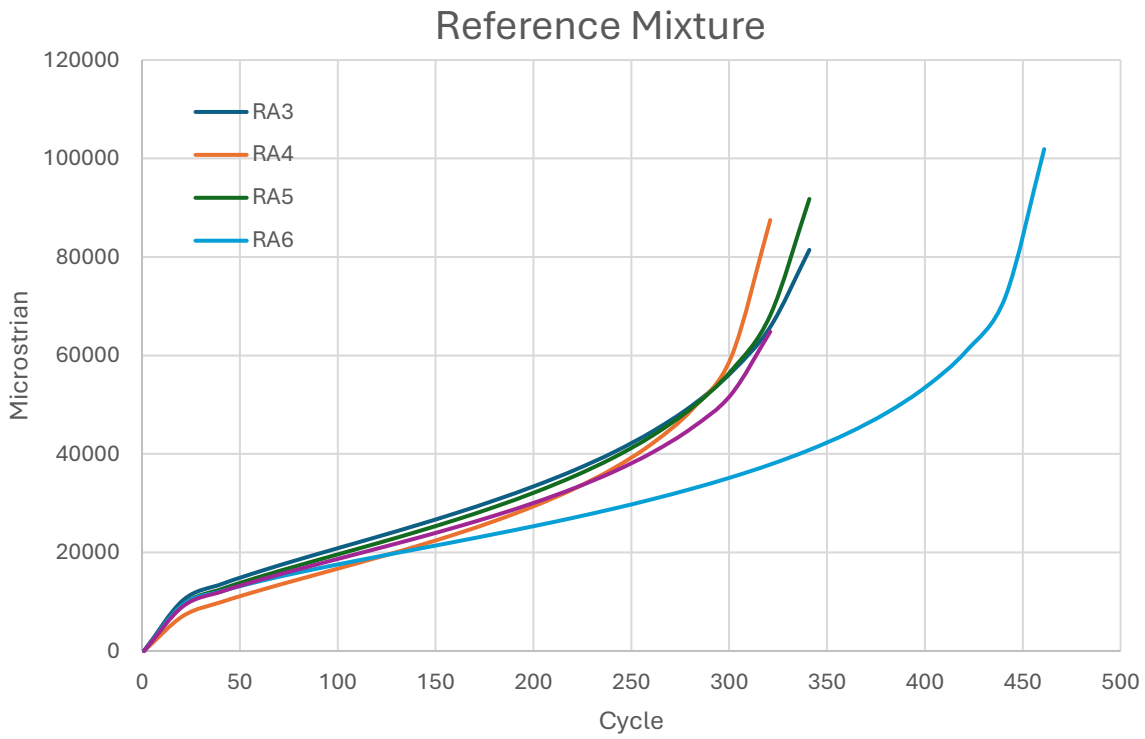


*Figure 127. Flow number results (Reference)*

*Table 22. Core Sample voids of Mixture with 0.3% Fibers*

| ID | $M_{air}$ | $M_{H2O}$ | $M_{SSD}$ | T | $\rho_w$ | $\rho_{SSD}$ | $\rho_{mv}$ | v |
|---|---|---|---|---|---|---|---|---|
| (-) | (g) | (g) | (g) | (°C) | ($Mg/m^3$) | ($Mg/m^3$) | ($Mg/m^3$) | (%) |
| **FB1** | 2828.9 | 1678.5 | 2836.2 | 26.9 | 0.997 | 2.435 | 2.537 | 4.01 |
| **FB2** | 2778.5 | 1646.6 | 2788.2 | 26.4 | 0.997 | 2.426 | 2.537 | 4.38 |
| **FB3** | 2778.2 | 1638.4 | 2785.4 | 27.4 | 0.996 | 2.414 | 2.537 | 4.86 |
| **FB4** | 2775.8 | 1638.8 | 2786.2 | 27.4 | 0.996 | 2.411 | 2.537 | 4.98 |
| **FB5** | 2820.0 | 1666.3 | 2826.4 | 26.5 | 0.997 | 2.423 | 2.537 | 4.50 |
| **FB6** | 2806.0 | 1661.4 | 2814.4 | 26.5 | 0.997 | 2.426 | 2.537 | 4.39 |

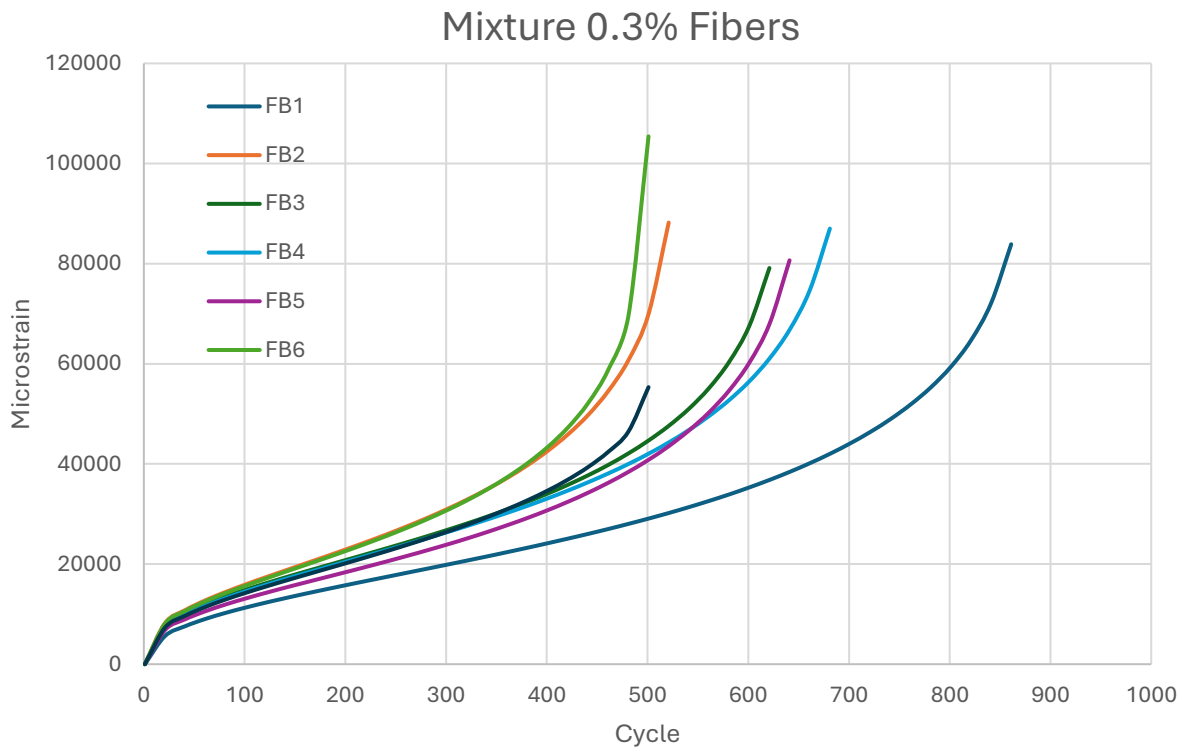


*Figure 128. Flow number results (0.3% Fibers)*